CSD-2002-01

MDOT

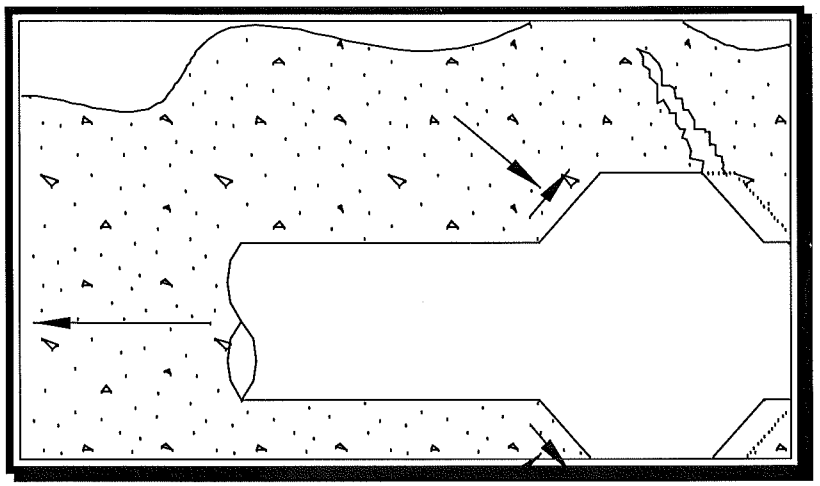

A Comparative Bond Study of Stainless Steel Reinforcement in Concrete

Final Report – January 2002

TESTING AND RESEARCH SECTION
CONSTRUCTION AND TECHNOLOGY DIVISION
RESEARCH REPORT # RC-1406
CONTRACT NO. 96-5434
AUTHORIZATION NO. (01-MTU-1)
PROJECT MANAGER: STEVE KAHL

MichiganTech
Center for Structural Durability

Technical Report Documentation Page

1. Report No. RC 1406	2. Government Accession No.	3. Recipient's Catalog No.
4. Title and Subtitle: A Comparative Bond Study of Stainless Steel Reinforcement in Concrete		5. Report Date January 2002
7. Author(s): Dr. Theresa M. (Tess) Ahlborn Mr. Timothy C. DenHartigh		6. Performing Organization Code: MTU
9. Performing Organization Name and Address: Michigan Technological University Civil & Environmental Eng. Department Center for Structural Durability 1400 Townsend Drive Houghton, MI 49931		8. Performing Org. Report No. CSD-2002-01
12. Sponsoring Agency Name and Address Michigan Department of Transportation Construction and Technology Division P.O. Box 30049 Lansing, MI 48909		10. Work Unit No. 11. Contract/Grant No. (C) 96-5434
15. Supplementary Notes		13. Type of Report / Period Final Report, 2001-2002 14. Sponsoring Agency Code

16. Abstract

Concrete bridge decks in corrosive environments have utilized several methods to prevent corrosion of the reinforcing steel including the use of stainless steel as reinforcement. While proven for corrosion resistance, very little information is available about the bond strength of stainless reinforcement. The bond strength of stainless steel reinforcement in concrete compared to conventional carbon steel reinforcement was studied in working stress ranges between 34% to 100% of yield.

One hundred and ninety one bond tests were performed with beam-end specimens similar to the ASTM A944 (1995) specimen. Bar types used in the bond tests were conventional A615 Gr. 60 carbon steel reinforcement, 316LN stainless steel reinforcement, and 2205 Duplex stainless steel reinforcement. Bonded lengths of 4-in. to 10-in. were used for the No. 4 bars, and 5.5-in. to 12-in. for the No. 6 bars. Concrete clear cover for all tests was 1½-in. to conduce cracking bond failure. No transverse reinforcement was present in the tests.

Comparisons of stainless reinforcement test results to predicted values revealed that there was no reason to believe the bond strength of stainless reinforcing bars, independent of bar type studied, was less than predicted. No. 4 reinforcing bar comparisons involving stainless steel reinforcement to carbon steel reinforcement showed that there was no reason to believe that the stainless steel bond strength was different than the carbon steel bond strength. The comparison of No. 6 stainless steel reinforcement bond tests to carbon steel bond tests revealed a weaker bond for some stainless bars. However, the conservatism of the AASHTO development length relationship (as well as other comparative relationships including OJB, ACI and Darwin) predicted lower bond strengths than observed at all bonded lengths for all bar types. Therefore, no modifications are suggested when determining the development length of stainless reinforcement on a one-to-one replacement of stainless steel 316LN or Duplex 2205 for Gr. 60 A615 reinforcement, No. 4 to No. 6 bars.

17. Key Words: Stainless steel, concrete reinforcement, bond, development length, bridge decks, 316LN stainless, Duplex 2205		18. Distribution Statement	
19. Security Classification Unclassified	20. Security Classification Unclassified	21. No. Pages 131	22. Price

Form DOT F 1700.7 (8-72)

A Comparative Bond Study of Stainless Steel Reinforcement in Concrete

Final Report
CSD 2002-01

Dr. Theresa (Tess) M. Ahlborn
Mr. Timothy C. DenHartigh

Michigan Technological University
Center for Structural Durability
Civil & Environmental Engineering Department
College of Engineering
Houghton, Michigan 49931

January 2002

ACKNOWLEDGEMENTS

The research reported herein was sponsored by the Michigan Department of Transportation. This support is gratefully acknowledged.

The authors are thankful to Steve Kahl and Dave Juntunen, the co-project managers of the Research Advisory Panel, and also to all RAP members including Steve Beck, David Calabrese, Ali Mahdavi and Tony Olson. Their guidance and supervision of the project and valuable input regarding these research efforts are appreciated.

This report presents the results of research conducted by the authors and does not necessarily reflect the views of the Michigan Department of Transportation. This report does not constitute a standard or specification.

EXECUTIVE SUMMARY

Concrete bridge decks in corrosive environments have utilized several methods to prevent corrosion of the reinforcing steel including the use of stainless steels as reinforcement. While proven for corrosion resistance, very little information is available about the bond strength of stainless reinforcement. The bond strength of stainless steel reinforcement in concrete compared to conventional carbon steel reinforcement was studied in working stress ranges between 34% to 100% of yield.

One hundred and ninety one bond tests were performed with beam-end specimens similar to the ASTM A944 (1995) specimen. Bar types used in the bond tests were conventional A615 Gr. 60 carbon steel reinforcement, 316LN stainless steel reinforcement, and 2205 Duplex stainless steel reinforcement. Bonded lengths of 4-in. to 10-in. were used for the No. 4 bars, and 5.5-in. to 12-in. for the No. 6 bars. Concrete clear cover for all tests was 1½-in. to produce cracking bond failure. No transverse reinforcement was present in the tests. The concrete was MDOT Grade D, typical of that used in Michigan bridge decks. Comparisons of stainless reinforcement test results to predicted values for bond strength of A615 reinforcement, revealed that there was no reason to believe the bond strength of stainless reinforcing bars, for either 316LN or Duplex 2205, was less than predicted. No. 4 reinforcing bar comparisons involving stainless steel reinforcement to carbon steel reinforcement showed that there was no reason to believe that the stainless steel bond strength was different than the carbon steel bond strength. However, the comparison of No. 6 stainless steel reinforcement bond tests to carbon steel bond tests revealed a weaker bond for some stainless bars. However, the conservatism of the AASHTO development length relationship (as well as other comparative relationships including OJB, ACI and Darwin) predicted lower bond strengths than observed at all bonded lengths for all bar types.

Realizing that the AASHTO 16th ed. Standard Specifications and LRFD codes currently limit the use of reinforcing materials above Gr. 75, the potential use of these high strength materials is limited. However, the results of tests show that the AASHTO development length relationship can conservatively be used for stainless 316LN and Duplex 2205 reinforcing bars. Therefore, no modifications are suggested when determining the development length of stainless reinforcement, specifically 316LN or Duplex 2205, on a one-to-one replacement for Gr. 60 A615 reinforcement, No. 4 to No. 6 bars.

TABLE OF CONTENTS

LIST OF FIGURES

LIST OF TABLES

CHAPTER 1: INTRODUCTION

The corrosion of reinforcing steel in concrete structures can be of serious concern, especially in bridge decks where de-icing salts are commonly used. To date, options to reduce corrosion of standard black bars have mainly included epoxy coating the bars. However, epoxy coated bars have some disadvantages particularly susceptibility to damage incurred during the transportation or installation of the steel. This damage can cause a concentration of corrosion resulting in a weaker bar than would otherwise have existed had no steps been taken to protect the bar from corrosion. Another problem with coated reinforcing is that changes to a bar cannot easily be made in the field. For example if a particular bar needs to be cut to fit into a particular form, if the bar is coated the newly cut end defeats the purpose of the coating. Another form of corrosion resistance found in reinforcing bars is cathodic protection. This form of protection utilizes an electrical current running through the bar to resist corrosion. Cathodic protection is effective but the drawback is the continuous required electrical current. Because of these failures in corrosive resistant reinforcing material, the use of stainless steel has become a more frequently used alternative. The use of stainless steel allows workers to cut and weld reinforcing steel as required in the field without negative results from this manipulation. However, stainless as an option is not currently addressed in terms of bond or development length by the American Concrete Institute (ACI), American Association of State Highway and Transportation Officials (AASHTO), or other design codes. This type of reinforcement has not been seriously considered in current concrete bond research.

1.1 BOND

When reinforcing bars are embedded into concrete and consequently loaded in tension, a certain bond stress associated with this load develops in the concrete. This bond stress nonlinear and is a function of load, reinforcing bar material properties, and reinforcing bar geometric properties. Bond stress is higher near the end of the bar that is being loaded and lower at the other end of the bar. Qualitatively, the nonlinear stress distribution can be thought of as follows; if the bond stress in the first part of the bar does not reach some critical point, the rest of the bar beyond that first part will not be required to transfer force

from itself to the concrete. In order for the entire bar to transmit force, the first part of the bar must reach this critical point, slip some unnoticeable amount, and then redistribute the bond stresses. This cycle continues until the entire bar is transmitting load from itself to the surrounding concrete.

When studying bond stress it is common practice to assume an average distribution of the bond stress in order to compute working bond strength. The working bond strength is equal to the bar load. From the bar load, the bar stress can be calculated. Bond strength equations generally deal with bar stresses and compute bond lengths that will produce these bar stresses. Typical design code equations attempt to predict a bonded length that will result in yielding the bar before bond is broken.

Bond strength is typically thought of as being made up of 3 components, friction and adhesion, which are dependent on the bar surface condition, and bearing, which is dependent on the bar deformation pattern. Further discussion of the components of bond can be found in Section 2.1.

A specific failure point must be defined for the purpose of normalization between various bond studies. A logical way to define this failure point would be some specific value for free-end displacement. Small values of free end displacement generally indicate that bond failure has occurred. In other words, if the free end of the test bar is sliding out of the specimen then obviously bond failure has occurred. The value that has been chosen throughout previous tests is a free-end displacement of 0.002-in. *Herein all references to bond failure shall be the load occurring at a free-end displacement value of 0.002-in.*

Bond failure is typically made up of 4 steps (Fédération Internationale du Béton, 2000):

- Step 1: Low bond stresses; all 3 bond components are present (adhesion, bearing, and friction). No displacement of the bar relative to the concrete can be seen. The only movement of the bar is due to elastic deformation of the concrete around the bar.
- Step 2: The bar starts to move with respect to the concrete. Microcracks form behind the bar deformation (see Figure 1-1). Two bond components remain, bearing and friction.

- Step 3: Microcracks spread radially outward from the bar. Confinement produced by either surrounding concrete or transverse reinforcing steel resist the spreading of the cracks.
- Step 4: Bond failure occurs by either pullout or bond cracking. Pullout will occur if the confinement is greater than the transverse bond force. Cracking occurs if the confinement is not greater than the transverse bond force.

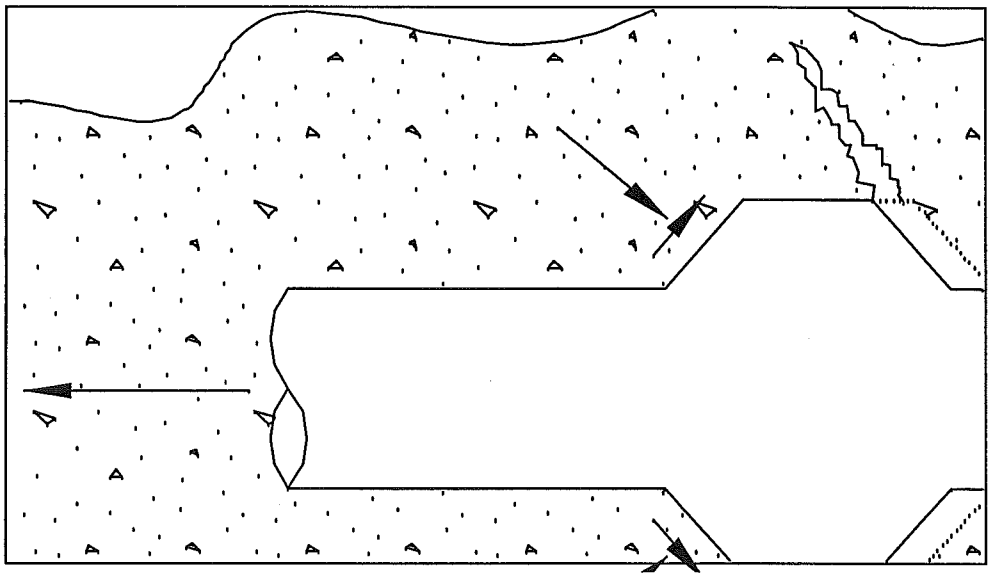

Figure 1-1: Step 2, Microcrack Formation

1.2 OBJECTIVE

This project investigated the tension development length of two types of solid stainless steel reinforcing bars in comparison to standard A615 Gr.60 black bars and theoretical equations, including AASHTO, ACI and others. Two types of stainless reinforcing bars were tested in this project, type 316LN and Duplex 2205. Reinforcing bar sizes typically used in bridge deck applications, No. 4 and No. 6 bars, ½-in. and ¾-in. diameter, respectively, were the focus of this study.

1.1 SCOPE

One hundred and ninety one semi-beam specimens were produced with the various reinforcing bars. Considering the schematic shown in Figure 1-2 the total number of semi-beam specimens used in this comparative study can be seen. Four bonded lengths were used for each bar type (black bar, and the two types of stainless bars) and size tested (No. 4 and

No. 6). Within each bar type and size, a minimum of seven semi-beam specimens were tested for each bonded length.

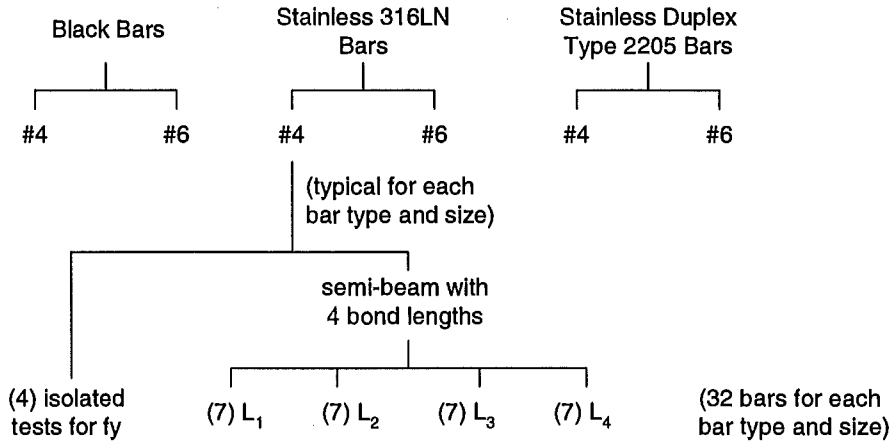

Figure 1-2: Number of Semi-beam Bond Specimens

1.2 ORGANIZATION

Chapter 2 presents bond studies starting with a historical review, then looking at the effects of epoxy coating on bars, finally looking at the effect the deformation pattern of the bar has on the bond strength. Epoxy bond tests were reviewed because many of these reports deal with comparative bond studies, similar to this project. Chapter 3 explains the experimental setup used in this study. Chapter 4 presents the experimental results and statistical discussion. Finally Chapter 5 presents conclusions and the significance of the results from this study.

CHAPTER 2: PREVIOUS RESEARCH

2.1 BOND HISTORY

D. A. Abrams was first to study the bond between concrete and steel in a clear scientific manner (Abrams, 1913). Abrams conducted 1500 pullout tests on smooth and deformed bars. He claimed that previous research that had been done on bond strength involved a lack of uniformity of the test specimen and only reported the maximum bond strength. With a purpose of investigating the effects of settlement and shrinkage on bond strength, he found that bars held against settlement, with respect to the concrete, exhibited 60% lower bond strength than bars that were allowed to settle with the concrete. He also found that when bars were cast in a vertical position rather than in a horizontal position, the bond for the vertical position was slightly stronger than the horizontal. He concluded from the evidence of his tests that the adhesive component was the most important component of bond. Abrams also found that the bond stress is not uniformly distributed along a bar embedded any considerable length and having the load applied at one end. One other main result was that for tests where the bar was given additional anchorage by means of nuts and washers attached to the bars, significant slip must occur before these factors come into action. All of Abrams' conclusions can be explained by today's known bond mechanics.

A. P. Clark looked at the effect of deformation patterns on the strength of bond (Clark, 1946). He studied 17 different deformation patterns, with bonded lengths of 8-in. and 16-in., for both top and bottom bars using pullout type tests. All the bars studied were 7/8-in. diameter. Slip was measured at both the free and loaded end. As stated, all of Clark's work was based on pullout tests, which are not the most reliable type of tests due to the unrealistic state of stress surrounding the bonded bar. Clark based the performance of the bar on a usable range of bond stress rather than bond strength. He averaged the bond stresses at loaded end-slip measurements of 0.0005, 0.001, 0.002, 0.003, 0.004, 0.005, 0.0075, and 0.01-in. for each bar. He then averaged the values for top and bottom-cast bars to obtain a single representative bond stress for each deformation pattern. The current deformation pattern criterion for deformed bars, found in ASTM A615 and A617, is based on this research. Clark also made recommendations that the ratio of shearing area to rib bearing area be

limited to a maximum of 10, ideally 5 to 6. Today's criteria used to describe the relative size and spacing of deformations is called relative rib area, which is proportional to the inverse of Clark's criteria. Relative rib area is proportional to the ratio of rib deformation height to rib spacing. Converting Clark's recommendations, it can be shown that he recommended equivalent values between 0.20-0.17 with a minimum value of 0.10. Today's standard bar deformation patterns have relative rib areas between 0.057 to 0.084. The equation commonly used to calculate relative rib area, R_r, can be seen in Equation 2-1. Figure 2-1 depicts the concept of bearing area and shear area.

$$R_r = \frac{BearingArea}{ShearArea} = h_r \cdot \frac{(d_b + h_r)}{(r_s \cdot d_b)} \qquad \textbf{Equation 2-1}$$

Where d_b = Diameter of bar.
h_r = Height of rib or deformation.
r_s = Rib spacing, center to center.

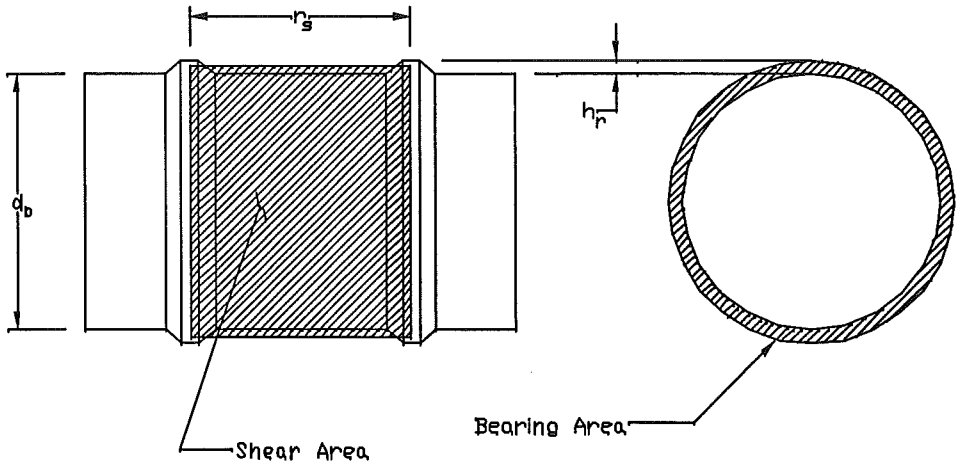

Figure 2-1: Relative Rib Area Diagram

R. M. Mains (1951) was the first to conduct a series of tests that measured the actual distribution of bond stress rather than assuming a uniform distribution of the bond stress. He accomplished this by placing strain gauges inside the reinforcing as opposed to previously mounting the strain gauges directly to the bar. The previous method of mounting the gauges is not desirable because it reduces the bond strength by reducing the area of steel in contact with the surrounding concrete. Mains' procedure included removing the top of

the rebar and putting a groove on the inside the bar. Strain gauges were then placed inside the groove. After this the top of the bar was welded back to the bottom section of bar with tack welds spaced 2-in. o/c. Mains tested both smooth and deformed bars. The main difference between the two was that the deformed bars, confirming previous speculation, developed much higher bond stress than the smooth bar. Two different types of tests were performed: pull-out specimens that were 21-in. long, 8-in. wide, and 12-in. high, with the center of the bars 2 ½-in. from the bottom, and beam specimens 78-in. long, 8-in. wide, and either 12 ½-in. or 18-in. high, with the bars located similarly to the pullout specimens.

Ferguson and Thompson (1965) were the first to test bond strength using a "new" type of beam that would place the development length in a negative moment region so that the maximum steel stresses and average bond stresses could be calculated. The investigation looked at the following different variables: strength of concrete, clear cover of the bars, development length and bar size, effect of end anchorage or hooks, effect of multiple cutoffs, and the effect of stirrups. The five different types of beams that they tested were: cantilevered beam, cantilevered beam with several bars (all with different development lengths), simple span beams with several development lengths, and a simple span beam with strain gages for flexural calibration. From the testing it was found that the beams with several different development lengths all in one beam did not produce accurate results. One conclusion from the remaining beams was that the bond strength increases with increased concrete strength, approximately in proportion to the square root of the compressive concrete strength, f'_c, thus 5000 psi concrete develops about 1.23 times the bond strength of 3300 psi concrete. Another main conclusion reached was that stirrups increased bond strength, however, they did not evaluate any type of relationship between bond strength and confinement by stirrups.

Lutz (1967) demonstrated that bond fails either by pullout of the bar or by cracking of the concrete around the bar. The pullout is a failure that "plows" or shears the concrete between the deformations of the bars. The cracking failure is due to the radial tensile stresses induced into the concrete surrounding the bar when the deformation acts as a wedge. This occurs when the cover cannot resist these tensile forces, and is the most common type of failure in structures.

Orangun, Jirsa, and Breen (1977) conducted a study on past bond research because they felt that the current code requirements did not accurately reflect the proper bond length required. They studied 62 different beams that were tested previously by various researchers and performed a regression analysis on the data which helped them produce the well-known OJB equation, see Equation 2-2.

$$l_{dOJB} = \frac{d_b \cdot \left(\frac{f_s}{4 \cdot \sqrt{f'_c}} - 50 \right)}{1.2 + 3 \cdot \frac{c}{d_b} + \frac{A_{tr} \cdot f_{yt}}{500 \cdot s \cdot d_b}} \qquad \textbf{Equation 2-2}$$

Where: d_b = Diameter of bar.
f_s = Steel stress at bond failure.
f'_c = Compressive strength of concrete.
c = Shortest distance of either clear cover to the bottom, side cover, or half the distance to the next adjacent bar.
A_{tr} = Area of transverse reinforcement across the horizontal plane through the center of the rebar being tested.
f_{yt} = Yield stress of horizontal reinforcement.
s = Center to center spacing of horizontal reinforcement.

They proposed a new perspective on bond mechanics stating that bond could be looked at as similar to a thick walled cylinder with an even pressure distribution, analogous to a pressurized pipe. The 'pressure' is due to the radial stresses that are induced when the bar is stressed. The cylinder radius is the smallest of either the side or clear cover to the centroid of the bar or half the spacing between adjacent bars plus half the bar diameter. There are three components of bond for a deformed bar: bearing, friction, and adhesion (see Figure 2-2). Adhesion is only a factor for low bond stresses; at higher stresses the adhesion component fails and is often ignored in computing bond strength. At these higher stress levels, bearing and friction combine to produce the total bond stress, which can be broken into two components, radial stress and longitudinal bond stress. From the figure it can be seen that with a decrease in the frictional component, both the total and longitudinal bond stresses would decrease and the radial pressure would increase. The derived equation developed took into account clear cover, diameter of the bar, length of the splice, the bond stress, and the concrete compressive strength.

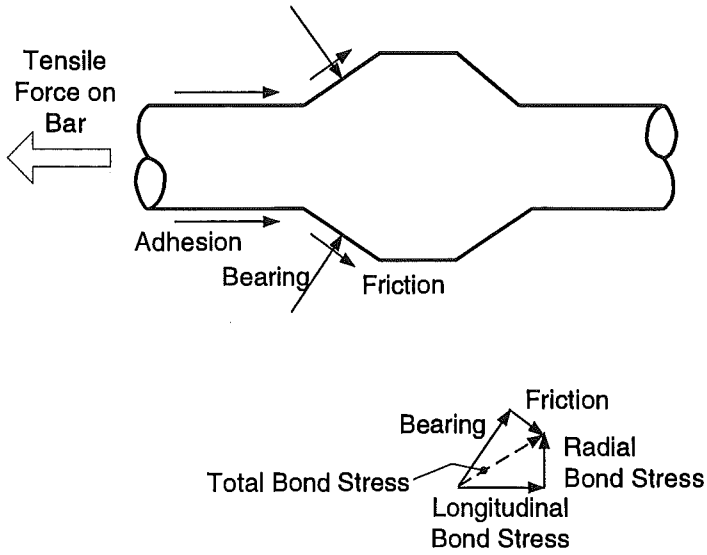

Figure 2-2: Bond Components

The influence of casting position and shear on development and splice lengths was studied by Jirsa and Breen (1981). Three different levels of shear intensity were studied. From this study shear was found to have virtually no influence on bond strength for both development bars and splices. They provide an excellent historical review of the evolution of the ACI code requirements on bond which is as follows:

> "The 1951 ACI Code provisions for top bars were heavily influenced by the work done by Clark (Clark 1946, 1949). Clark assumed that a loaded end slip of a bar in a pullout test corresponded to half the crack width that would develop in a beam with the reinforcement at an equal level of stress as in the test. Therefore a loaded end slip of .02-in would correspond to a crack width of .04-in. The 1951 ACI Code used this information, and a serviceability limit crack width of .02-in., to develop a maximum allowable bond stress. Ultimate stress design was implemented into the ACI Code in 1971. With that implementation, the requirements were changed from limiting the bond stress to development length equations."

Luke et al (1981) studied the influence of casting position of bars for both development length and splice length. Bars were cast at varying heights from the bottom and compared to

that of bottom bar ultimate bond strength. The bond strength was found to decrease with an increase in depth of concrete cast below the bar. Bar size had very little effect on the strength reduction of the bond. Concrete slump was also found to have a significant impact on the bond strength. The higher the slump, the greater the impact bar position had on the strength reduction of the bond. One significant result was that the 40% increase in the development length required by the current ACI Code (318-77) was found to be conservative, even for test bars cast with 70 inches of concrete below. These results were the basis for a change in the bar position reduction factor in the 1989 ACI 318 Building Code. Bar size did not seem to change the effects of reduction due to casting position.

2.2 ACI COMMITTEE 408

The American Concrete Institute (ACI) Committee 408 – Bond and Development of Reinforcement was originally organized in 1930. In 1997, the Committee adopted the mission to: *Develop and report information, and develop and maintain standards for analysis and design of concrete structures as influenced by bond, development, and anchorage of reinforcement.* The committee's current goals include development of recommended design procedures for development and splicing bars in tension, and to produce a state-of-the-art report on the topic. The committee has produced "Suggested Development, Splice, and Standard Hook Provisions for Deformed Bars in Tension" (ACI 408.1R-90); "State-of-the-Art Report: Bond Under Cyclic Loads" (ACI 408.2R-92) (Reapproved 1999). The committee has also adopted Provisional Standard "Splice and Development Length of High Relative Rib Area Reinforcing Bars in Tension (ITG-2-98)" which was developed and produced by the TTTC Innovative Task Group 2. This document became ACI 408.3-01 and Commentary, ACI 408.3R-01. Furthermore, the committee has produced *Bond and Development of Reinforcement - A Tribute to Peter Gergely, SP-180,* and has sponsored several sessions at ACI conventions covering topics related to state-of-the-art practices and models, and practical problems related to bond.

In 1966 the ACI Committee 408 reviewed the knowledge available at that time. A significant conclusion was that, since bond strength usually fails with cracking of the member, which is related to the tensile strength of the concrete, it was not unexpected that bond strength seems to vary approximately linearly with the square root of f'_c. This agrees

with work done by Ferguson and Thompson one year before. Another conclusion from this report was that pinching stresses at reaction locations tend to produce confining stresses which tend to increase bond strength. This report concluded that since bond stress has such an extreme variability it is better to look at an average of bond stresses or strengths rather than an individual test. A very important finding was also the fact that when bars are cut off in tension zones large stress concentrations occur and the shear strength in that location is significantly reduced.

The ACI Committee 408 produced a report investigating the behavior of bond under cyclic loads (1992). There are two types of cyclic loads. The first is called "low cycle" and are loads that contain only a few cycles, but develop very large bond stresses. Low cycle loads are often caused by earthquake loads or in high wind loads. The second type of cyclic load is called "high cycle", these contain loads that have a high frequency, but low bond stresses, similar to what is often thought of as vibration. These high cycle loads are generally seen in bridge members or members supporting vibrating machinery. High cycle loads were the focus of this report. High cycle loading is usually a dilemma at service levels compared to low cycle loading which usually is problematic for ultimate loading conditions. This report observed that concrete structures are typically not subjected to stress reversals under high cycle loading. High cycle loading typically produces low stresses, usually between 25-30% of the yield stress. Because of this and the fact that anchor lengths are usually long in bridge type structures bond failure in high cycle loading is rare. A major conclusion from this report was that if the bond does not fail by a fatigue failure then this type of loading does not adversely affect the stress-slip relationship near ultimate loading compared to the stress-slip relationship for a statically loaded member. They also concluded that friction and adhesion play a greater role in members where splitting is the failure mechanism.

2.3 Epoxy Coated Reinforcing

David Johnston and Paul Zia (1980) conducted a study of bond for epoxy coated bars. They used a beam end test similar to the ASTM A944 test used today. The specimen size was 15 inches deep, 8-in. wide, and 36-in. long. The tests were static loads as well as a dynamic loading. From the dynamic load tests they concluded that there was little difference in bond characteristics when compared to the static load tests. They found that the first cycle

difference found for epoxy coated bars became negligible when the number of cycles increased. Results were similar to other tests conducted on epoxy coated bars, that is a required 20% to 30% increase in the required development length.

Treece and Jirsa (1989) studied the bond strength of epoxy coated reinforcing. At that time epoxy bars were being used in virtually all forms of construction as a method of corrosion control for standard reinforcing bars. It was thought that the epoxy coating could adversely affect bond. In the study, 21 beam lap splice specimens were tested in areas of constant moment and the bond strength of epoxy coated bars were compared to uncoated bars. The test setup was such that the bond would fail by splitting of the concrete rather than pullout. In this manner of setup the bond stress could be found directly from the steel stress rather than having to look at a shear failure in the concrete for the pullout case. In the report, they referred to the critical bond stress as the lesser of the bond stress that was developed corresponding to the loaded-end slip of 0.01-in, or to a free-end slip of 0.002-in. For the final results of the tests free end slip measurements were used. They also made a note to emphasize that bond stress at 0.002-in is not the ultimate bond stress that the bar would develop, this is the bond stress that developed for a certain length below the required development length that would bring the bond stress up to ultimate. Epoxy coated bars were found to develop 17% less stress than the uncoated bars. With the epoxy coated bars, it was found that after cracks developed there was little increase in the load to failure, whereas with the uncoated bars there was a significant increase in load after cracks appeared before failure. No concrete dust was found on the epoxy coated bars after failure, and the epoxy-coated bars did not appear to crush the concrete against the rib deformations as would normally be found on uncoated bars.

The effects of bar deformation patterns and the reduction of bond of epoxy coated bars was studied by Choi et al (1990a). Three different types of deformation patterns were tested, designated type S, C, and N. Type S had patterns that were perpendicular to the axis of the bar, type C had deformations that were at an angle of 60 deg. to the axis of the bar, and type N had deformations that were at an angle of 70 deg. to the axis of the bar. Similar to Treece and Jirsa (1989), they found that the epoxy-coated bars had no concrete powder from the wedges sticking to the ribs. The effect of epoxy coating was found to vary considerably with

deformation pattern. For the three bar sizes that were tested (No. 5, No. 6 and No. 8), the S pattern was affected the most. The ratio of coated bar bond strength to uncoated bar bond strength for the C and the N patterns were very close for the No. 6 and No. 5 bars. Also, it was observed that the smaller bars were affected, on the average, greater than the larger bars. It was found that as the relative rib area increased the effects of epoxy coating decreased.

The effects of epoxy coating have also been investigated for splices (Hester, 1990). The investigation found that, as with development length tests, the epoxy coated splice lap was weaker. It was recommended that the uncoated bar equation be multiplied by a factor of 1.35 for the ACI Building Code, and 1.20 for the AASHTO Bridge Specification for bars with transverse reinforcement. The increase in bond strength due to transverse reinforcement was found to be roughly the same for both coated and uncoated reinforcing.

Choi et al (1990b) studied the effects of various parameters on bond strength. The parameters studied included epoxy-coating thickness, deformation pattern, bar size, concrete cover, and casting position. The testing method, beam end specimens, was similar to the proposed testing method of this study, 9-in. wide, 24-in. long, with 15-in. of concrete above the bars. Failure was assumed when the slip at the unloaded end of the bar reached 0.002 inches. It was again found that bond strength was reduced with the application of epoxy coating. However, the reduction in bond was greater for No. 5 bars and smaller, whereas the epoxy coating had little affect for No. 6 bars and larger. This confirmed the findings of Choi et al (1990a) in that the bond strength reduction was found to be less for bars with larger rib bearing areas. The bond strength increased as the concrete cover increased, as seen by Luke et al. (1981), but the decrease in bond due to epoxy coating was independent of the concrete cover. Hadje-Ghaffari et al (1991) confirmed the results of previous research and was similar in all aspects to Choi et al (1990a).

French et al (1992) studied bond behavior of uncoated and epoxy coated reinforcing was for the following parameters: concrete strength (6, 10, 12, and 14 ksi), the addition of micro silica to concrete (6, 10, 12, and 14 ksi), and bar size (No. 6, 8, and 11). This test was the first time that strain distribution in epoxy coated reinforcing had been measured. The testing method that was used was a beam end test, similar to those used by Choi et al (1990a,

1990b) and Hadje-Ghaffari et al (1991), which is similar to ASTM A944, the standard test for comparing bond strength. The new phenomenon that was found was that epoxy coated bars has different strain distributions than uncoated bars for low bar stresses and near bond failure. At low bar stress the epoxy-coated bars developed the same load as the uncoated bars, but over a much longer length. Near failure, the epoxy coated bars showed less strain in the bar than the uncoated bars. This was due to the fact that the epoxy-coated bars were unable to resist slip, which caused the strain in the epoxy-coated bars to be relieved.

2.4 Effect of Deformation Pattern

Darwin and Graham (1993) released a report on the effects of deformation height and spacing on bond strength. Bars were machined to 1-in. diameter in the investigation with deformation heights of 0.05, 0.075, and 0.10 and deformation spacings ranging from 0.26 to 2.2-in. These combinations produced relative rib areas of 0.20, 0.10, and 0.05 for each deformation height. "Conventional" reinforcing bars were also studied, which had a relative rib area of 0.07. Bond was studied using standard beam end tests similar specifications for bond tests given by ASTM A944. The variables of confinement were: 2-in. cover without transverse reinforcement, 2-in. with transverse reinforcement, and 3-in. cover without transverse reinforcement. Bars with 2-in. cover had an initial unbonded length of ½-in. and a bonded length of 12-in. Bars with 3-in. cover had an initial unbonded length of 4-in. and a bonded length of 8½-in. It was found that bond strength is a function of relative rib area of the bars, independent of the specific combination of rib height and rib spacing, for conditions in which confinement inhibits specimen cracking. Under conditions where the bar confinement was small enough so that bond failed by splitting of the concrete, the bond strength was found to be independent of deformation pattern. Where the cover was enough so that the bond failed in pullout, the bond strength was found to increase with the increase of relative rib area. The observed relationships between deformation pattern, degree of confinement, and bond strength appear to explain the large scatter obtained in earlier splice and development tests for bars that are confined by transverse reinforcement.

Darwin and Tholen (1996) again studied the effects of deformation properties on bond strength. Beam end tests were used to investigate the effects of bar size, relative rib area, and the ratio of rib width (measured parallel to the longitudinal axis of the bar) to center-to-

center spacing on bond strength. One hundred thirty-nine (139) specimens containing bars with relative rib areas, R_r, ranging from 0.05 to 0.28 were tested both with and without transverse stirrup confining the test bar. Finite elements were also used to model and study the fundamental behavior of bond. Bond strength was not affected by R_r for bars not confined by transverse stirrups, but increased as bar size and R_r increase for bars confined by transverse stirrups. Bond strength decreased when the ratio of rib width to center-to-center rib spacing was greater than 0.45. Under all conditions of confinement, epoxy coating had a less detrimental effect on splice length of high relative rib areas than on the splice length of conventional bars, which had a relative rib of 0.0727. This confirms the findings of Choi et al (1990a and 1990b). For the uncoated bars, deformation properties did not affect the splice length for relative rib areas of 0.065 all the way up to relative rib areas of 0.140. From the finite element analysis the relationship between bond strength and the product of embedded length and cover to the center of the bar was found to be nearly linear. They also found from this analysis that the increase in bond strength is not in proportion to the increase in embedded length.

2.5 OTHER BOND RELATIONSHIPS

In 1993 Darwin et al performed a reliability strength study of bond using a Monte Carlo statistical analysis. From this study they produced a bond relationship (Equation 2-3) that yielded very accurate tensile bond strength values compared to the bond tests that they were studying. The equation produces a mean test to prediction ratio of 1.00 with a coefficient of variation of 0.107 for beams with no transverse reinforcement and a mean test to prediction ratio of 1.01 with a coefficient of variation of 0.125 for beam with transverse reinforcement.

$$l_{dDARWIN} = \frac{\frac{f_s}{f'^{\frac{1}{4}}_c} - 2130 \cdot \left(.1 \cdot \frac{c_M}{c_m} + .9 \right)}{80.2 \cdot \left(\frac{c + K_{tr}}{d_b} \right)} \qquad \textbf{Equation 2-3}$$

Where: d_b = Diameter of bar being tested or developed.
f_s = Steel stress at bond failure.
f'_c = Compressive strength of concrete.
c_{so}, c_b= Side cover or bottom cover of reinforcing bars.
c_s = min(c_{si}+0.25-in., or c_{so}.)
c_M = Maximum value of c_s or c_b.
c_m = Minimum value of c_s or c_b.
K_{tr} = Transverse reinforcement index = $\frac{35.3 \cdot t_r \cdot t_d \cdot A_{tr}}{s \cdot n}$
A_{tr} = Total area of transverse reinforcement within the spacing s which crosses the plane of splitting through the center of the bar being tested or developed.
R_r = Relative rib area, ratio of projected rib area normal to bar axis to the product of the nominal bar perimeter and the center to center rib spacing.
t_r = $9.6 \cdot R_r + 0.28$
t_d = $0.72 \cdot d_b + 0.28$
s = Spacing of transverse reinforcement.
n = Number of bars being developed along the splitting plane.

In practice, design codes contain equations for tensile bond strength in the form of development length. Development length is the required embedment length of a particular reinforcing bar into concrete that will result in yielding of the bar before the bar pulls out. The two most commonly used code development length equations are found in the ACI 318-99 Building Code Requirements for Structural Concrete and the AASHTO Standard Specifications for Highway Bridges code. The ACI 318-99 Building Code development length equation can be seen in Equation 2-4 and the AASHTO Standard Specifications equation can be seen in Equation 2-5.

$$l_{dACI} = \frac{3}{40} \cdot d_b \cdot \frac{f_y}{\sqrt{f'_c}} \cdot \frac{\alpha \cdot \beta \cdot \lambda \cdot \gamma}{\left(\frac{c + K_{tr}}{d_b}\right)} \qquad \textbf{Equation 2-4}$$

Where: d_b = Diameter of bar.
f_y = Yield stress of the bar being tested.
f'_c = Compressive strength of concrete.
c = Shortest distance of either clear cover to the bottom, side cover, or half the distance to the next adjacent bar.
α = Reinforcement location factor.
β = Coating factor.
γ = Reinforcement size factor.
λ = Lightweight aggregate concrete factor.

K_{tr} = Transverse reinforcement index = $\dfrac{A_{tr} \cdot f_{yt}}{1500 \cdot s \cdot n}$

A_{tr} = Total area of transverse reinforcement within the spacing s which crosses the plane of splitting through the center of the bar being tested or developed.

f_{yt} = Yield strength of transverse reinforcement.

s = Center to center spacing of horizontal reinforcement.

n = Number of bars being developed.

$$l_{dAASHTO} = \frac{0.04 \cdot A_b \cdot f_y}{\sqrt{f'_c}} \cdot \alpha \cdot \beta \cdot \lambda \cdot \gamma \qquad \textbf{Equation 2-5}$$

Where: f'_c = Compressive strength of concrete.

A_b = Area of bar being developed.

f_y = Yield stress of the bar being tested.

α = Reinforcement location factor.

β = Coating factor.

γ = Reinforcement size factor.

λ = Lightweight aggregate concrete factor.

2.6 REVIEW OF BOND TEST SPECIMENS

There are three types of tests that are generally used to determine bond strength in tension: pullout test, beam-end tests, and lap-splice tests. In pullout tests the bar to be tested is cast in the center of a concrete block. The bar is then pulled out of the block with the reactive force acting on the face of the block (see Figure 2-3). This reaction causes compressive stresses in the concrete surrounding the bar, which are not representative of an actual beam. These compressive stresses cause a clamping effect on the bar thus this type of test often yields higher bond strength values compared to actual field bond values. This test is useful because of the size of the concrete specimen. The concrete block that the bar is embedded can be as small as 6-in. in diameter and 8 to 10-in. long. However, the disadvantage of the clamping compressive stresses often outweighs this advantage.

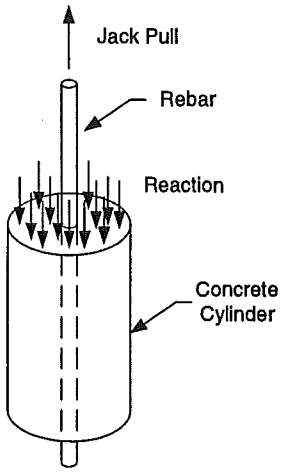

Figure 2-3: Pullout Test

The beam-end test (also referred to as the semi-beam test) is the method currently specified under ASTM A944. This test involves taking a small section of a beam and simulating the forces that would be seen if it were a whole beam (discussed in detail in upcoming sections and shown in Figure 2-4 and Figure 2-5). This test models the stresses in an actual beam much better than the pullout test. The size of specimen as specified by ASTM A944 is 24-in. long, 8-in. plus the diameter of the bar wide, and the depth is at least the concrete cover plus the embedment length plus the diameter of the bar. The disadvantage of this test is the size; typical specimens weigh up to 350 pounds.

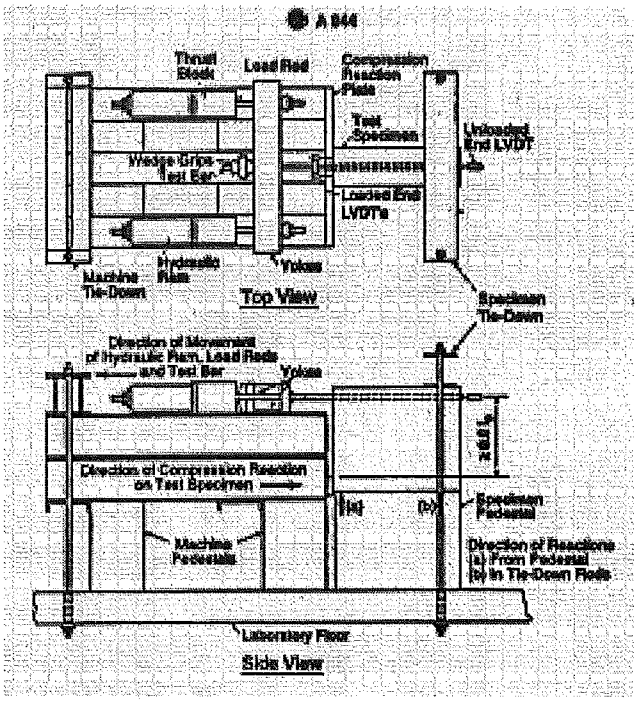

Figure 2-4: ASTM A944 Specimen Testing Configuration (ASTM A944, 1996)

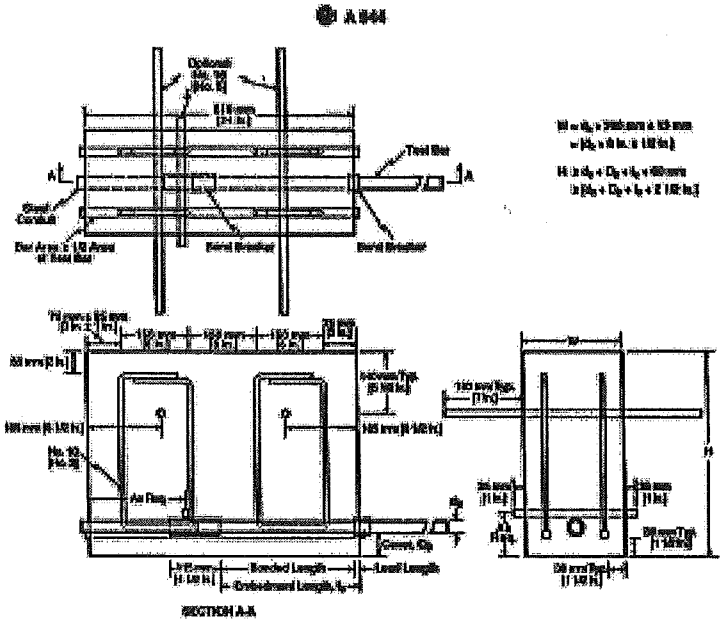

Figure 2-5: ASTM A944 Specimen Geometry and Reinforcement

The lap-splice test consists of a full-scale beam with two point loads applied at cantilevered ends on each side of the beam, see Figure 2-6. This loading causes an area of constant moment and zero shear in the area where the bars are being tested. The bars are spliced in the middle of the beam where the splice length is such that the beam will fail in bond. From the load at failure, the force in the bars can be calculated from simple beam mechanics. Also, the bond stress can be calculated from the force in the bar. The advantage of this test is the fact that it simulates beam stresses exactly. The obvious disadvantage of this test is the size. Typical beams are 8 to 10-in. wide, 12-in. deep, and span between 5 to 10 feet.

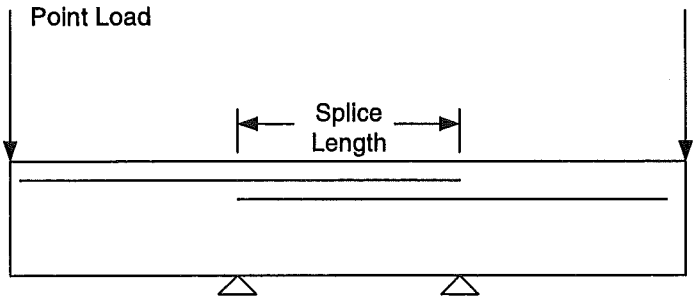

Figure 2-6: Lap-Splice Test

2.7 BOND TEST SPECIMEN

Although several bond specimens have been used in previous research regarding bond, a recent study conducted at Michigan Technological University (Foo, 1998) evaluated the behavior of a version of the commonly used semi-beam specimen (ASTM A944) that is smaller in size compared to past studies. The resulting specimen was easier to handle, less expensive to make, and easier to dispose. The test data compared well to the equation developed by Orangun, et al (1977) which is the basis for the current development length equation for the ACI 318-99 Building Code (1999) and the AASHTO 16th ed. Standard Specifications (1996).

A schematic of the semi-beam test specimen used in this study is shown in Figure 2-7. This set-up represents a beam in flexure (shown as a free-body diagram with a support reaction R_1) whereas the bar stress is induced from external loading and an internal moment couple develops between the bar in tension and the concrete in compression near the top of the beam (R_2). In this set-up, the bar stress is created from a jacking force of the test machine

and the testing jig applies the remaining reactions (the reaction R_3 is required for equilibrium). Debonded zones are used for two reasons. A debonded lead length at the pull end eliminates coning failures and reduces surface stresses that do not exist in a full beam specimen. The debonded length at the free end reduces effects of confining pressures from the support reaction while also allowing for the bonded length to be varied such that the development length can be accurately determined. Debond zones are created by wrapping plastic or some similar material around the bar so that the concrete does not come into contact with the reinforcing bar.

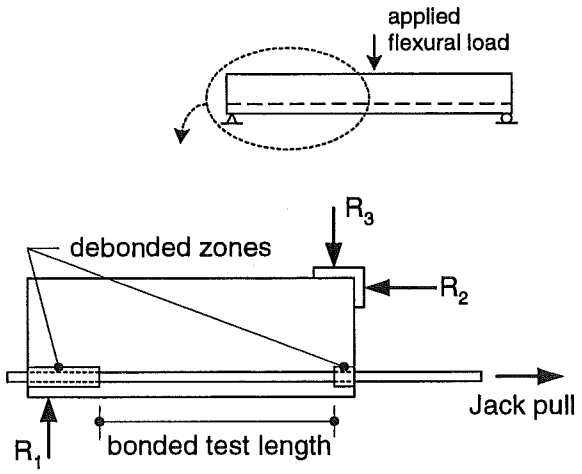

Figure 2-7: Semi-Beam Test Specimen

Figure 2-8 depicts the test specimen in the testing apparatus that has been designed and built to fit within the testing machine constraints. The lower cross-head will move down to apply a vertical bar force.

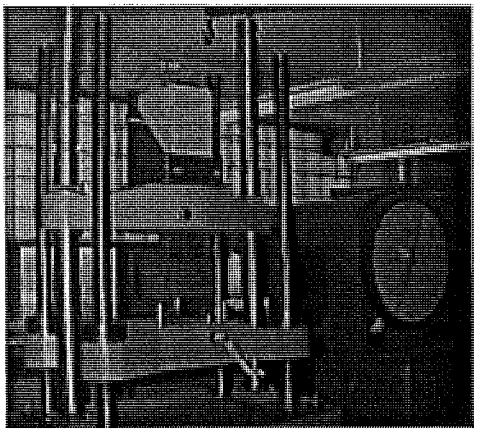

Figure 2-8: Specimen Configuration in Loading Jig

CHAPTER 3: EXPERIMENTAL PROGRAM

3.1 GENERAL

This chapter explains the experimental rationale used to test bond strength of the various bars in this study over a specific bonded length range of 4-in to 12-in. Beam end specimens used were similar to ASTM A944 specimen configuration and based on research by Foo (1998). Foo researched bond failures in a test specimen with reduced section area that produced comparable results with the OJB equation. Load and free end displacement were recorded using a Megadec 3016AC Data Acquisition device manufactured by OPTIM Electronics which was controlled by TCS for Windows, version 3.2.0, developed by OPTIM Electronics. Free end displacement was measured using a Sensotec LVDT (Linear Variable Differential Transformer) with a range of ± 0.1-in. The data acquisition system was set up to sample at a rate of ten data points per second.

Each specimen was identified with a specific specimen label in the following manner:

$ =	B for normal Black Bars S for stainless 316LN bars D for duplex type 2205 stainless bars
# =	4 for No. 4 bars 6 for No. 6 bars
** =	04, etc. for bonded length
&&& =	619, etc. for date specimens were casted
@@ =	01, etc. for specimen number

Specimen Label: $#-**-&&&-@@

Table 3-1: Specimen Label Key

For example, a specimen poured on the 25th of June, third one tested, number four stainless type 316LN, with four inches of bonded length would be labeled as follows: S4-04-625-03.

3.2 TEST VARIABLES

The primary variables in the tests were the bar size (diameter), bond length, and type of bar (conventional carbon bar ASTM A615 Gr. 60, stainless type 316LN and stainless type 2205 Duplex). The concrete strength was forecasted to be 4500 psi according to the MDOT grade D mix that is used in most bridge decks.

3.3 MATERIALS

All materials used in the tests are discussed in this section.

3.3.1 Reinforcing Bars

Three types of bars were tested in this study, conventional carbon bar (A615 Gr. 60), and two types of stainless bar (type 316LN, and Duplex type 2205). Carbon bar shall be referred to as black bar for the remainder of this report. Relative rib area as defined in Section 2.1 was measured by taking four random measurements for each of the variables used to compute R_r. The mean from these measurements was used to compute R_r for each of the different bar types and sizes, which can be seen in Table 3-2. While it has been shown (Darwin and Tholen, 1996) that the relative rib area of bars tested for bond in the configuration used in this study has no influence on bond strength, these measurements are included for completeness.

	#4 Black	#4 Stainless	#4 Duplex	#6 Black	#6 Stainless	#6 Duplex
Relative Rib Area	0.0992	0.1083	0.0865	0.1728	0.1008	0.1156

Table 3-2: Measured Relative Rib Area

From a visual inspection performed on the surface condition of the bars there was little difference found. Neither the black bar nor both types of stainless appeared to have mill scale remaining on their respective surfaces. Mill scale is a metallic "dust" typically remaining on the bar surface after the rolling process unless the surface is blasted clean. From comparisons of the two stainless bars, the Duplex bar appeared to have a shinier and smoother surface than the 316LN bars. This was due to the higher chromium content (discussed in Section 3.3.1.3) found in the Duplex bars. The higher chromium content of the Duplex bars resulted in the Duplex bars having the highest cost out all three types of bars. The second most expensive bar type was the stainless 316LN. Reinforcing bar cost data can be seen in Table 3-3. Supplier information for the bars used in this study is also included in the table. Suppliers indicated that these were standard costs and were not increased because of the small quantities ordered for this study.

Rebar Type	Supplier	Cost		S&H
		No. 4	No. 6	
Black Bar A615, Gr.60	Moyle Concrete Building Supply Houghton, MI Contact: 906-482-3042	$0.22/lb ($0.49/kg)	$0.22/lb ($0.49/kg)	local - no charge $15 cut
Stainless Type 316LN	Empire Specialty Steel Inc. Dunkirk, NY *out of business as of 7/1/01	$1.85/lb ($4.08/kg)	$1.85/lb ($4.08/kg)	~$175
Stainless Duplex Type 2205	Denman & Davis Slatersville, RI Tom Proulx, 401-767-0011	$5.28/lb ($11.64/kg)	$5.96/lb ($13.14/kg)	~$290

Table 3-3: Rebar Cost and Supplier Data

3.3.1.1 Yield Tests

The yield strength for all bars was tested in the Tinius Olsen testing machine, see Figure 3-1.

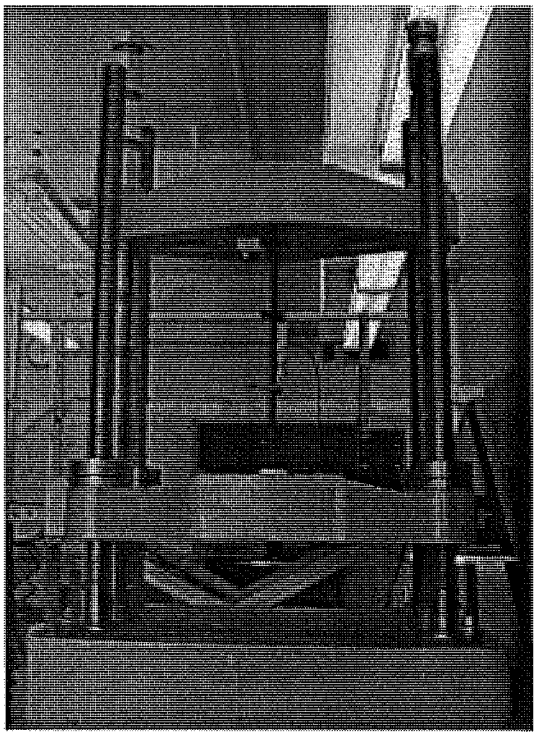

Figure 3-1: Rebar Tensile Yield Test Set-up

The Tinius Olsen is a screw-type driven machine that is primarily used to create tensile forces.

Bars were loaded in the machine with jaw style grips at the top and bottom heads of the machine anchoring the bar as the force was applied. Yield testing was done at a rate of 20000 psi/min according to ASTM A370 section 11.4.3. The LVDT was connected to an aluminum bar via a wormgear hose clamp, see Figure 3-2.

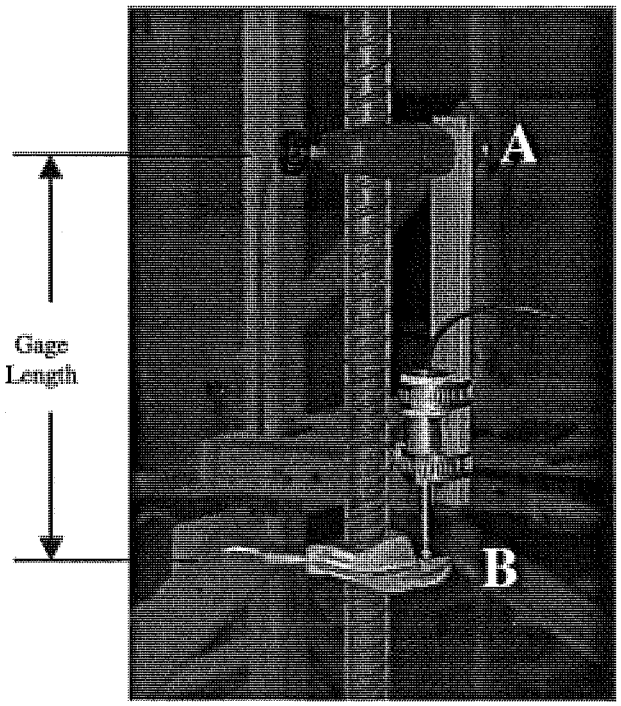

Figure 3-2: Tensile Yield Test LVDT Configuration

The aluminum bar was bolted to a pipe clamp that was attached to the rebar specimen at point A. The floater end of the LVDT was pushing against another pipe clamp with one side ground flat at point B. ASTM A370, annex 9, states that bars tested for yield strength should have a gage length of 8-in. The 8-in. gage length was measured to be between the centerline of the bolts of the two pipe clamps. In Figure 3-2 that is approximately the centerline of the two finger fasteners in the left of the figure.

Eight random bars were yield tested for each material type, four of each size. The mean yield strength, using a 0.2% offset is what shall be henceforth referred to as the yield strength. The offset was based off the point where the straight line section of the stress-strain curve intersected the x-axis to eliminate grip seating effects, not offset from the origin. This is in accordance with ASTM A370, section 13.2.1.

3.3.1.2 Black Rebar

Black bar was used as a control to verify the test set-up and to compare similar bonded lengths of the different type bars. All black bar used met ASTM A615 requirements and was of Grade 60; 420 in metric. These specifications state that the Grade 60 bars must simply have a minimum yield strength of 60000 psi. They also state that the cross-sectional area for No. 4 bars must be 0.20-in^2 and 0.44-in^2 for the No. 6 bars. The black bars used also met ASTM A615 standards for deformation. The deformation measurements can be seen in Appendix A.

The yield strength for the black bars was found to be 65.8 ksi with a coefficient of variation of $\pm$ 1.24% for the No. 4 bars, and 62.5 ksi with a coefficient of variation of $\pm$ 0.48% for the No. 6 bar. The coefficient of variation, also denoted as V_x, is a normalized quantity based on the standard deviation and the mean. It is used to determine the imprecision in measurement due to sampling error, i.e., it is a relative measure of dispersion. V_x is calculated by taking the standard deviation (σ_x) and dividing by the mean (μ_x), see Equation 3-1. This produces a dimensionless quantity showing the variation as a percentage of the mean.

$$V_x = \frac{\sigma_x}{\mu_x} \qquad \textbf{Equation 3-1}$$

Where: σ_x = Standard deviation of data.
μ_x = Mean of data.

Yield test data can be seen in Table 3-4. Graphs from the yield testing can be seen in Appendix B.

	f_y, No. 4 bars		f_y, No. 6 bars	
	Mean (4 samples)	V_x	Mean (4 samples)	V_x
Black Bar A615 Gr. 60	65.8 ksi	$\pm$ 0.92%	62.5 ksi	$\pm$ 0.48%
Stainless 316LN	101.2 ksi	$\pm$ 11.94%	81.4 ksi	$\pm$ 3.37%
Stainless Duplex 2205	88.4 ksi	$\pm$ 1.27%	82.3 ksi	$\pm$ 0.61%

Table 3-4: Rebar Yield Data

3.3.1.3 Stainless Steel Rebar Type 316LN

Stainless steel is generally thought of as a single type of steel. In fact the term stainless refers to a group of metallic materials containing a minimum of 12% chromium (Cox et al). When metals are composed of this minimum level of chromium they produce a passive film, which in turn fights against corrosion. Other types of alloys can be added to provide different mechanical properties such as weldability, corrosion resistance, and other service properties. Stainless steels suitable for reinforcement in concrete structures generally fall into three categories, ferritic, ferritic-austentic, and austentic. Ferritic steels contain less than 17% chromium, ferritic-austentic (duplex) steels contain 22-28% chromium, and the austentic steels typically contain 18% chromium and 8% nickel. The stainless steels used in this study were stainless Type 316LN and Duplex type 2205. Stainless 316LN steel is classified as an austenitic steel, and the Duplex 2205 steel is classified as ferritic-austentic with 22% chromium and 5% nickel.

Stainless steel rebar, Type 316LN was selected to be studied primarily due to the fact that it is in the Michigan Department of Transportation Special Provisions for Reinforcement, Stainless Steel (1999) as a replacement for A615 black bars in corrosive environments. These bars met all requirements for ASTM A955M for yield strength and deformation patterns.

The bars were yield tested in the same manner as the black bars. Nine bars were tested total, five No. 4's and four No. 6's. The additional No. 4 bar was tested due to the large variability observed in the first four tests. The yield strength was found to be 101.2 ksi with a coefficient of variation of $\pm 11.94\%$ for the No. 4 bars, and 81.4 ksi with a V_x of $\pm 3.37\%$ for the No. 6 bars. The No. 4 bars were rolled from a different heat than the No. 6 bars, which explains the difference in yield strengths. See Appendix B for plots showing stress-strain curves of the yield tests. Yield test results for the 316LN bars can be seen in Table 3-4.

3.3.1.4 Duplex Stainless Rebar Type 2205

Type 2205 Duplex stainless steel rebar was selected because it is specified as an alternative to Type 316LN in the Michigan Department of Transportation Special Provisions for Reinforcement, Stainless Steel (1999). The bars were yield tested in the same manner as the

black bars and stainless bars. The yield strength of the bars was found to be 88.4 ksi for the No. 4 bars with a coefficient of variation of ± 1.27%. The yield strength of the No. 6 bars was 82.3 ksi with V_x equal to ± 0.61%. Yield test results for the Duplex bars can be seen in Table 3-4.

3.3.2 Concrete

The mix for all concrete used was MDOT Grade D, typical of that used in bridge deck construction. The concrete used for the test specimens was delivered by Moyle Construction, Houghton, MI and was typically delivered in 1½ cubic yard deliveries. A normal delivery made 56 test specimens plus 12 test cyclinders as well as air and slump tests. The predicted concrete strength was 4500-psi versus the resulting concrete strength of approximately 5500-psi. The specified mix can be seen and compared to the delivered mix in Table 3-5.

Mix	Date Cast	Cement (lbs/yd)	Coarse Aggregate (lbs/yd)	Fine Aggregate (lbs/yd)
MDOT, Grade D	--	*658 min.*	*1772*	*1237*
Batch 1	6-Jun-01	680	1792	1360
Batch 2	25-Jun-01	693	1773	1333
Batch 3	4-Sep-01	663	1787	1323
Batch 4	9-Oct-01	647	1822	1236

Table 3-5: Concrete Mix Data

3.3.2.1 Casting

The concrete was poured on four different occasions, June 6, June 25, September 5, and October 9, 2001. The delay in the third pour was due to the late procurement of the Duplex stainless bars. The concrete was poured outdoors into the forms that were placed on a flat parking lot. All pours typically took approximately half an hour each. Specimens were vibrated to consolidate the concrete using a normal construction type hand-held concrete vibrator. The concrete was screeded off to the top of the forms then finished using a hand trowel. After the tops of the specimens were finished the specimens were covered with polyethylene sheeting and then watered roughly once every two hours. The day of the second pour had temperatures around 90-deg. Due to the high temperatures of that day, the

specimens were watered for roughly five minutes repeated every half an hour with cold water and covered between waterings for the first 6 hours after casting.

On each pour cylinders were made according to ASTM C31, air content was measured according to ASTM C231, and slump was measured according to ASTM C143. Values for slump, air, and cylinder strength can be seen in Table 3-6. In all cases values were within the acceptable range as specified by MDOT Standard Specification for Construction.

Mix	Date Cast	Slump (in)	Air (%)	Compressive Strength (psi)
MDOT, Grade D	--	*0-3.5*	*6.5 ± 1.5*	*4500 min.*
Batch 1	6-Jun-01	2.5	5.5	5210
Batch 2	25-Jun-01	0.5	5.0	5458
Batch 3	4-Sep-01	2.5	5.5	5909
Batch 4	9-Oct-01	2.5	5.0	5500

Table 3-6: Concrete Results

3.3.2.2 Curing

As previously stated, the specimens were cured immediately after finishing the top surface by putting polyethylene sheeting over the specimens and watering them periodically. The day after the pour the specimen forms were stripped, and specimens were moved indoors where they were covered with plastic and burlap and watered 3 times per day to simulate a typical bridge deck field cure. After seven days the burlap and plastic covers were taken off the specimens as they continued to cure for an additional 21 days thus allowing the concrete to cure for a total of 28 days before being tested. The cylinders were taken to a 100% humidity room and left to cure until they were broken on the first day of bond testing and the last day of bond testing.

3.4 TEST SPECIMENS

3.4.1 Selected Bond Length

Bond stress varies along the length of a bar. The closer to the loaded end of the bar the higher the bond stresses. It has long been agreed upon that in order to get working bond

stresses with an associated bond length a mean value for bond stress can be used. This mean bond stress equation can be seen in Equation 3-2.

$$u = \frac{A_b \cdot f_s}{l \cdot \pi \cdot d_b} \qquad \textbf{Equation 3-2}$$

Where u = Bond Stress.
d_b = Diameter of Bar.
f_s = Steel Stress at bond failure.
A_b = Area of the bar being developed.
l = Length of bar bonded or exposed to the concrete.

These mean bond stresses can be converted to working bond strength through equilibrium concepts. The working force in the bar can be found by taking the bond stress and multiplying by the area of the bar in contact with the surrounding concrete. In other words, simply multiply the equation through by the denominator to get the equation into a form where it can easily be seen that bond strength is equal to bar force.

Bond length was varied experimentally to determine the bond strength for comparison with predicted values. The predicted bond strength was based on the OJB equation (Equation 2-2) which has become one of the most recognized equations for predicting bond strength and is the basis of many design codes. The ACI Building Code (Equation 2-4) and the AASHTO 16th edition (Equation 2-5) were used to compare the actual bond strength with design code predictions. These comparisons can be seen in Chapter 4. It should be noted that the minimum bond length requirements as well as the resistance factors set by the two design codes were not taken into account. This was done because in experimental work the goal is to use equations that will be representative of the test data. If the equations utilized resistance factors the equations would have an inherent redundancy and not properly reflect the actual test data. The equation developed by Darwin et. al, 1995 (Equation 2-3) was also used to compare theoretical bond strength equations. The Darwin equation was formulated based on a reliability analysis using a Monte Carlo simulation and produces a mean test/predicted ratio of 1.01 for bars that are not confined by transverse reinforcement. Calculations using the four equations to compute theoretical bond strength for the bonded lengths used in this study can be found in Appendix C. These calculations were performed using the concrete strength from the first batch of specimens, i.e. 5210 psi.

The bar was debonded in two locations along the its length. The first location was at the face of the specimen to 1-in. into the specimen. This was done to try to eliminate tensile stresses along the free face of the specimen that do not exist in a full beam. After the selected length for the test was exposed, the bar was again debonded to the end of the bar. Figure 3-3 shows a typical specimen bond layout.

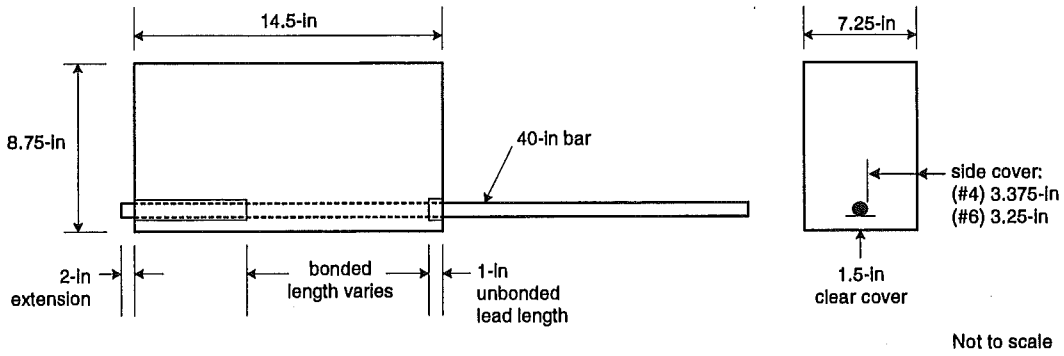

Figure 3-3: Debond Schematic with Specimen Dimensions

The bar was debonded using prestressing debond wrap from Prestress Supply Inc., in Lakeland, Florida. A 2-in. extension of the bar beyond the back face of the specimen was used for measuring free end displacement when the tests were taking place.

A matrix showing the bonded lengths used in this study can be seen in Table 3-7. Bold marks indicate bonded lengths that were used for comparative purposes between reinforcing bar material tyes. Non-bold marks indicate bonded lengths that were used simply to verify the linear relationship between bond strength and bonded length within a given bar type and size.

Bonded Length (in)	#4			#6		
	A615 Gr. 60	316LN	Duplex 2205	A615 Gr. 60	316LN	Duplex 2205
4	xx	xx	xx			
5				xx		
5.5	xx	xx	xx			
6				xx	xx	xx
6.5				xx		
7	xx					
8	xx	xx	xx	xx	xx	xx
8.5	xx					
10		xx	xx	xx	xx	xx
12				xx	xx	xx

Table 3-7: Test Specimen Matrix

The bonded lengths were selected to produce a range of tests along the stress curve in order to get a broader view of the bond strength as the stress in the bar increases. In order to confirm a linear relationship between bonded length and bond strength at least three points are needed. For test comparison purposes in the future, tests were also required to have similar bonded lengths.

3.4.2 Geometry

The specimen size was 14.5-in. long, 7.25-in. wide, and 8.75-in. tall (see Figure 3-3). The test was set up as a beam end specimen type. Clear cover for all tests was 1.5-in. This was selected so that the bond failure would be by cracking of the concrete caused by radial tensile stresses created by the bar sliding out of the concrete.

3.4.3 Form Work

Forms were made of ½-in. plywood sides and bottoms with ¾-in. plywood or particleboard ends. The forms were nailed together using 1.75-in. finishing nails. The inside of the forms were treated with Thompson's Water Sealer prior to use and were coated with hydraulic oil used to act as a form release agent the day of the pour. Meticulous care was taken to prevent the release agent from coming into contact with the test bar. The forms were stripped within 24 hours of castings, cleaned and reused.

3.5 TEST SETUP

3.5.1 Specimen Configuration

The specimens were positioned in such a manner so that they sat on the top cross-head (see Figure 2-8) in a self-resisting frame (see Figure 3-5). Specimens were loaded by hand into the self-resisting frame. The bar was then pulled out by the displacement of the bottom cross-head at a load rate of approximately 20000 psi per minute. No tests fell under the minimum three-minute requirement of ASTM A944. On the average, one test took between five and ten minutes.

3.5.2 Free End LVDT

Free end displacement was measured using the Sensotec LVDT with a range of ±.1-in. calibrated using a Mitutoyo micrometer with a precision of .00005-in. After calibration the LVDT had a precision reading of 9.5288×10^{-5}. See Appendix D for LVDT and load calibration data.

A steel angle was mounted to the specimen using five-minute quick set epoxy after the specimen was set in the resisting frame, plumbed and leveled. The epoxy was allowed to set until the angle was rigidly fixed to the specimen. Then the LVDT was mounted to the angle using a magnetic clamp. See Figure 3-4 for clarification.

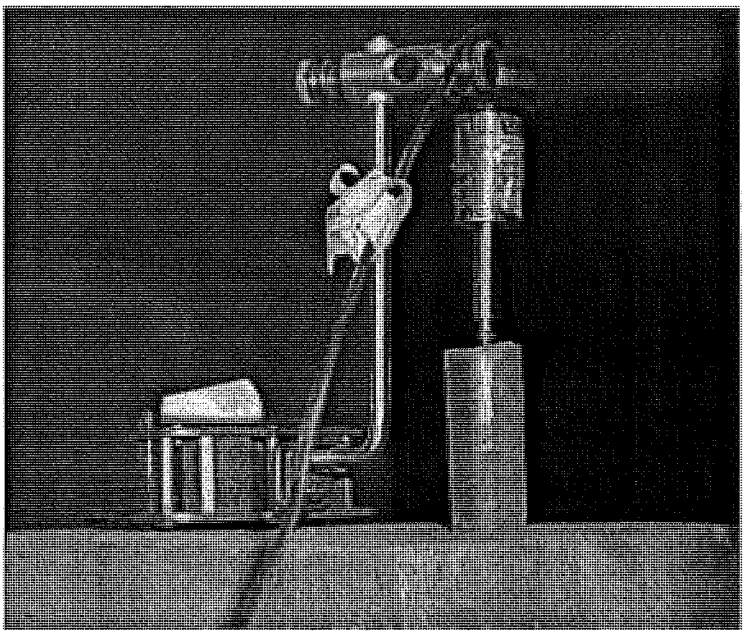

Figure 3-4: LVDT Mount Setup

3.5.3 Load Acquisition

The Tinius Olsen testing machine is outfitted with a dial gage for the four different load settings that it is equipped with. The Tinius Olsen machine is also capable of producing an output signal for the load in the form of resistance in ohms (Ω). This is accomplished by the use of an internal linear varying resistor. Load readings were taken and the resistance was recorded at each of the four different load settings to produce a calibration curve used to convert the signal from the machine to a usable load value in pounds.

3.5.4 Loading Frame

A self-resisting load frame was designed to create the desired flexural stresses within the specimen. The frame was made of steel (see Figure 3-5).

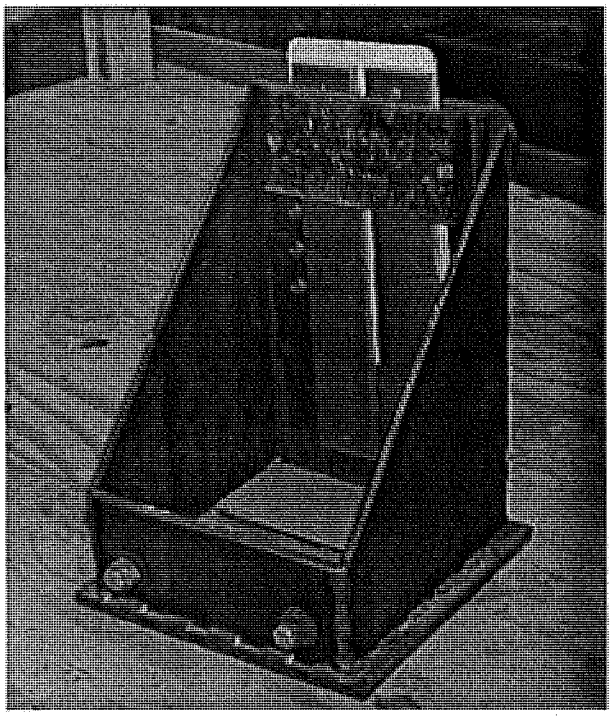

Figure 3-5: Self-Resisting Frame

Three reaction plates offset from the frame actually create the flexural stresses. These reactions as they occur on the specimen can be seen in Figure 3-6.

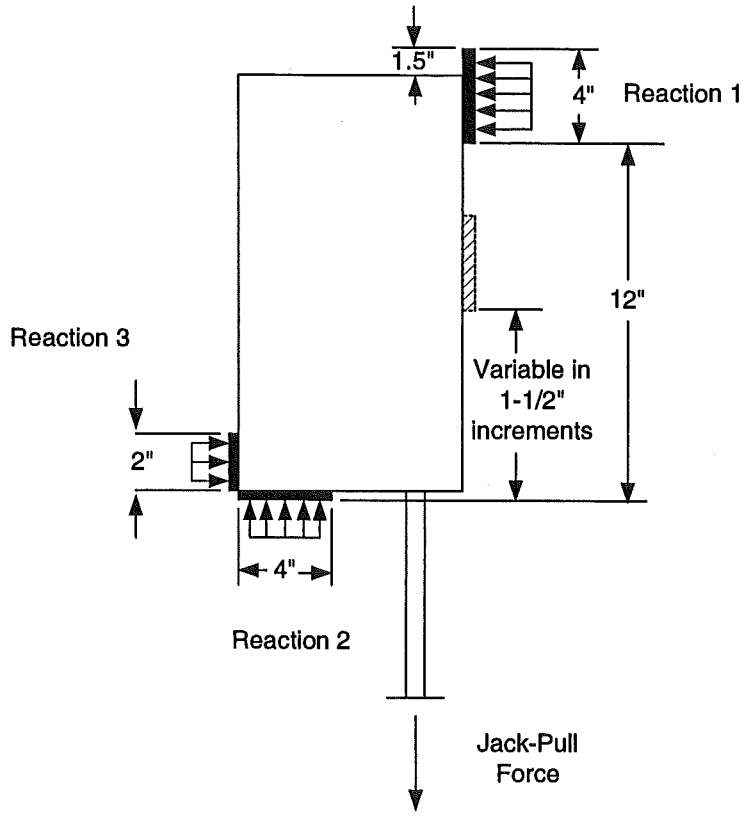

Figure 3-6: Reactions on Specimen

Discardable wood shims were used at the reaction plates to help distribute loads in locations where stress concentrations would be likely to occur due to disformity in the specimen. The wood shims were replaced after roughly 20 uses based on visual inspection of the shims.

During testing the upper reaction (Reaction 1) location was found to be crucial. The upper reaction plate was moveable such that the plate location could be adjusted in 1-½ inch increments. If the plate was located at too long of a distance the specimens were found to fail in flexure. More discussion of this plate location can be found in Chapter 4.

3.6 TEST PROCEDURE AND DATA MANIPULATION

As stated, specimens were loaded into the test frame by hand. Temporary scaffolding was built around the Tinius Olsen machine in order to accomplish this and make working with the specimen easier. After the test specimen was loaded, the angle was epoxied in the proper position. Whilst the epoxy was setting up the specimen was leveled and plumbed into exact

position and the data from the previous test was transferred from the Megadec system to the computer. After the epoxy was firm the LVDT was attached by means of the magnetic holding device. Next the Tinius was zeroed and the TCS software started recording the data. After the start of recording the jaws were set to grip the bar and the Tinius was turned on to start loading the specimen. The loading rate was approximately 20000 psi per minute. The test was considered finished when the load reached a plateau, when the free end displacement reached values in excess of 0.006-in., or when the specimen cracked in which case the free end displacement typically went in excess of 0.1-in. the instant the crack occurred. (Note that bond failure was defined at 0.002-in. of free-end displacement. However, specimens were tested beyond this displacement level to evaluate cracking patterns compared with other reported studies as noted in the literature review.) After the test was complete the specimen was lifted by hand out of the test frame, the next specimen was loaded into the testing jig and the whole process was repeated.

3.6.1 Data Smoothing

Load and free end displacement data was collected and transferred to computer. Due to the flutter, or noise from the LVDT, the raw data was smoothed using a running average of ten data points. This means that, for example, the data point corresponding to one second for the load-displacement plots is not just the one raw data point. This specific point is the mean of the next ten data points. Ten points were chosen simply because this would be one second data. This process continues for the next data point, in this example, 1.1 seconds, which would contain the mean of the next ten data points. Using this running averaging technique, data was not reduced, it was simply smoothed out. Below in Figure 3-7 are two contrasting plots showing the raw data next to the adjusted data for the test of B4-04-619-03.

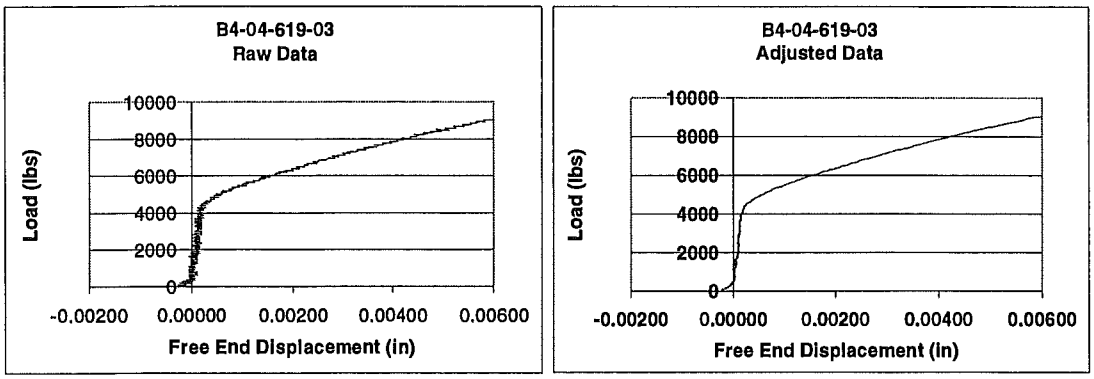

Figure 3-7: Raw vs. Adjusted Data Plots

3.6.2 Zero Offset

The zero load point had to be determined after the data was plotted. As shown in Figure 3-7, there was some initial slip at the beginning of the tests due to grip seating. This is seen in the initial 500 pounds of loading on the plots where the line is increasing in slope. Visual inspection of the plots led to the shifting of the zero point, or origin. The shift was such that if the line that had a virtually constant slope after all slip has been worked out of the system were to be extended, it would pass through the origin. Typical origin adjustments made were in the range of -0.00020 inches from the original data. Had these adjustments not been made, the failure loads (i.e., load at 0.002-in. of free end displacement) would have been lower than what they appear in Chapter 4 by approximately five percent.

3.6.3 Normalized Data

To allow comparison between bond strength in semi-beam specimens cast on different dates, data for later cast dates was normalized to the first casting. Three cylinders were broken on the first and last day of testing. The mean strength value of these two breaks was used to calculate the theoretical pullout value for each different bond length. For both types of stainless specimens the bond strength was normalized to compare with the bond strength of the control, i.e. the black bars. The normalized bond strength was calculated taking the square root of the mean of the first batch of specimens (cast 6/19/01), which was 5210 psi, divided by the actual concrete strength for the other batches, and multiplying this by the test bond strength. The equation form can be seen below in Equation 3-3. The value that was normalized was the failure load, or the load at 0.002-in.

$$NormalizedBond = \sqrt{5210 / f'_c} \cdot BondStrength \qquad \textbf{Equation 3-3}$$

As defined, the specimen name includes the date the specimen was cast. Bond strength data from any specimens that were cast on days different than the first batch has been normalized.

CHAPTER 4: EVALUATION OF EXPERIMENTAL RESULTS

In this chapter the experimental data will be looked at as each bar type individually, then compared with each other. Any observed differences will be described in detail.

Throughout the testing period large amounts of data were collected. The most efficient method to convey this data is in tabular form. Table 4-2 through Table 4-5 contains this data. Labels in the tables are as follows: The plate location column in the tables contains the distance, measured from the bottom of the self-reacting frame up to the bottom of the upper reaction plate, Reaction 1 (see Figure 3-6). The location of the upper reaction plate in the self-reacting frame was critical to obtain valid bond strength data. Further discussion of the significance of the plate location can be found in Section 4.2.2. Thus to get the distance from the loaded face of the specimen to the center of the reaction plate simply take the value given in the table and add 1½-in. to it. Most of the time the load from the Tinius Olsen had to be offset by 62.47 pounds. Occasionally the load had to be offset by 8.401 pounds. Regardless of the offset this is only a mere fraction of max load.

Throughout the tests the maximum load as measured from the Tinius Olsen machine was recorded in order to compare the maximum load as recorded by the MEGADEC data acquisition system. This load compared well with the data collected by the MEGADEC data acquisition system.

The bond failure load, or the column labeled "Load @ 0.002 in.", was observed in Microsoft Excel using the load-displacement graph for each test. After the graph was zeroed appropriately to eliminate grip-seating effects (see Section 3.6.2), the data point at 0.002-in. of free end displacement and the subsequent load was recorded in the tables. The normalized bond strength was calculated using Equation 3-3 (in Section 3.6.3). As stated above, the expected load was calculated using Equation 2-2, the OJB Equation. Appendix C contains theoretical bond strength calculations for the four bond relationships presented in Chapter 2. The "Percent Difference" column is the percent difference between the normalized load at failure (0.002-in. free end displacement) and the expected load with respect to the expected load. This was calculated by taking the failure load, subtracting the

expected load, then dividing the result by the expected load. See Equation 4-1 for clarification.

$$\%Difference = \left(\frac{NormalizedFailureLoad - ExpectedLoad}{ExpectedLoad} \right) \cdot 100 \qquad \textbf{Equation 4-1}$$

In the tables, the mean value is the mean for the valid data only. For example if a bar yielded there was no load at 0.002-in. Then the mean for that bonded length would not contain any value for bond strength since none existed and the mean of the remaining valid values would be shown in that specific mean location. Another example would be if there were flexural cracks before bond failure occurred, the mean value would not include this bond test. Also in the tables, the row labeled "Coeff. of Var." contains the coefficient of variation for the respective row.

The "Comments" column in all tables contains certain notes, observations, or conclusions from the tests. "Typical Failure" indicates that at the time of bond failure the bar had pulled out of the specimen without the specimen cracking. This type of failure exhibited specimen cracking at free end displacements in excess of 0.006-in. "Typical Crack" indicates the specimen revealed a bond failure crack at the point of bond failure. "Typical CrackA" indicates the specimen cracked after bond had failed but before the test was completed. "Bar Yielded" simply signifies the bar had yielded before bond failure could occur. "Flexural Crack" indicates that a flexural failure resulting in specimen cracking occurred before bond failure. Discussion of this failure mode can be found in Section 4.2.2. "Flexure CrackA" represents specimens that yielded flexural cracking after bond failure occurred. On occasion the recorder system failed to record data. In those instances "Observed" is indicated in the comments column. This simply means that the failure load was observed while the computer displayed the live test data.

4.1 COMPARISON OF DESIGN EQUATIONS

As stated in Chapter 3, all bond strength results were compared to design equations, which consisted of both the the AASHTO Standard Specifications (1996) (Equation 2-5) and the ACI 318-99 Building Code (Equation 2-4). In addition to being compared to the AASHTO

Code (Equation 2-5), the results were also compared to the theoretical OJB and Darwin equations (2-2 and 2-3, respectively). Plots showing the four different relationships can be seen in Figure 4-1 and Figure 4-2 plotted over the bonded length range tested. It is important to note that these figures represent predicted relationships based on previous research and are shown for comparative purposes. They do not incorporate test data herein. These figures show that for lower bonded lengths, and for the No. 4 bars, all the equations predict similar bar stress except for the ACI equation, which is approximately 22% lower than the other three equations. All four relationships have different slopes. Because of this the final predicted bar stress is different for all four relationships. At longer bonded lengths for No. 4 bars, the AASHTO equation predicts the strongest bond, then the OJB equation and the ACI equation are next both very close to each other, finally the Darwin equation predicts the lowest bond strength.

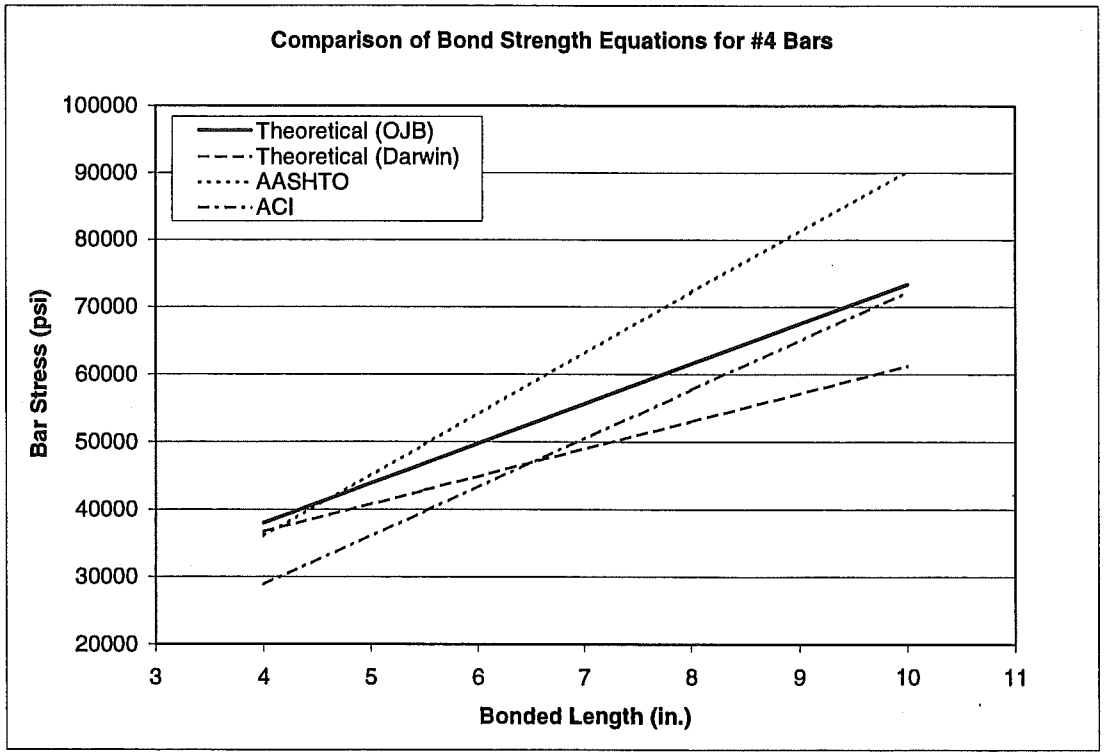

Figure 4-1: Comparison of Bond Strength Equations for No. 4 Bars

For the No. 6 bars, the predicted bond strengths are more scattered than the No. 4 bars at the lower end of the bonded length range. At the upper end of the bonded length range the

AASHTO equation again predicts the highest bar stress followed by the OJB and ACI equations and finally the Darwin equation. There is a somewhat closer relationship between the next two predictors, and then the Darwin predictor seems to be consistently less than the other three equations.

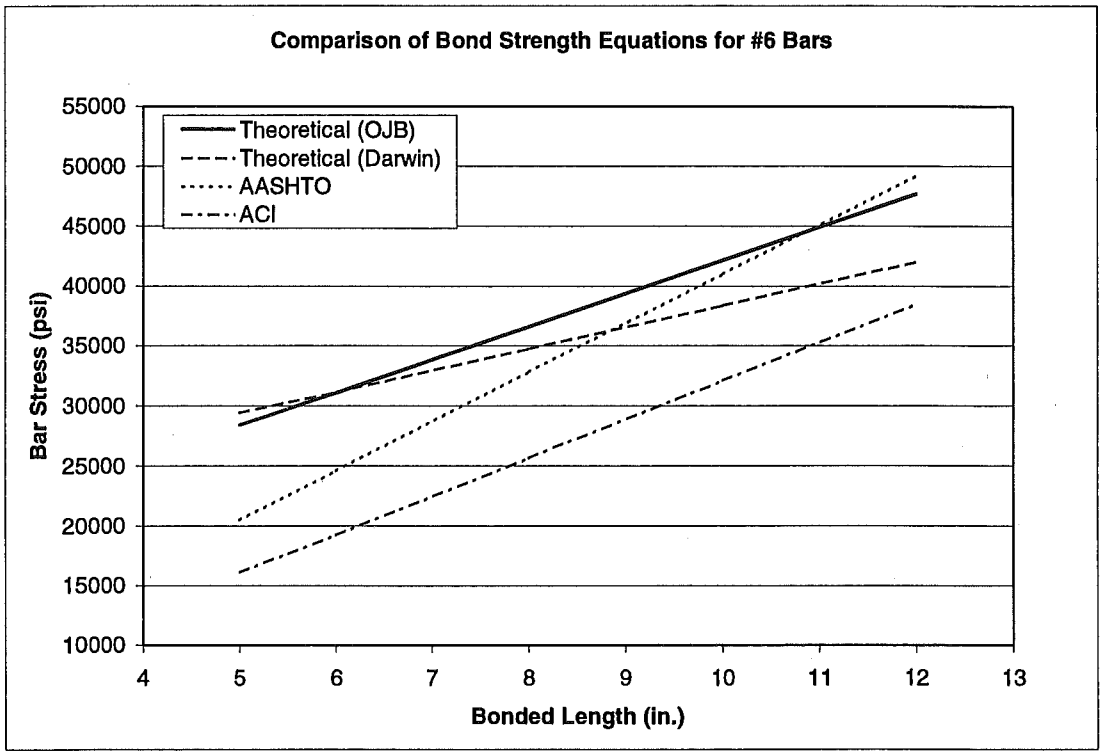

Figure 4-2: Comparison of Bond Strength Equations for No. 6 Bars

In design, development length is the term that refers to the required bonded length that would make the bar yield before bond failure occurred. In a design situation this would indicate that the Darwin predictor would be the most conservative by predicting longest development lengths whereas the AASHTO predictor would be the least conservative by predicting the shortest development lengths.

The development length of #4 and #6 bars for the four relationships, assuming 60-ksi steel and using the concrete strength from the black bar tests (5210-psi), can be seen in Table 4-1. Note that these are predicted lengths necessary to anchor the respective bar to achieve a yield stress of 60 ksi and do not represent data collected.

Development Lengths				
Bar Size	OJB	AASHTO	ACI	Darwin
#4	7.7-in	6.7-in	8.3-in	9.7-in
#6	16.4-in	14.6-in	18.7-in	21.9-in

Table 4-1: Development Lengths

From the tests, the only No. 4 bars that yielded were black bars with a bonded length of 8-in and 8.5-in. Of this bonded length over half the bars yielded before bond failure occurred and one specimen yielded as the bond failure point was reached during the test. This would indicate that either the ACI or the OJB equation produced the most accurate development length because by the Darwin equation the bars should not have yielded and by the AASHTO equation the bars should have yielded at the 7-in bonded length.

4.2 BLACK BAR RESULTS

Black bars, A615 Gr. 60, were used as a control to verify the test specimen with respect to bond strength equations and to compare the results from the tests involving other bar types. Black bars were chosen as a control because all equations that deal with tensile bond strength, as referred herein as bond strength, have been developed using black bars.

4.2.1 A615 Number 4 Bar Results

All the test data for the No. 4 black bars can be seen in Table 4-2. From the table it can be seen that overall the test bond strength was close to the theoretical OJB bond strength for each bonded length tested. It should be noted that the predicted bond strength, or expected load for a particular bond length, is based off of the OJB Equation (Equation 2-2) using the mean cylinder strength for the group being tested. Calculations for all expected loads for all bond lengths can be found in Appendix C. For the 4-in. bonded length the experimental bond strength was roughly 7% lower than the predicted bond strength of 7461-lb. The mean experimental bond strength was 6881-lb. with a coefficient of variation of $\pm$ 13.0%. The 5.5-in. bonded length had results that were very close to the predicted bond strength with the mean experimental bond strength, 9671-lb., being 5.2% higher than the predicted bond strength, 9195-lb. Despite this appearance of a close relation between experimental

and expected bond strength, the experimental bond strength had a large coefficient of variation of ± 19.8%. Both bonded lengths, 7-in. and 8.5-in., experienced bond failure approximately within 5% of the predicted bond strength. However, the 7-in. bonded length had much larger values for V_x than the 8.5-in. bonded length; ± 17.2% compared to ± 5.0% respectively. After the fourth pour, specimens were tested with bonded lengths of 8.0-in. This bonded length produced a normalized experimental bond strength of 12400-lb., which is 2.6% above the predicted bond strength. This bonded length had a coefficient of variation of ± 5.5%. Additional analysis is carried out in Section 4.5.1.

Specimen	Plate Location (in.)	Load @ .002 in. (lbs)	Normalized Bond Strength (lbs)	Expected Load (lbs)	Percent Difference	Comments
B4-04-619-01	12	5662	5662	7461	-24.11%	Typical Failure
B4-04-619-02	12	6939	6939	7461	-7.00%	Typical Failure
B4-04-619-03	12	6364	6364	7461	-14.70%	Typical Failure
B4-04-619-04	12	7924	7924	7461	6.21%	Typical Crack
B4-04-619-05	12	6947	6947	7461	-6.89%	Typical Failure
B4-04-619-06	12	8211	8211	7461	10.05%	Typical Failure
B4-04-619-07	12	6401	6401	7461	-14.21%	Typical Failure
Mean for 4" bond			*6921*		*-7.24%*	
Coeff. Of Var.			*0.1297*			
B4-05-619-01	12	--	--	9196	--	Recorder Malfunction
B4-05-619-02	12	11426	11426	9196	24.25%	Typical Failure
B4-05-619-03	12	10944	10944	9196	19.01%	Typical Failure
B4-05-619-04	12	10707	10707	9196	16.43%	Typical Failure
B4-05-619-05	12	7168	7168	9196	-22.05%	Typical Failure
B4-05-619-06	12	7394	7394	9196	-19.59%	Typical Failure
B4-05-619-07	12	8307	8307	9196	-9.67%	Typical Failure
B4-05-109-01	12	12072	11755	9196	27.78%	Typical Failure
Mean for 5.5" bond			*9671*		*5.17%*	
Coeff. Of Var.			*0.1982*			
B4-07-619-01	9	14601	14601	10931	33.58%	Typical Failure
B4-07-619-02	9	12226	12226	10931	11.85%	Typical Failure
B4-07-619-03	9	10480	10480	10931	-4.12%	Typical Failure
B4-07-619-04	12	10674	10674	10931	-2.35%	Typical Failure
B4-07-619-05	12	8834	8834	10931	-19.18%	Typical Failure
B4-07-619-06	12	--	--	10931	--	LVDT malfunction
B4-07-619-07	12	12285	12285	10931	12.39%	Typical Failure
Mean for 7" bond			*11517*		*5.36%*	
Coeff. Of Var.			*0.1719*			
B4-08-109-01	12	12246	11919	12418	-1.38%	Yield After Failure
B4-08-109-02	12	13234	12881	12418	6.57%	Yield After Failure
B4-08-109-03	12	--	--	12418	--	Bar Yield
B4-08-109-04	12	--	--	12418	--	Bar Yield
B4-08-109-05	12	--	--	12418	--	Bar Yield
B4-08-109-06	12	--	--	12418	--	Bar Yield
B4-08-109-07	12	--	--	12418	--	Bar Yield
Average for 8" bond			*12400*		*2.59%*	
Coeff. Of Var.			*0.0548*			

Table 4-2 continued on next page

continued from previous page

Specimen	Plate Location (in.)	Load @ .002 in. (lbs)	Normalized Bond Strength (lbs)	Expected Load (lbs)	Percent Difference	Comments
B4-08-619-01	12	--	--	12666	--	Bar Yielded
B4-08-619-02	12	13962	13962	12666	10.24%	Typical Failure
B4-08-619-03	12	12670	12670	12666	0.03%	Typical Failure
B4-08-619-04	12	--	--	12666	--	Bar Yielded
B4-08-619-05	12	--	--	12666	--	Bar Yielded
B4-08-619-06	12	13040	13040	12666	2.96%	Yielded @ .002-in.
B4-08-619-07	12	--	--	12666	--	Bar Yielded
Mean for 8.5" bond			*13224*		*4.41%*	
Coeff. of Var.			*0.0503*			

Table 4-2: No. 4 Black Bar A615 Test Results

Based on work done by Foo (1998), the load-displacement curve was expected to climb along the load axis until bond failed, at which point the curve would go horizontal. Visual inspection was done on the results of bond tests from: Tholen and Darwin (1996), Choi et al (1990A), Choi et al (1990B), Hadje-Ghaffari (1991), and French et al (1992). From this inspection it was deduced that a normal load-displacement curve looks very similar to the curves produced from this study. As stated before, the experimental specimens were designed with 1½-in. of clear cover on the bottom. This was originally done so that bond failure would be a cracking type of failure. In a cracking type of failure it has been shown that relative rib area, R_r, has no effect on bond strength. However, the failure modes observed in all No. 4 black bars initially revealed no cracking in the specimen at the time of defined bond failure, i.e. at a free end displacement of 0.002-in. After further studying the No. 4 black bar bond tests, this type of failure seems to be consistent with a cracking failure; had the tests been continued to a free end displacement greater than 0.006-in., the specimens would have experienced bond cracking. This is based on the similarities that exist between the load-displacement curves produced from this study compared to other bond studies. In one instance (B4-04-619-03) the bar was loaded well after bond failure. The load-displacement curve for this case with an extended free-end displacement scale can be seen in Figure 4-3. The free end displacement axis has been extended approximately ten times that of a typical load-displacement plot.

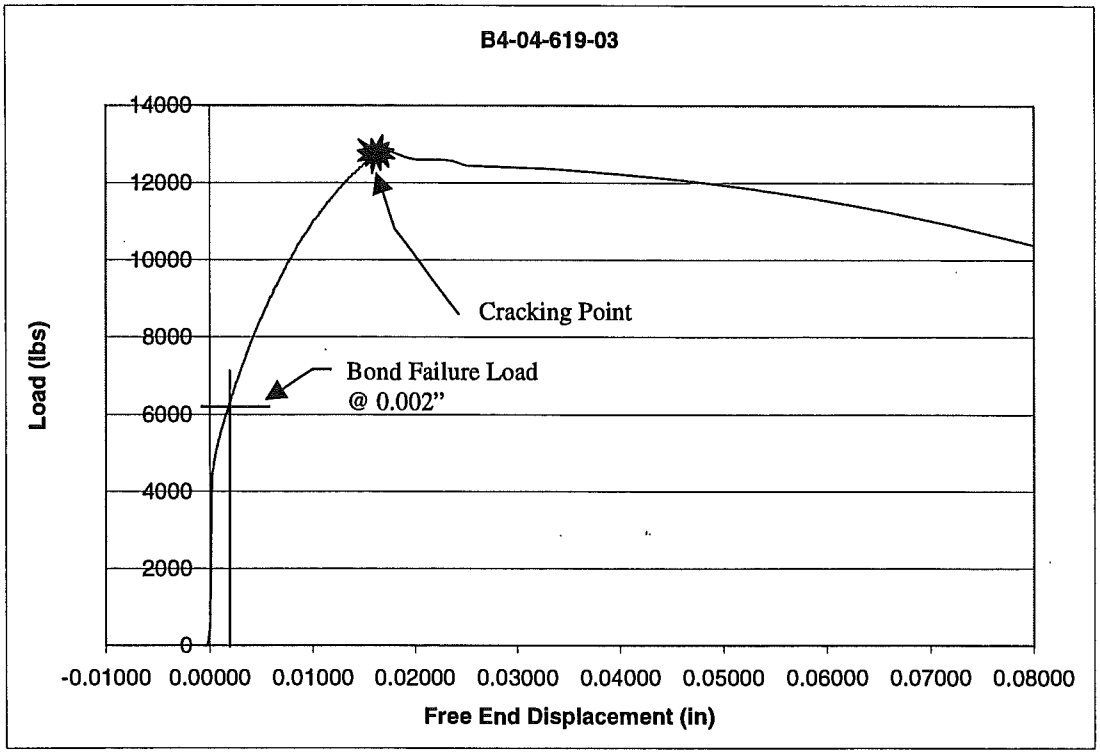

Figure 4-3: Load-Displacement Curve for B4-04-619-03, Extended Scale

Specimen B4-04-619-03 exhibited cracking patterns that were typical to bond cracking failure. This crack pattern as well as the load-displacement plot, with a typical scale, can be seen below in Figure 4-4.

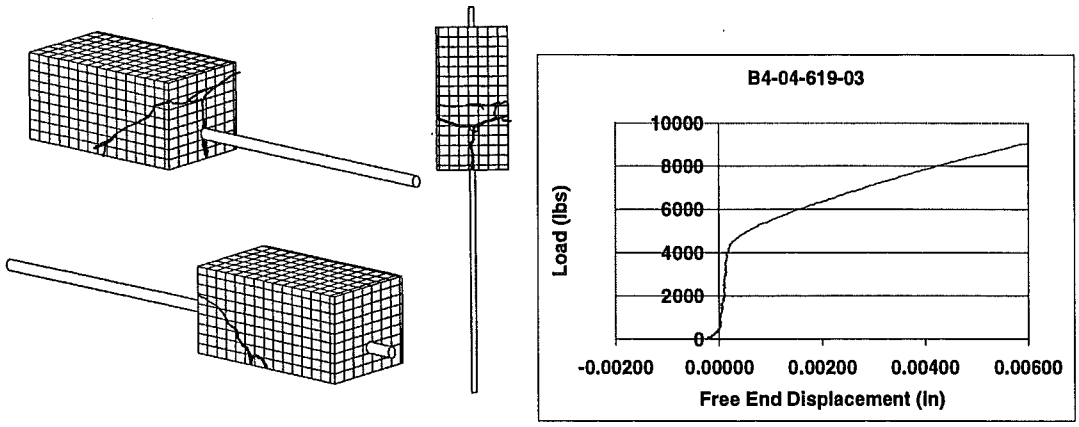

Figure 4-4: Crack Pattern and Load-Displacement for Specimen B4-04-619-03

All load-displacement plots show a bilinear curve similar to what can be seen in Figure 4-4. It is established that bond is made up of three components; bearing, friction, and adhesion (see Figure 2-2). In order for a load-displacement plot to display a bilinear curve, one of these components must be broken and the bar must move relative to the surrounding concrete. The movement as seen in the bilinear curve causes microcracks to form at the back side of the reinforcing bar deformations (see Figure 1-1). It is obvious that the bearing component of bond will not be broken unless the specimen is entirely broken apart. Because friction is dependent on a force normal to the bar surface, the only way for a bilinear curve produced by frictional bond failure would be if the confining pressure of the concrete around the bar were to somehow be relieved. This relief in confining pressure would have to be accompanied by cracking of the specimen. Therefore it follows that the bilinear curve must be due to the formation of microcracks at the back of the bar deformation accompanied by the breakdown of the adhesion bond component at lower bond stresses. The point where the microcracks form (i.e. the point where the slope changes) increases in load as the bond increases in length. After the microcracks form the load continues to increase, because the bond still has bearing and frictional components and the confinement of the concrete is still greater than the outward pressure due to the radial component of bond stress. However, the increase in load is accompanied by larger increases in free end displacement as the cracks spread radially outward from the bar. In other words the slope of the line for load versus free end displacement is less than before the microcracks formed (the line is not as steep).

Several bars with a bonded length of 8.0-in. and 8.5-in. yielded before bond failure occurred. This was not unexpected, as the bond length was right at the length where yielding of the bar was predicted to occur. The load data from these samples that yielded does not indicate bond strength, rather it gives a lower limit for the bond strength, i.e. the bond strength is known to be larger than the yield strength of the bar.

4.2.2 A615 Number 6 Bar Results

All the test data for the No. 6 black bars can be seen in Table 4-3. From the table it can be seen that the normalized mean experimental bond strength, herein after referred to as experimental bond strength, for all bonded lengths was within 18.7% to 40.7% above the

predicted bond strength. The 5-in. bonded length mean experimental bond strength of 17152-lb. was 37.2% above the predicted bond strength of 12501-lb. The experimental bond strength had a small coefficient of variation of ± 5.0%. The 6.5-in. bonded length mean experimental bond strength was 38.4% above the predicted bond strength. The mean experimental bond strength for this length, 19848-lb., had a coefficient of variation of ± 4.3%. The 8-in. bonded length produced results that were the highest above the predicted bond strength with a mean experimental bond strength (22763-lb.) 40.7% above the predicted strength (16175-lb.). This bonded length had a V_x of ± 8.9%. The length with results closest to the predicted was the 12-in. bonded length. These specimens had a mean experimental bond strength that was 18.7% above the predicted bond strength and had a coefficient of variation of ± 5.3%. After the fourth pour specimens were tested with bonded lengths of 6-in. and 10-in. This was to provide bond strength data for the black bars with lengths identical to the stainless bars. The 6-in. bonded length produced a normalized mean experimental bond strength of 18580-lb. with a coefficient of variation of ± 10.1%. The 10-in. bonded length had a normalized mean experimental bond strength of 25123-lb. and a coefficient of variation of ± 5.0%. Both normalized mean experimental bond strength results were approximately 35% higher than their respective predicted bond strengths. Additional data analysis is carried out in Section 4.5.2.

Specimen	Plate Location (in.)	Load @ .002 in. (lbs)	Normalized Bond Strength (lbs)	Expected Load (lbs)	Percent Difference	Comments
B6-05-619-01	12	--	--	12501	--	Flexure Crack
B6-05-619-02	7.5	17245	17245	12501	37.95%	Typical Crack
B6-05-619-03	7.5	17232	17232	12501	37.84%	Typical Crack
B6-05-619-04	12	16250	16250	12501	29.99%	Typical Crack
B6-05-619-05	12	--	--	12501	--	Flexure Crack
B6-05-619-06	7.5	18482	18482	12501	47.84%	Flexure CrackA
B6-05-619-07	6	16550	16550	12501	32.39%	Flexure CrackA
Mean for 5" bond			*17152*		*37.20%*	
Coeff. of Var.			*0.0502*			
B6-06-109-01	7.5	20315	19773	14101	44.07%	Typical CrackA
B6-06-109-02	7.5	--	--	14101	--	LVDT Malfunction
B6-06-109-03	7.5	15700	15281	14101	11.34%	Typical CrackA
B6-06-109-04	7.5	20298	19756	14101	43.95%	Typical Crack
B6-06-109-05	7.5	19616	19092	14101	39.11%	Flexure CrackA
B6-06-109-06	7.5	--	--	14101	--	LVDT Malfunction
B6-06-109-07	7.5	19521	19000	14101	38.44%	Typical Crack
Average for 6" bond			*18580*		*35.38%*	
Coeff. of Var.			*0.1012*			
B6-06-619-01	9	20633	20633	14338	43.90%	Typical Crack
B6-06-619-02	7.5	18655	18655	14338	30.11%	Flexure CrackA
B6-06-619-03	7.5	--	--	14338	--	Flexure Crack
B6-06-619-04	12	19989	19989	14338	39.41%	Typical Crack
B6-06-619-05	12	--	--	14338	--	Flexure Crack
B6-06-619-06	12	--	--	14338	--	Flexure Crack
B6-06-625-07	7.5	20113	20113	14338	40.28%	Typical CrackA
Mean for 6.5" bond			*19484*		*38.42%*	
Coeff. of Var.			*0.0425*			
B6-08-619-01	10.5	24679	24679	16175	46.39 %	Typical Crack
B6-08-619-02	10.5	24513	24513	16175	51.55%	Flexure CrackA
B6-08-619-03	10.5	--	--	16175	--	Flexure Crack
B6-08-619-04	9	24451	24451	16175	51.17%	Typical Crack
B6-08-619-05	9	22864	22864	16175	41.35%	Typical Crack
B6-08-619-06	9	19066	19066	16175	17.87%	Typical Crack
B6-08-619-07	9	22336	22336	16175	38.09%	Typical Crack
B6-08-109-01	9	23047	22432	17000	35.57%	Typical Crack
Mean for 8" bond			*22763*		*40.73%*	
Coeff. of Var.			*0.0892*			

Table 4-3 continued on next page

continued from previous page

Specimen	Plate Location (in.)	Load @ .002 in. (lbs)	Normalized Bond Strength (lbs)	Expected Load (lbs)	Percent Difference	Comments
B6-10-109-01	12	27686	26947	19134	44.70%	Typical Crack
B6-10-109-02	12	24971	24304	19134	30.51%	Typical Crack
B6-10-109-03	12	26785	26070	19134	39.99%	Typical Crack
B6-10-109-04	12	26785	26070	19134	39.99%	Typical Crack
B6-10-109-05	12	24972	24305	19134	30.51%	Typical Crack
B6-10-109-06	12	25424	24745	19134	32.88%	Typical Crack
B6-10-109-07	12	24060	23418	19134	25.75%	Typical Crack
Average for 10" bond			*25123*		*34.90%*	
Coeff. of Var.			*0.0501*			
B6-12-619-01	12	24123	24123	21073	14.47%	Typical Crack
B6-12-619-02	12	26785	26785	21073	27.10%	Typical Crack
B6-12-619-03	12	24509	24509	21073	16.30%	Typical Crack
B6-12-619-04	12	26580	26580	21073	26.13%	Typical Crack
B6-12-619-05	12	--	--	21073	--	Bar Yielded
B6-12-619-06	12	24507	24507	21073	16.29%	Typical Crack
B6-12-619-07	12	23600	23600	21073	11.99%	Typical Crack
Mean for 12" bond			*25017*		*18.72%*	
Coeff. of Var.			*0.0533*			

Table 4-3: No. 6 Black Bar A615 Test Results

Most specimens cracked as expected for bond failure. The cracks start at the loaded face and continue for the length of bonded bar. At the free-end where the bar was debonded the cracks generally ran out to the sides of the specimens at angles varying from 45 to 90 degrees from the longitudinal axis of the bar. A typical crack pattern along with its associated load-displacement plot can be seen in Figure 4-5.

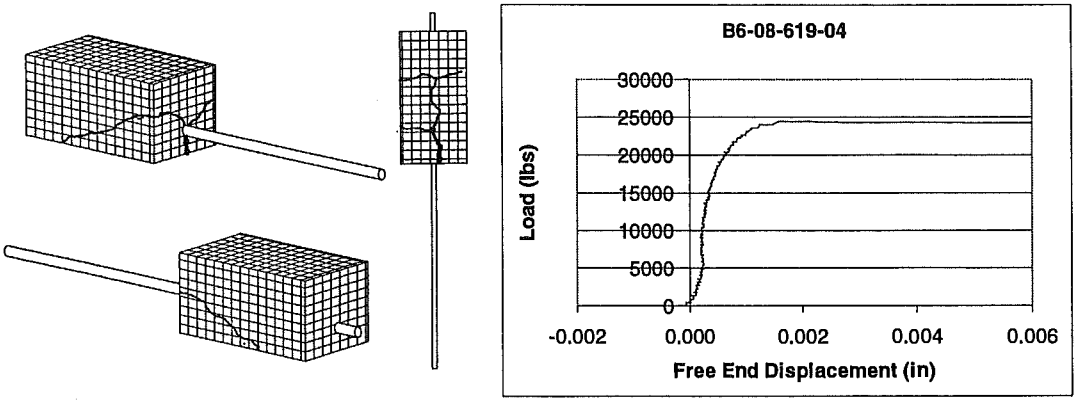

Figure 4-5: Crack Pattern and Load-Displacement for Specimen B6-08-619-04 (Bond Failure)

During the testing some specimens cracked differently than expected. The odd cracks were similar to flexure cracks in a beam. Figure 4-5 shows the typical cracking associated with bond failure produced in this study with its respective load-displacement plot whereas Figure 4-6 displays a specimen with a typical load-displacement and crack pattern for a flexural failure. This type of failure poses a problem for bond strength studies because when the specimen cracks the maximum strength obtained is based on concrete failure, not bond failure. Because of this, the only pertinent bond strength information from one of these tests is the fact that the bond strength is definitely stronger than the cracking strength of the concrete. In other words, the load obtained is a lower bound for bond strength when this type of failure occurs. Some tests where the specimens showed flexure cracks still provided valid bond strength data. In these tests the free end displacement reached 0.002-in. before the specimen cracked. These specimens are noted as "Flexure CrackA" and are included in the data analysis. All specimens noted as "Flexure Crack" were eliminated from further analysis because the load at 0.002-in would be reflective of the concrete flexural strength, not the true bond strength.

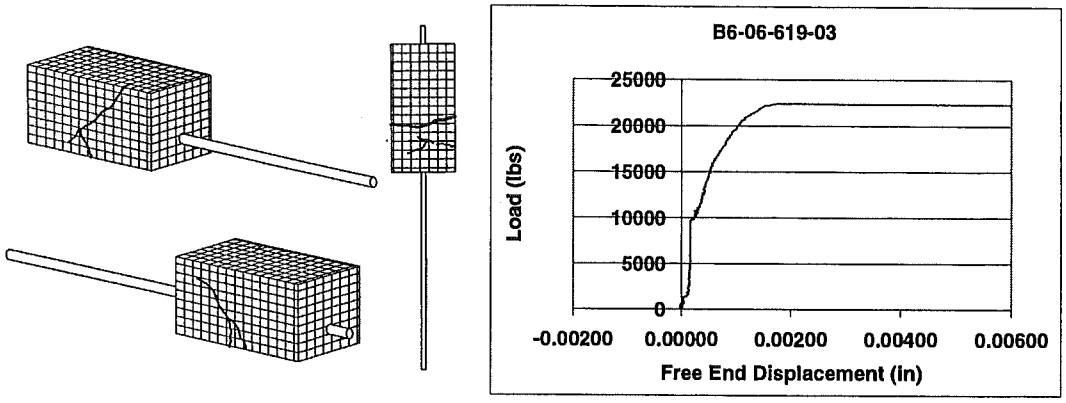

Figure 4-6: Crack Pattern and Load-Displacement for Specimen B6-08-619-03 (Flexure Failure)

Flexural cracks are caused when tensile stresses in the concrete exceed the concrete tensile capacity. Qualitatively, these tensile stresses are caused by the action of transferring the tensile load from the bar to the concrete at the point where the bar is no longer bonded to the concrete. This phenomenon was previously observed by ACI Committee 408 (1966). If the debonded section at the end of the bar is thought of as not existing, this becomes easier to picture. To avoid this flexural failure mode, the upper reaction plate (Reaction 1, see Figure 3-6) was moved down closer to the bonded end of the bar. This was achieved by moving the bolts that held the reaction plate in place down to the closest appropriate hole that was in the self-reacting frame. These holes were spaced at 1½-in. on center starting at 8-in. from the bottom of the frame going up to 14-in. from the bottom of the frame. The plate was kept far enough away from the bonded section of the test bar to try to eliminate any pinching stresses that would make the bond strength appear to increase.

The maximum tensile stress in concrete before cracking can be found by analyzing the specimen the same way that a concrete beam would be analyzed. An example of the flexural capacity of the specimen is as follows: The load when the flexural crack occurred for specimen B6-05-619-01 was 16080 pounds. From statics the three unknown reactions can be found (Figure 4-7). Dimensional values used to calculate the reactions can be seen in Figure 4-8.

$R_2 := P$	*(Vertical Equilibrium)*	$R_2 = 16.08kip$
$R_1 := P \cdot \frac{(8.75 - 2 - 1.875)}{[14.5 - (1 + 1.25)]}$	*(Moment about point A)*	$R_1 = 6.399kip$
$R_3 := R_1$	*(Horizontal Equilibrium)*	$R_3 = 6.399kip$

Figure 4-7: Sample Calculation of Specimen Reactions

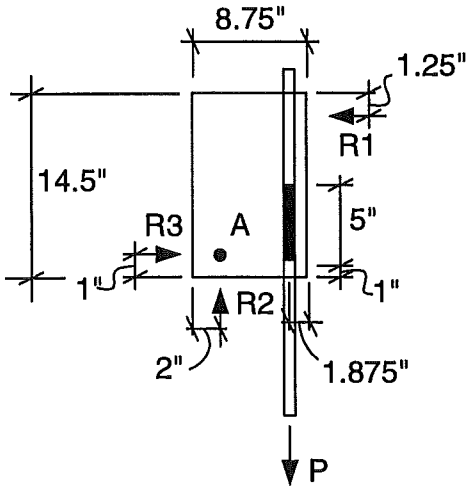

Figure 4-8: Reaction Locations for Sample Calculation for Specimen B6-05-619-01

With the reactions known, the flexural stresses and forces were calculated. Given that the crack on this particular specimen appeared approximately 8-in. from the free face of the specimen (i.e. the back of the specimen), or 6.75-in down from the location of reaction 1, this was considered the critical section. The standard 7.5 multiplier used in ACI 318-99 (section 9.5.2.3) to calculate the modulus of rupture is actually the bottom of a range of possibilities. This range of possibilities can be found in the ACI Manual of Concrete Practice, published in 1997, part 3, section 224.2R-4, which states that for an assumed concrete weight of 150 pounds per cubic foot the multiplier can range from 7.5 to 12.2. The cracking moment was calculated for both the high and the low possible values for the modulus of rupture to see where the applied moment fell in relation to these suggested capacity extremities. The continuation of the example for specimen B6-05-619-01 is seen in Figure 4-9.

$M_{applied} := R_1 \cdot 6.75 \cdot in$ $\quad M_{applied} = 43.194 kip \cdot in$

$MOR1 := 7.5 \cdot \sqrt{f_c} \cdot psi$ *(Low Modulus of Rupture)*

$MOR2 := 12.2 \cdot \sqrt{f_c} \cdot psi$ *(High Modulus of Rupture)*

$I := \frac{7.25 \cdot in \cdot (8.75 \cdot in)^3}{12}$ *(Moment of Inertia)*

$M_{crlow} := \frac{MOR1 \cdot I}{c}$ $\quad M_{crlow} = 51.262 kip \cdot in$

$M_{crhigh} := \frac{MOR2 \cdot I}{c}$ $\quad M_{crhigh} = 83.387 kip \cdot in$

Figure 4-9: Sample Calculation for Computing the Modulus of Rupture and the Associated Flexural Capacity

After examining the above calculations it can be seen that the applied moment ($M_{applied}$) is below the lowest expected cracking moment (M_{crlow}). It should be noted that the calculations do not take into account shear deformations that would cause a non-linear stress distribution in the beam. This non-linearity would cause higher tensile stresses than what was calculated. Because many specimens cracked at similar loads, further investigation was desired. The investigation path chosen was the finite element method. This investigation would consider the shear deformations.

A very rough finite element model was made using a student version of SAP90. The model consisted of 182 constant strain triangle elements. Constant strain triangles were initially used because of the limitations of the student version of SAP90 allowing a maximum of 99 nodes. Use of the CST (Constant Strain Triangles) allowed for the creation of a finer mesh in the areas of interest. The rough model did not take into consideration the inherent tensile stresses at the free face of the specimen, i.e. no attempt to model the debonded zone in the first 1-in. of the specimen was made. Concrete elements were 7.5-in wide throughout the model except where the rebar was located. At these locations 6.75-in wide elements were used with concrete properties along with ¾-in. wide elements with steel properties. Several bonded lengths were modeled with the reaction plate, i.e. restrained nodes, located both at the top of the self-reacting frame and approximately 1-in. from the end of the bonded section of bar. The load that produced flexural failure during the tests was used in each

model. Results from the model showed that at the end of the bonded bar section very high tensile stresses were being developed thus correlating with the observed flexural cracking. With this finite element model and the findings of ACI Committee 408 (1966), the action of moving the reaction plate nearer to the end of the bonded section of rebar as discussed in the beginning of this chapter becomes justifiable.

4.3 STAINLESS TYPE 316LN RESULTS

4.3.1 316LN Number 4 Bar Results

Test data for the No. 4 stainless 316LN bars can be seen in Table 4-4. Test results were much more sporadic than the previously discussed black bar tests. The bonded length of 4-in. had a normalized mean test bond strength of 8233-lb. that was 10.4% above the predicted strength of 7636-lb. Experimental bond strength for the 4-in. bonded length had a coefficient of variation of ±28.6%. Tests with bonded lengths of 5.5-in. produced a normalized experimental bond strength mean of 11370-lb., 23.6% higher than predicted bond strength value of 9411-lb. The experimental bond strength for the 4-in. bonded length had a coefficient of variation of ±15.7%. Normalized mean bond strength results for the bonded length of 8-in. were the closest to the predicted values with 14216-lb. being 17.6% above the predicted bond strength of 12371-lb. The experimental bond strength for 8-in. bond lengths had a coefficient of variation of ±9.8%. The 10-in. bond length tests had a normalized mean experimental bond strength of 19640-lb., which was 36.4% above the predicted bond strength of 14738-lb. and had a coefficient of variation of ±7.1%. Further data analysis can be found in Section 4.5.1. The large coefficients of variation were somewhat expected based on yield strength tests performed (see Table 3-4). Subsequent conversations with the supplier indicated that the bars did come from the same lot. However, this is somewhat suspect as the supplier has since gone out of business.

Specimen	Plate Location (in.)	Load @ .002 in. (lbs)	Normalized Bond Strength (lbs)	Expected Load (lbs)	Percent Difference	Comments
S4-04-625-01	12	8944	8738	7636	17.13%	Typical CrackA
S4-04-625-02	12	12461	12174	7636	63.18%	Typical Failure
S4-04-625-03	12	7577	7403	7636	-0.78%	Typical Failure
S4-04-625-04	12	5878	5743	7636	-23.02%	Typical Failure
S4-04-625-05	12	8198	8009	7636	7.36%	Typical Failure
S4-04-625-06	12	10270	10034	7636	34.49%	Typical CrackA
S4-04-625-07	12	5663	5533	7636	-25.84%	Typical Failure
Mean for 4" bond			*8233*		*10.36%*	
Coeff. of Var.			*0.2860*			
S4-05-625-01	12	10408	10168	9412	10.58%	Typical CrackA
S4-05-625-02	12	13973	13651	9412	48.46%	Typical Failure
S4-05-625-03	12	12584	12294	9412	33.70%	Typical Failure
S4-05-625-04	12	9429	9212	9412	0.18%	Typical CrackA
S4-05-625-05	12	10880	10630	9412	15.60%	Typical CrackA
S4-05-625-06	12	10315	10078	9412	9.60%	Typical Failure
S4-05-625-07	12	13880	13560	9412	47.47%	Typical CrackA
Mean for 5.5" bond			*11370*		*23.66%*	
Coeff. of Var.			*0.1572*			
S4-08-625-01	12	12345	12061	12371	-0.21%	Typical Failure
S4-08-625-02	12	15440	15085	12371	24.81%	Typical Failure
S4-08-625-03	12	13781	13464	12371	11.40%	Typical Failure
S4-08-625-04	12	15397	15043	12371	24.46%	Typical Failure
S4-08-625-05	12	16263	15889	12371	31.46%	Typical Crack
S4-08-625-06	12	--	--	12371	--	Bar Yielded
S4-08-625-07	12	14081	13757	12371	13.82%	Typical Crack
Mean for 8" bond			*14216*		*17.62%*	
Coeff. of Var.			*0.0978*			
S4-10-625-01	12	--	--	14738	--	Bar Yielded
S4-10-625-02	12	--	--	14738	--	Bar Yielded
S4-10-625-03	12	--	--	14738	--	Bar Yielded
S4-10-625-04	12	22069	21561	14738	49.74%	Cracked as bar yielded
S4-10-625-05	12	20070	19608	14738	36.17%	Cracked as bar yielded
S4-10-625-06	12	18751	18319	14738	27.22%	Cracked as bar yielded
S4-10-625-07	12	19521	19072	14738	32.45%	Typical Failure
Mean for 10" bond			*19640*		*36.40%*	
Coeff. of Var.			*0.0705*			

Table 4-4: No. 4 Stainless Type 316LN Test Results

Bond failure was similar to the No. 4 black bar bond tests and most failures were a two step process. Initially all components of bond were present. At a certain load the adhesion component of bond failed leaving friction and bearing bond components to transfer tensile forces. After adhesion had failed microcracks formed at the backside of the deformation of the reinforcing bar. Hence the tests produced bilinear curves. The point where the slope changes, or mircrocracks form, again, increases in load as the bonded length increases. This can be seen in Figure 4-10, which shows a typical crack pattern and load-displacement curve for the No. 4 316LN bond tests.

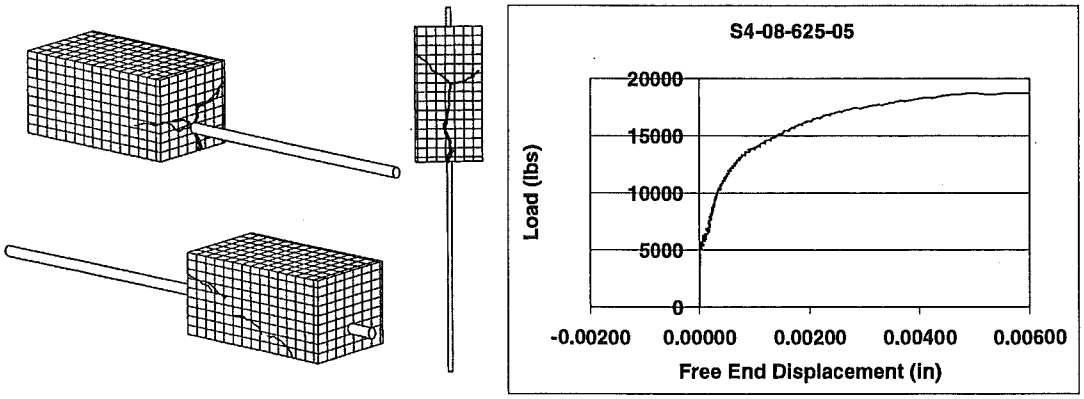

Figure 4-10: Crack Pattern and Load-Displacement Curve for Specimen S4-08-625-05

Like the No. 4 black bar specimens, the No. 4 stainless 316LN specimens did not exhibit cracking at the time when defined bond failure occurred. Therefore, several specimens were pulled past the typical shut off point (0.006-in. free end displacement) to force the specimens to crack. These specimens are noted in Table 4-4 in the "Comments" section as "Typical CrackA". The crack pattern produced by these specimens was a typical bond crack pattern with a longitudinal crack running along the bar at the bonded locations and then spreading out to the sides of the specimen running at angles of 45 to 90 degrees from the longitudinal axis of the bar (see Figure 4-10). The crack patterns and graphs seen are very similar to the black bar crack patterns that can be seen in Figure 4-5. DenHartigh (2001) shows crack patterns and load-displacement plots in his report. Specimens with bonded lengths of 10-in. yielded the bars which is as expected. Some of these specimens cracked just as the bar yielded and are noted as such in the "Comments" column.

4.3.2 316LN Number 6 Bar Results

The results for the No. 6 stainless 316LN bars can be seen in Table 4-5. The bonded length of 6-in. resulted in a normalized mean experimental bond strength of 15717-lb. that was 14.5% above the predicted bond strength of 14048-lb. The experimental bond strength had a coefficient of variation of ± 14.2%. Tests with a bonded length of 8-in. yielded normalized results that were 23.7% higher than expected bond strength. Mean normalized experimental bond strength was 20011-lb. with an associated coefficient of variation of ± 6.3%. The bonded length of 10-in. produced a normalized mean experimental bond strength of 25274-lb, which was 35.7% higher than predicted bond strengths of 19061-lb. The experimental bond strength had a coefficient of variation of ± 4.9%. Finally, tests with a bonded length of 12-in. resulted in a normalized mean experimental bond strength of 27718-lb. that was 31.5% higher than predicted bond strength values. These tests had a coefficient of variation of only ± 1.7%. Additional analysis is carried out in Section 4.5.2.

Specimen	Plate Location (in.)	Load @ .002 in. (lbs)	Normalized Bond Strength (lbs)	Expected Load (lbs)	Percent Difference	Comments
S6-06-625-01	7.5	13627	13313	14048	-3.00%	Typical CrackA
S6-06-625-02	7.5	14803	14462	14048	5.37%	Typical Crack
S6-06-625-03	7.5	16158	15786	14048	15.02%	Typical Crack
S6-06-625-04	7.5	20435	19965	14048	45.46%	Typical CrackA
S6-06-625-05	7.5	14171	13845	14048	0.87%	Typical CrackA
S6-06-625-06	7.5	17086	16693	14048	21.62%	Typical CrackA
S6-06-625-07	7.5	16328	15952	14048	16.23%	Typical CrackA
Mean for 6" bond			*15717*		*14.51%*	
Coeff. of Var.			*0.1421*			
S6-08-625-01	10.5	22248	21736	16555	34.39%	Typical CrackA
S6-08-625-02	10.5	18612	18184	16555	12.43%	Flexure CrackA
S6-08-625-03	10.5	20472	20001	16555	23.66%	Typical CrackA
S6-08-625-04	10.5	19852	19395	16555	19.92%	Typical CrackA
S6-08-625-05	10.5	19367	18921	16555	16.99%	Typical CrackA
S6-08-625-06	10.5	21485	20990	16555	29.78%	Typical CrackA
S6-08-625-07	10.5	21340	20849	16555	28.91%	Typical Crack
S6-08-107-01	10.5	22000	21430	16555	32.39%	Typical Crack
Mean for 8" bond			*20186*		*24.81%*	
Coeff. of Var.			*0.0624*			
S6-10-625-01	10.5	24059	23505	19062	26.22%	Typical CrackA
S6-10-625-02	12	28145	27497	19062	47.65%	Typical Crack
S6-10-625-03	12	26167	25565	19062	37.28%	Typical CrackA
S6-10-625-04	12	26326	25720	19062	38.11%	Typical CrackA
S6-10-625-05	12	24918	24344	19062	30.72%	Typical CrackA
S6-10-625-06	12	25377	24793	19062	33.13%	Typical Crack
S6-10-625-07	12	26096	25495	19062	36.90%	Typical Crack
Mean for 10" bond			*25274*		*35.72%*	
Coeff. of Var.			*0.0498*			
S6-12-625-01	12	28953	28286	21568	34.24%	Typical Crack
S6-12-625-02	12	28598	27940	21568	32.59%	Typical Crack
S6-12-625-03	12	28094	27447	21568	30.26%	Typical Crack
S6-12-625-04	12	27684	27047	21568	28.36%	Typical Crack
S6-12-625-05	12	28140	27492	21568	30.47%	Typical CrackA
S6-12-625-06	12	28989	28322	21568	34.41%	Typical Crack
S6-12-625-07	12	28140	27492	21568	30.47%	Typical Crack
Mean for 12" bond			*27718*		*31.54%*	
Coeff. of Var.			*0.0172*			

Table 4-5: No. 6 Stainless Type 316LN Test Results

Bond failure was similar to previous No. 6 black bar tests. Failure was again a two step process involving the formation of microcracks and the breakdown of the adhesion component of bond. Many of the specimens cracked just after bond failure had technically occurred. This is to say that just as the free end displacement surpassed 0.002-in of displacement the specimens cracked. These are denoted as "Typical CrackA" in the "Comments" column in Table 4-5. The plots of the test data again show a bilinear curve prior to 0.002-in. of free-end displacement. The point where the curve changes slope (shown here at approximately 14,000-lb.) increases in load as the bond length increases. The point where the specimen cracks can be seen on the plot where the slope of the line goes to zero. Figure 4-11 shows a typical crack pattern and load-displacement curve for the No. 6 stainless 316LN bars.

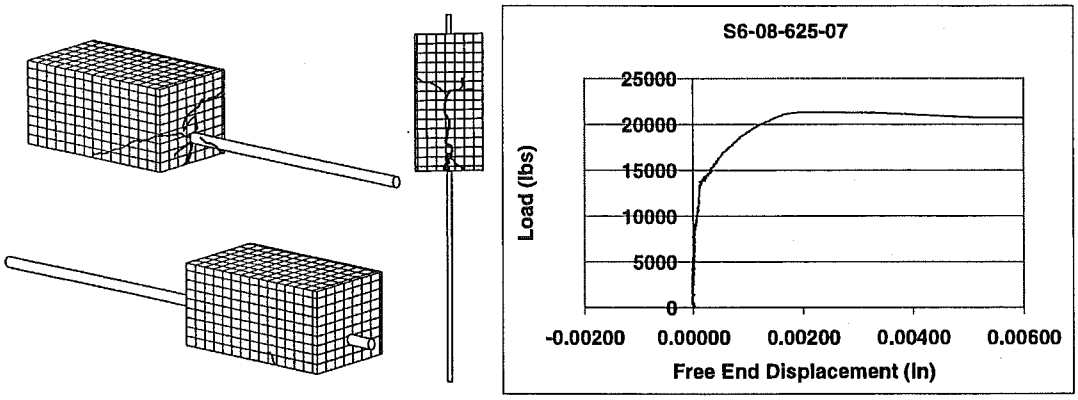

Figure 4-11: Crack Pattern and Load-Displacement Curve for Specimen S6-08-625-07

During the tests the upper reaction plate was kept in a lower location similar to the No. 6 black bars to prevent flexural failures. The location used was determined by observing the plate location of the black bar tests which eliminated the flexural failure. Consideration was taken to prevent the reaction plate from encroaching on the bonded end of the bar and thus creating confining stresses that would increase the apparent bond strength.

4.4 DUPLEX STAINLESS TYPE 2205 RESULTS

4.4.1 Duplex 2205 Number 4 Bar Results

Test data for the No. 4 Duplex 2205 bars can be seen in Table 4-6. Test results were quite consistent producing bond strengths that were approximately 17% higher than the predicted bond strength. The bonded length of 4-in. had a normalized mean bond strength of 8784-lbs with a coefficient of variation of ± 17.7%. This was 17.7% higher than the predicted bond strength. Normalized mean experimental bond strength for the bonded length of 5.5-in. was 10043-lbs which was 9.2% above the predicted bond strength. This mean bond strength had a V_x of ± 29.8%. The 8-in. bonded length normalized mean bond strength was 14155-lb. with a coefficient of variation of ± 12.6%. This was 17.1% above the predicted bond strength. The 10-in. bonded length had a normalized mean experimental bond strength of 16848-lb. that was 17.0% above the predicted bond strength of 15335-lb. This bond strength had a coefficient of variation of ± 10.7%. Additional analysis is carried out in Section 4.5.1.

Specimen	Plate Location (in.)	Load @ .002 in. (lbs)	Normalized Bond Strength (lbs)	Expected Load (lbs)	Percent Difference	Comments
D4-04-925-01	12	8716	8184	7946	9.70%	Typical Failure
D4-04-925-02	12	6393	6003	7946	-19.54%	Typical Failure
D4-04-925-03	12	9676	9085	7946	21.78%	Typical Failure
D4-04-925-04	12	9767	9171	7946	22.92%	Typical Failure
D4-04-925-05	12	8945	8399	7946	12.58%	Typical Failure
D4-04-925-06	12	11859	11136	7946	49.26%	Typical Failure
D4-04-925-07	12	10130	9511	7946	27.49%	Typical Failure
Mean for 4" bond			*8784*		*17.74%*	
Coeff. of Var.			*0.1772*			
D4-05-925-01	12	9300	8732	9793	-5.03%	Observed
D4-05-925-02	12	10319	9689	9793	5.37%	Typical Failure
D4-05-925-03	12	16424	15421	9793	67.71%	Typical Crack
D4-05-925-04	12	7259	6816	9793	-25.88%	Typical Failure
D4-05-925-05	12	13137	12335	9793	34.15%	Typical Failure
D4-05-925-06	12	10589	9942	9793	8.13%	Typical Failure
D4-05-925-07	12	7843	7364	9793	-19.91%	Typical Failure
Mean for 5.5" bond			*10043*		*9.22%*	
Coeff. of Var.			*0.2977*			
D4-08-925-01	12	13594	12764	12875	5.58%	Typical Failure
D4-08-925-02	12	15833	14867	12875	22.98%	Typical Failure
D4-08-925-03	12	14692	13796	12875	14.12%	Typical Failure
D4-08-925-04	12	18796	17648	12875	45.99%	Typical Crack
D4-08-925-05	12	14236	13367	12875	10.57%	Typical Crack
D4-08-925-06	12	15330	14394	12875	19.07%	Typical Failure
D4-08-925-07	12	13049	12252	12875	1.35%	Typical Failure
Mean for 8" bond			*14155*		*17.09%*	
Coeff. of Var.			*0.1260*			
D4-10-925-01	12	19248	18073	15336	25.51%	Typical, Yield
D4-10-925-02	12	16826	15799	15336	9.72%	Typical, Yield
D4-10-925-03	12	--	--	15336	--	Bar Yielded
D4-10-925-04	12	17608	16533	15336	14.82%	Typical, Yield
D4-10-925-05	12	15605	14652	15336	1.75%	Typical Failure
D4-10-925-06	12	--	--	15336	--	Bar Yielded
D4-10-925-07	12	20429	19182	15336	33.21%	Typical, Yield
Mean for 10" bond			*16848*		*17.00%*	
Coeff. of Var.			*0.1069*			

Table 4-6: No. 4 Stainless Duplex 2205 Test Results

Bond failure was similar to the No. 4 black bars and the No. 4 stainless 316LN bars. The load-displacement curve showed a bilinear curve for most bond test specimens. As explained in Section 4.2.1, the bilinearity of the curve is due to the formation of microcracks at the backside of the deformation of the reinforcing bars after the adhesion loss. For specimens that were allowed to crack (pulled to a free end displacement greater than 0.006-in.) the load-displacement curve is similar to the other No. 4 specimens that exhibited bond cracking. These specimens have a tri-linear relationship. The new third portion of the curve occurs when all components of bond are broken. At this point the free end displacement goes beyond the limits of the LVDT as the load drops off. This was previously shown in Figure 4-3. Because most specimens did not crack at free-end displacements less than 0.006-in, only a typical load-displacement curve is shown in Figure 4-12.

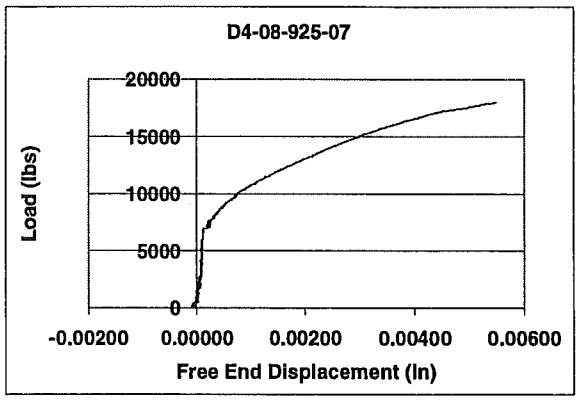

Figure 4-12: Load-Displacement Curve for D4-08-925-07

Some specimens exhibited bond cracking. These three specimens cracked just at the bond failure point and are noted in Table 4-6 as "Typical Crack". The cracks associated with these specimens were typical bond crack patterns with a longitudinal crack running along the bar at the bonded locations and then spreading out to the sides of the specimen running at angles of 45 to 90 degrees from the longitudinal axis of the bar. The crack patterns are similar to the crack patterns for both black bar and stainless 316LN bar. Some specimens with bonded lengths of 10-in. yielded as expected for this bonded length.

4.4.2 Duplex 2205 Number 6 Bar Results

Test data for the No. 6 Duplex bars can be seen in Table 4-7. Test results produced normalized experimental bond strengths that were approximately 9.0% higher than the

predicted bond strength using the OJB equation. Specimens with a bonded length of 6-in. had a normalized experimental mean bond strength of 14248-lbs with a coefficient of variation of ± 7.6%. Experimental bond strength was only 3.81% higher than the predicted bond strength. Normalized mean bond strength for the bonded length of 8-in. was 18443-lb which was 7.1% above the predicted bond strength. This mean bond strength had a V_x of ± 7.8%. Ten inch bonded lengths had a normalized experimental mean bond strength of 21244-lb. with a coefficient of variation of ± 5.5%. This was 14.1% above the predicted bond strength. The 12-in. bonded length had a normalized mean bond strength of 23091-lb. that was 9.6% above the predicted bond strength of 22441-lb. This bond strength had a coefficient of variation of ± 5.7%. Additional analysis can be found in Section 4.5.2.

Specimen	Plate Location (in.)	Load @ .002 in. (lbs)	Normalized Bond Strength (lbs)	Expected Load (lbs)	Percent Difference	Comments
D6-06-625-01	9	16000	15023	14617	9.46%	Flexure CrackA
D6-06-625-02	7.5	14600	13709	14617	-0.12%	Typical CrackA
D6-06-625-03	7.5	15282	14350	14617	4.55%	Typical CrackA
D6-06-625-04	7.5	17124	16079	14617	17.15%	Typical CrackA
D6-06-625-05	7.5	14929	14017	14617	2.13%	Typical CrackA
D6-06-625-06	7.5	14865	13958	14617	1.70%	Typical CrackA
D6-06-625-07	7.5	13420	12601	14617	-8.19%	Typical CrackA
Mean for 6" bond			*14248*		*3.81%*	
Coeff. of Var.			*0.0764*			
D6-08-625-01	10.5	--	--	17225	--	Flexure Crack
D6-08-625-02	9	19068	17904	17225	10.70%	Typical CrackA
D6-08-625-03	9	18205	17093	17225	5.69%	Typical Failure
D6-08-625-04	9	19018	17857	17225	10.41%	Typical CrackA
D6-08-625-05	9	20256	19020	17225	17.60%	Typical CrackA
D6-08-625-06	9	18182	17072	17225	5.55%	Typical CrackA
D6-08-625-07	9	15932	14959	17225	-7.51%	Typical CrackA
Mean for 8" bond			*18443*		*7.07%*	
Coeff. of Var.			*0.0783*			
D6-10-625-01	12	21075	19788	19833	6.26%	Typical CrackA
D6-10-625-02	12	23602	22161	19833	19.00%	Typical CrackA
D6-10-625-03	12	22239	20882	19833	12.13%	Typical CrackA
D6-10-625-04	12	23900	22441	19833	20.50%	Typical Crack
D6-10-625-05	12	23600	22160	19833	18.99%	Typical Crack
D6-10-625-06	12	21334	20032	19833	7.57%	Typical CrackA
D6-10-625-07	12	--	--	19833	--	LVDT Malfunction
Mean for 10" bond			*21244*		*14.08%*	
Coeff. of Var.			*0.0550*			
D6-12-625-01	12	25868	24289	22442	15.27%	Typical Crack
D6-12-625-02	12	25870	24291	22442	15.28%	Typical Crack
D6-12-625-03	12	25412	23861	22442	13.24%	Typical Failure
D6-12-625-04	12	22245	20887	22442	-0.88%	Typical Failure
D6-12-625-05	12	24792	23279	22442	10.47%	Typical Crack
D6-12-625-06	12	24900	23380	22442	10.96%	Observed
D6-12-625-07	12	23054	21647	22442	2.73%	Typical Failure
Mean for 12" bond	*12*		*23091*		*9.58%*	
Coeff. of Var.			*0.0574*			

Table 4-7: No. 6 Stainless Duplex 2205 Test Results

Bond failure was similar to the A615 black bar and the stainless 316LN bar. The graphs displayed the bilinear action associated with the formation of microcracks. A typical crack pattern and load-displacement curve can be seen in Figure 4-13.

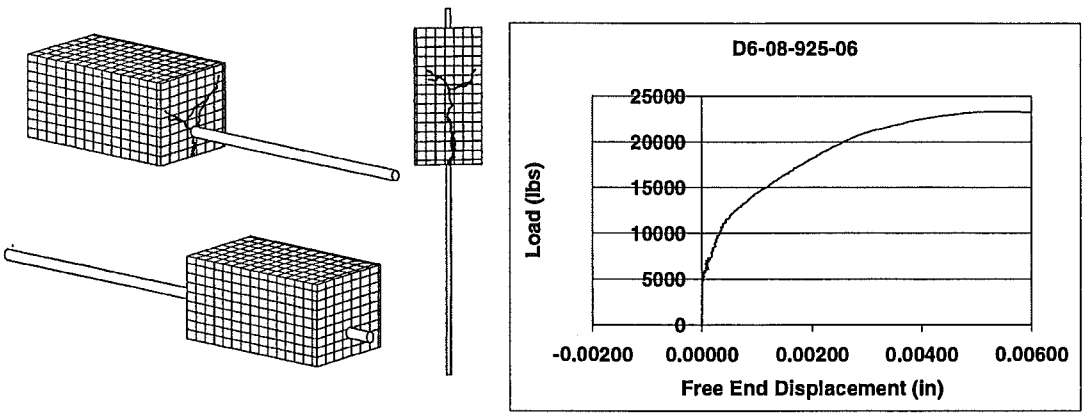

Figure 4-13: Crack Pattern and Load-Displacement Curve for Specimen D6-08-925-06

4.5 COMPARISON OF RESULTS

4.5.1 Number 4 Bar Comparisons

The No. 4 black bars and the No. 4 stainless bars (316LN and 2205) behaved similarly in the fact that every specimen had a failure mode that involved the formation of microcracks before bond failure. All specimens that were pulled to a free end displacement greater than 0.006-in. exhibited bond cracking. As previously stated the relative rib (R_r) area does not affect bond strength when bond fails by cracking the concrete. Past research by Darwin and Graham (1993) has shown that a higher R_r value produces stronger bond in pullout type bond failures. The research also showed that for bars with similar R_r values the bond strength gathered from these bars are comparable. In these tests, ultimate bond failure involved cracking of the specimen. The specimen cracking at ultimate bond indicates the type of failure that is referred to as cracking failure. Thus it can be concluded that even though the relative rib area for the No. 4 bars varies somewhat between the different types of bars, the normalized experimental bond strength for the different types of bars can be compared to each other without adjustment for relative rib area.

Load-Displacement plots of all three bar types also reveal a bilinear curve, all of which are similar in shape. These plots also reveal comparable values for the point where the slope changes, i.e. the point where microcracks form, for similar bonded lengths. For example, Figure 4-14 shows three load-displacement plots comparing black bar to stainless 316LN and Duplex 2205 bar, both having a 4-in. bonded length. A simple examination of these three graphs demonstrates the similarity between the different types of bars.

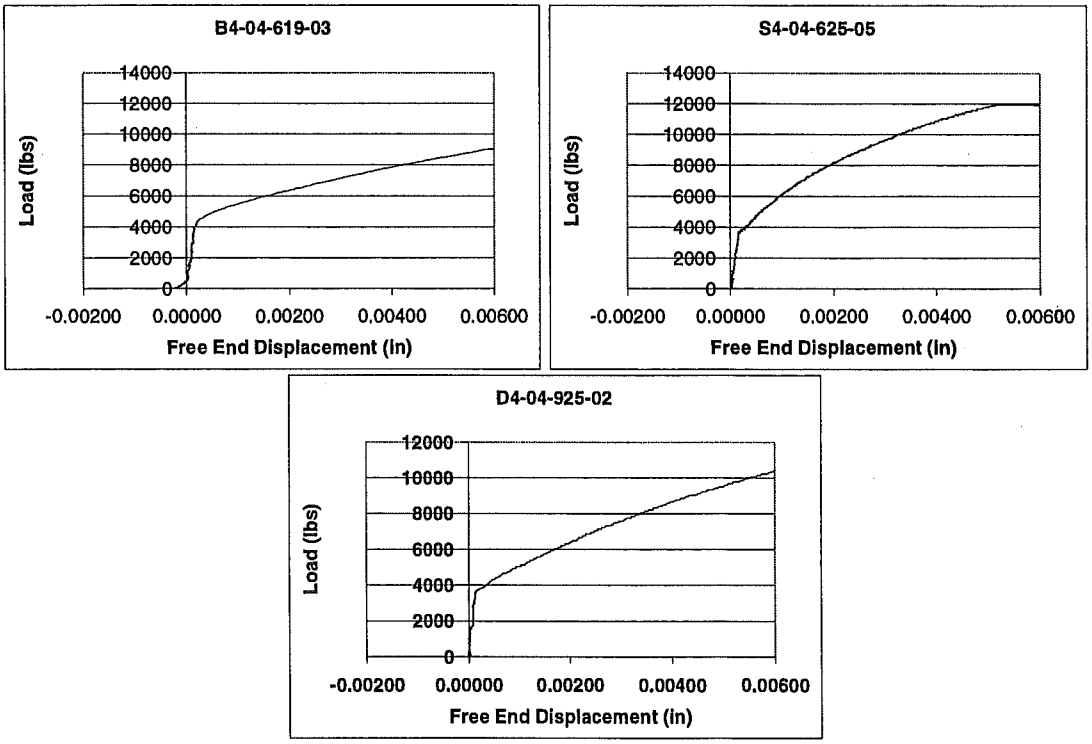

Figure 4-14: Comparison of Load-Displacement Plots for Specimens B4-04-619-03, S4-04-625-05 and D4-04-925-02

Statistical t-tests were performed on the data to determine if the point where the microcracks formed was similar for identical bonded lengths between the three types of bars. A 5% significance level was used. From the t-tests it was found that the point where the microcracks formed for the different types of bars was from similar populations. The load at which microcracks formed was also compared between the two types of stainless bars. This comparison revealed that the data was again from similar populations.

Had all specimens been allowed to crack, the load-displacement plots would have shown a tri-linear curve. The first portion of the curve being the steepest which would include all three components of bond: adhesion, friction, and bearing (see Figure 2-2) with no cracks.

The only movement of the bar is due to elastic deformation of the concrete around the reinforcing bar. The second portion of the curve was after the adhesion component had been broken, leaving friction and bearing components to provide the bond strength while microcracking propagated. Concrete mircocracking occurs on the backside of the deformed ribs as the bar is being pulled away from the stationary concrete, hence reducing the slope of the curve in this section. The third portion of the curve (previously shown in Figure 4-3), which is only seen for the specimens that were allowed to crack, would be the point where the cracks, formerly microcracks, reach the specimen face. As this third portion takes shape, the load is decreasing because the bearing component had started crushing and shearing the concrete between the deformations.

A comparison of crack patterns between the black bar and stainless type 316LN for identical bonded lengths is shown in Figure 4-15. When the crack patterns are compared to each other many similarities are seen. On the face of the specimen with the smallest cover, the crack followed the bar up to the point where the bar became debonded, then the crack progressed out to each side of the specimen. On the sides of the specimen the crack ran at approximately a 45-deg. angle starting near the debonded free-end of the bar. The front face shows the typical "Y" crack pattern that is commonly seen in bond tests involving semi-beam specimens.

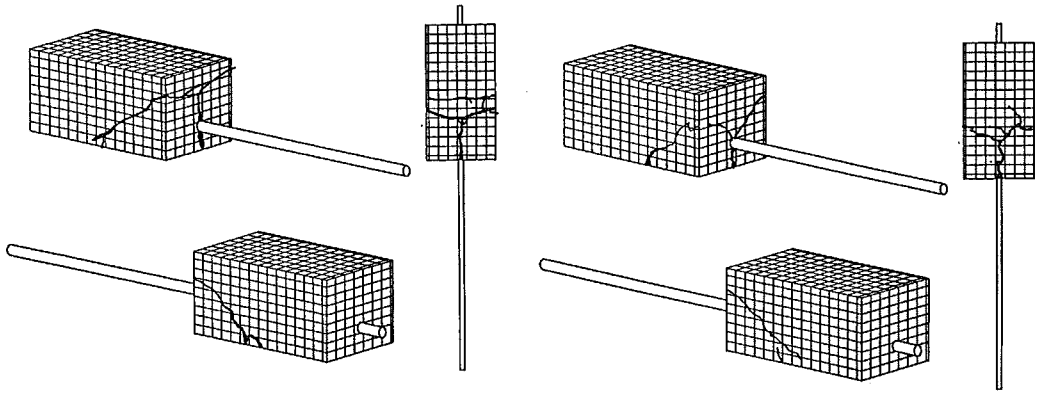

Figure 4-15: Comparison of Crack Patterns for B4-04-619-03 and S4-04-625-06

Normalized mean experimental bond strength for all the bonded lengths for the black bars had a range between 7.2% below predicted bond strength to 5.4% above the predicted bond

strength (Table 4-2). The normalized mean experimental bond strength for all bonded lengths for the stainless type 316LN bars ranged from 10.4% above predicted bond strength to 36.4% above the predicted bond strength (Table 4-4). The Duplex 2205 stainless normalized mean experimental bond strength ranged from 9.22% to 19.7% above the predicted bond strength (Table 4-6).

Results from both types of stainless bar bond tests were statistically compared to the normalized experimental bond strength of the black bars. In addition, results were statistically compared to the predicted bond strength based upon all four bond strength equations (Equations 2-2 to 2-5) with an emphasis on the AASHTO relationship. The statistical analysis tool used to compare results was a t-test. The t-test is generally used to distinguish a mean and variance taken from a sample in which the population mean and variance are unknown and can be performed on data with dissimilar variances. The t-tests were conducted on alike bonded lengths; a single t-test would compare normalized bond strength data from two equal bonded lengths. When performing t-tests, a significance level, α, must be chosen. This represents the probability of making a Type I error. A Type I error occurs when the null hypothesis, H_o, is rejected when in fact it is actually true. For all statistical t-tests α was taken as 0.05. This means that there is a 5% chance of wrongfully rejecting H_o. The significance level of 0.05 was chosen because this is typically an acceptable level for a Type I error.

Black bar experimental bond strength was statistically compared to the predicted bond strength (OJB, AASHTO, ACI and Darwin) using a two-tailed t-test with a significance level, α, equal to 0.05 in order to verify the bond strength experiment. The null hypothesis, H_o, was stated such that the normalized experimental bond strength of stainless bars was equal to the experimental bond strength of the black bars. The alternative hypothesis for this round of statistical tests was that the experimental bond strength was not equal to the predicted bond strength. This was done because it is important, when comparing the black bar experimental bond strength to the theoretical bond strength, to check if the bond tests are coming from a different population that the theoretical bond strength population. From the statistical tests comparing the experimental bond strength of black bar to the predicted

bond strength there was no statistical reason to assume that the experimental bond strength and the predicted bond strength for the No. 4 bars came from different populations. Table 4-8 contains the hypotheses used for all t-tests as well as the t-test results. In Table 4-8, μ_1 and μ_2 indicate the mean of the data being tested. In the black bar tests μ_1 is the mean of the black bar experimental bond strength and μ_2 is the theoretical bond strength. For the stainless t-tests μ_1 is always the stainless mean and μ_2 is either the mean of the black bar or the theoretical bond strength. Statistical tests that produced results requiring the alternate hypothesis to be accepted are highlighted in Table 4-8.

No. 4 Black Bar							
Hypotheses	Bonded Length	Black Bar	316LN Bar	AASHTO	OJB	ACI	Darwin
	4	--	--	$\mu_1=\mu_2$	$\mu_1=\mu_2$	$\mu_1\neq\mu_2$	$\mu_1=\mu_2$
H_0: $\mu_1=\mu_2$	5.5	--	--	$\mu_1=\mu_2$	$\mu_1=\mu_2$	$\mu_1=\mu_2$	$\mu_1=\mu_2$
H_A: $\mu_1\neq\mu_2$	7	--	--	$\mu_1=\mu_2$	$\mu_1=\mu_2$	$\mu_1=\mu_2$	$\mu_1=\mu_2$
	8	--	--	$\mu_1=\mu_2$	$\mu_1=\mu_2$	$\mu_1=\mu_2$	$\mu_1=\mu_2$
	8.5	--	--	$\mu_1=\mu_2$	$\mu_1=\mu_2$	$\mu_1=\mu_2$	$\mu_1\neq\mu_2$
No. 4 316LN							
Hypotheses	Bonded Length	Black Bar	316LN Bar	AASHTO	OJB	ACI	Darwin
	4	$\mu_1\neq\mu_2$	--	$\mu_1\neq\mu_2$	$\mu_1\neq\mu_2$	$\mu_1\neq\mu_2$	$\mu_1\neq\mu_2$
H_0: $\mu_1=\mu_2$	5.5	$\mu_1\neq\mu_2$	--	$\mu_1\neq\mu_2$	$\mu_1\neq\mu_2$	$\mu_1\neq\mu_2$	$\mu_1\neq\mu_2$
H_A: $\mu_1<\mu_2$	8	$\mu_1\neq\mu_2$	--	$\mu_1\neq\mu_2$	$\mu_1\neq\mu_2$	$\mu_1\neq\mu_2$	$\mu_1\neq\mu_2$
	12	--	--	$\mu_1\neq\mu_2$	$\mu_1\neq\mu_2$	$\mu_1\neq\mu_2$	$\mu_1\neq\mu_2$
No. 4 Duplex							
Hypotheses	Bonded Length	Black Bar	316LN Bar	AASHTO	OJB	ACI	Darwin
	4	$\mu_1\neq\mu_2$	$\mu_1\neq\mu_2$	$\mu_1\neq\mu_2$	$\mu_1\neq\mu_2$	$\mu_1\neq\mu_2$	$\mu_1\neq\mu_2$
H_0: $\mu_1=\mu_2$	5.5	$\mu_1\neq\mu_2$	$\mu_1\neq\mu_2$	$\mu_1\neq\mu_2$	$\mu_1\neq\mu_2$	$\mu_1\neq\mu_2$	$\mu_1\neq\mu_2$
H_A: $\mu_1<\mu_2$	8	$\mu_1\neq\mu_2$	$\mu_1\neq\mu_2$	$\mu_1\neq\mu_2$	$\mu_1\neq\mu_2$	$\mu_1\neq\mu_2$	$\mu_1\neq\mu_2$
	12	--	$\mu_1<\mu_2$	$\mu_1\neq\mu_2$	$\mu_1\neq\mu_2$	$\mu_1\neq\mu_2$	$\mu_1\neq\mu_2$

Table 4-8: No. 4 Bar Statistical T-Test Results

Statistical tests comparing normalized stainless (316LN and Duplex 2205) experimental bond strength to normalized black bar experimental bond strength were performed with the null hypothesis, H_o, stated such that the normalized stainless bond strength was equal to the normalized black bar experimental bond strength. The alternative hypothesis for these tests was that the normalized experimental bond strength of the stainless bars was less than the

normalized experimental bond strength of the black bars. Because of the way that H_a was set up, the t-tests were lower tail one-sided tests. From the t-tests involving both types of stainless compared to normalized experimental bond strength, it can be concluded there is no statistical reason to reject the null hypothesis. In other words there is no statistical reason to conclude that bond strength for No. 4 stainless (316LN and Duplex 2205) bars is less than the bond strength of black bars.

T-tests were also used to compare the normalized experimental bond strength of the stainless bars to the theoretical equations. The null hypothesis of these tests was that the normalized experimental bond strength was equal to the theoretical bond strength. The alternative hypothesis was that the normalized experimental bond strength was less than the theoretical bond strength. This setup again makes a lower tail one-sided test. From the t-tests there was no reason to conclude that the stainless bond strength was less than the theoretical bond strength, for all four bond relationships.

Normalizing the bond strength with respect to the black bar test concrete strength allowed comparisons between the other types of bars with varying concrete strengths. This normalized data can be seen below in terms of bar stress in Figure 4-16 for the No. 4 bars. From Figure 4-16, it can be seen that the conclusions based on the statistical analysis are valid. That is to say the normalized experimental bond strength for both types of the No. 4 stainless bars does not seem to be less than either the predicted bond strength based off the AASHTO relationship or the experimental bond strength of the black bars.

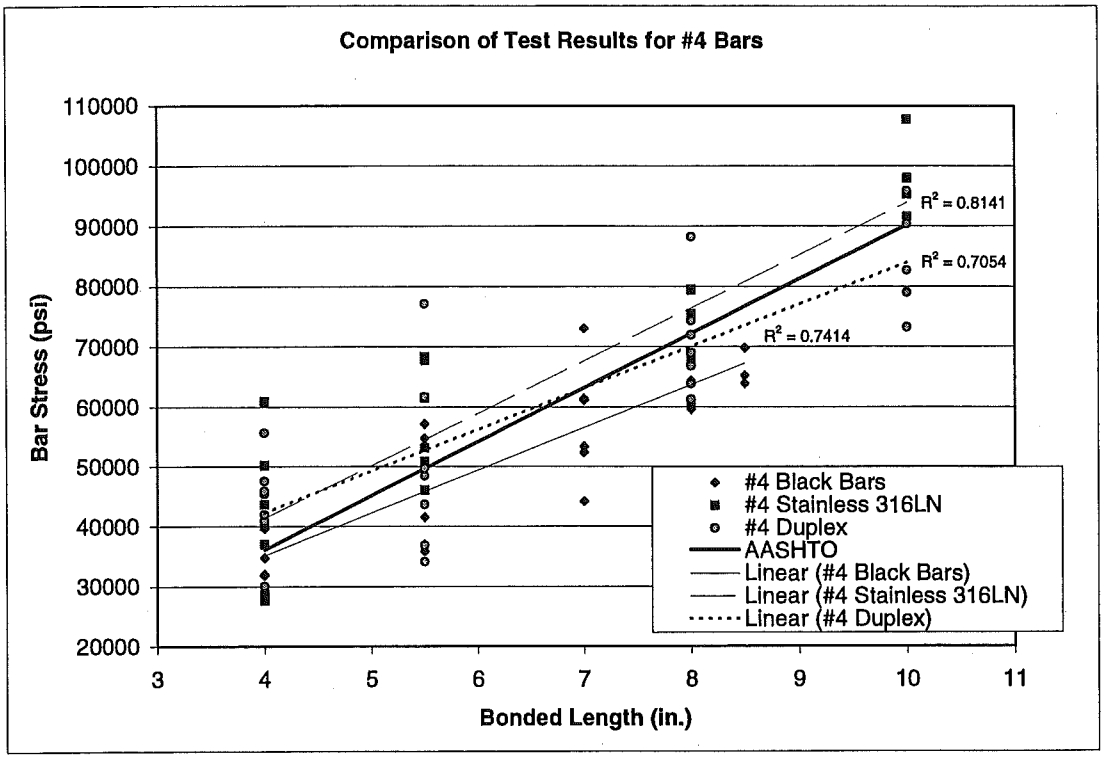

Figure 4-16: Linear Regression for No. 4 Bars

One of the primary goals of this investigation was to determine if bond strength of stainless bars (316LN and Duplex 2205) is less than conventional black bar bond strength. Conclusions based upon the statistical analysis of the No. 4 bars indicate that *there is no reason to believe that the bond strength of stainless bars is less than black bar experimental bond strength or theoretical bond strength.* T-test results for the No. 4 bars can be seen in Table 4-8.

4.5.2 Number 6 Bar Comparisons

The No. 6 black bar and the No. 6 stainless bar bond test resulted in similar bond failure behavior. Nearly all No. 6 bond specimens cracked before the test was shut off at 0.006-in of free end displacement. Consequently the bond strengths for bar types with different relative rib area, R_r values can be compared to each other.

Most black bar specimens with bonded lengths of 6-in and 8-in exhibited the two-step bond failure in which adhesion fails for lower bond stresses and microcracks cause a bilinear load-displacement curve. After the microcracks form the bond strength is less rigid, i.e. the curve

has more slope than before the adhesion component failed. Black bar specimens with bonded lengths of 10-in and 12-in failed in a different manner than the bonded lengths of 6-in and 8-in. As the load increased virtually no free-end displacement occurred. This would indicate that the bar was not moving relative to the concrete until the point when the specimen cracked.

Comparison of plots containing load-displacement curves for No. 6 black bar and No. 6 stainless bars show similar behavior for the shorter bonded lengths. Similarly to Figure 4-14 for the No. 4 bar, the point where the microcracks form is at a similar load for alike shorter bonded lengths (6-in and 8-in). Figure 4-17 shows load-displacement plots for all three types of bars for comparative purposes with a bonded length of 8-in.

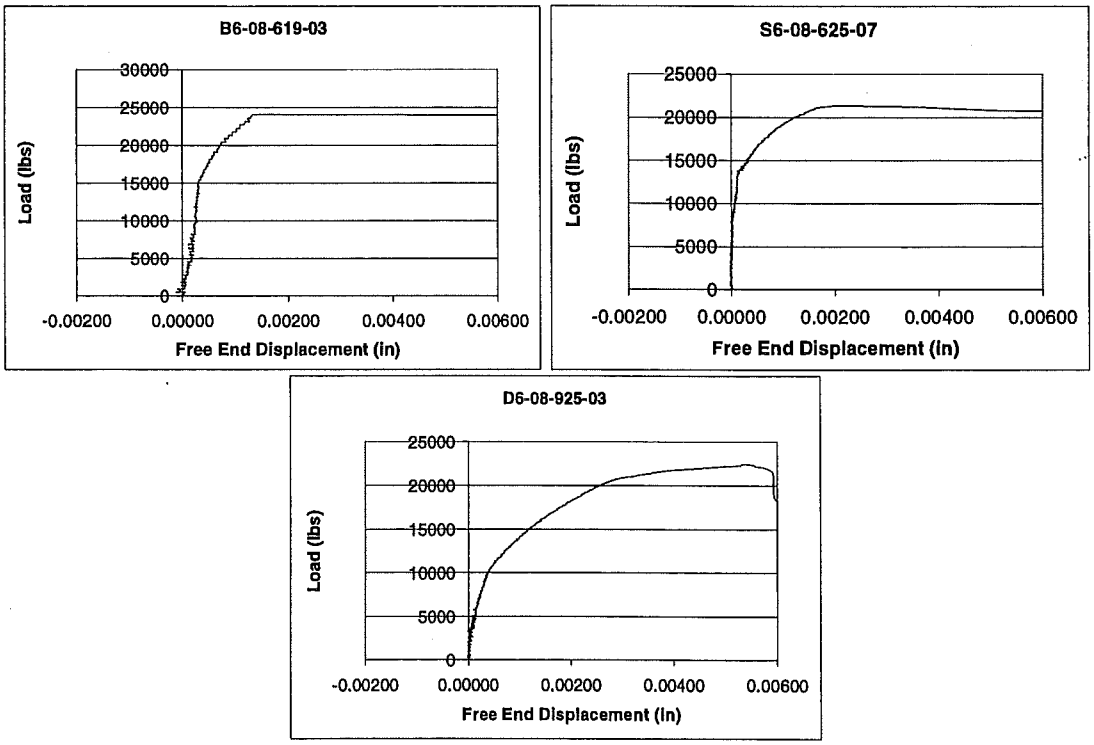

Figure 4-17: Comparison of Load-Displacement Plots for Specimens B6-08-619-03, S6-08-625-07, and D6-08-925-03

Further comparison of the load-displacement curves reveal that the curve for black bar seems to become increasingly different as the bonded length increases. The curve follows the load axis until the specimen cracks. Stainless 316LN bars are somewhat similar to this, but the Duplex 2205 stainless bars are different. Duplex bars seem to be exhibiting the

formation of microcracks at approximately the same load as the shorter bonded lengths. When viewing the load-displacement plots, the curve for black bar and 316LN bar with bonded lengths of 10-in and 12-in. stay near the load axis until the specimen cracks, whereas the curve for the Duplex bars veer away from the axis once microcracks form. Figure 4-18 shows load-displacement curves for all three bar types with bonded lengths of 12-in. From this figure the difference between the black bar and 316LN bar compared to the Duplex bar is inherently obvious. The entire shape of the curve for the Duplex bar is different than the other two types of bars.

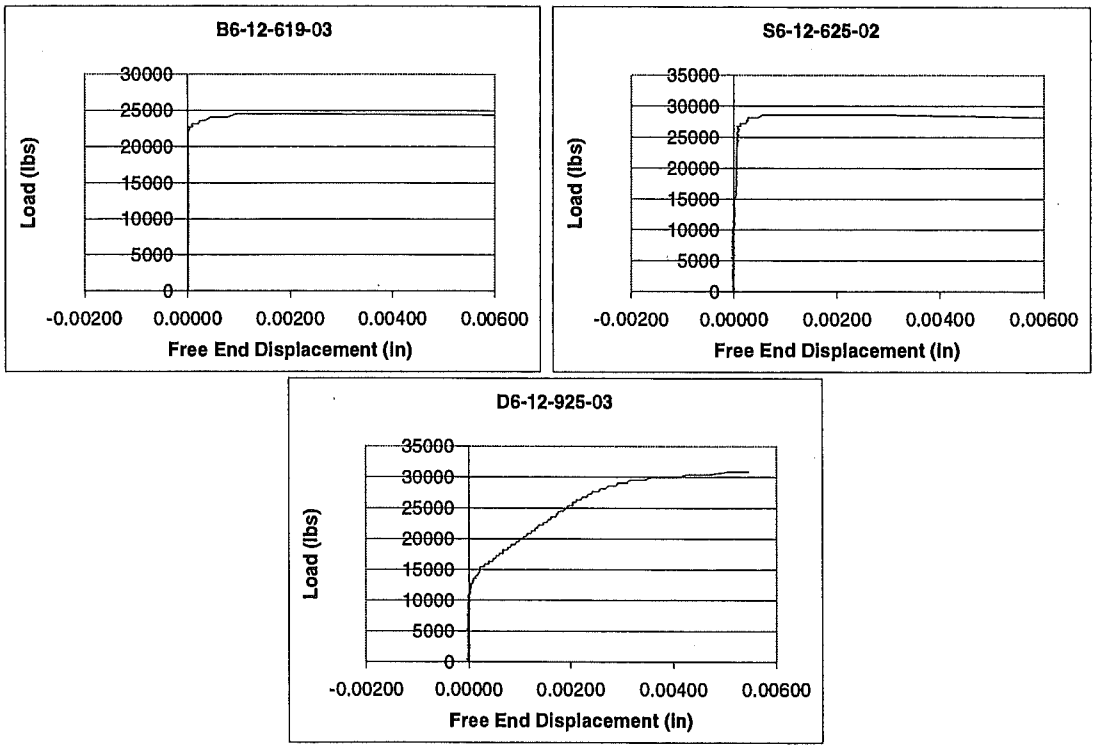

Figure 4-18: Comparison of Load-Displacement Plots for Specimens B6-12-619-03, S6-12-625-02, and D6-12-925-03

As previously observed for bonded lengths, particularly the 10-in. and 12-in. bonded lengths for black bar and stainless 316LN, the failure mode showed the free end displacement virtually stationary until bond was broken. This means that the all three components of bond failed at the same time. It appears that as the bonded length increases bond failure tends to occur at lower bond stresses. Bond stress can be computed from the bond strength using Equation 3-2. Figure 4-19 shows the bond stress at failure for the No. 6 bond tests.

From the linear regression fit to these data points it can be seen that the bond stress is in fact decreasing as the bonded length increases.

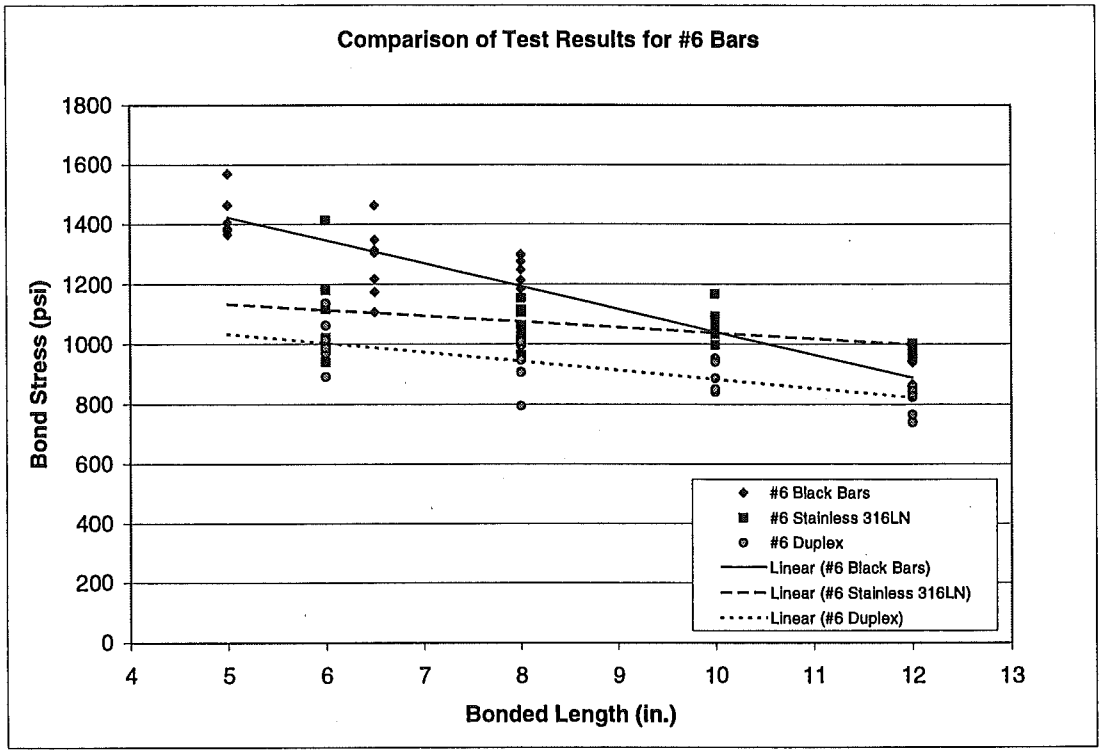

Figure 4-19: No. 6 Bar Bond Stresses

A comparison of the bond crack patterns of No. 6 black bar and No. 6 stainless bars shows nearly identical patterns between the different bars types for similar bonded lengths. Figure 4-20 shows all three specimens crack patterns, the black bar crack pattern located in the upper-left, the stainless bar crack pattern in the upper-right, and the Duplex crack pattern in the bottom-center. The crack patterns for the No. 6 bars are typical of all bond failure crack patterns. On the face with the least clear cover a longitudinal crack ran until the bar became debonded. Then the crack ran to either side of the specimen. Cracks on the sides of the specimens ran at approximately a 45-deg. angle starting near the debonded end of the bar. Similar to the No. 4 bars, the front face exhibited the typical Y-crack patterns that are commonly seen in bond tests involving semi-beam specimens.

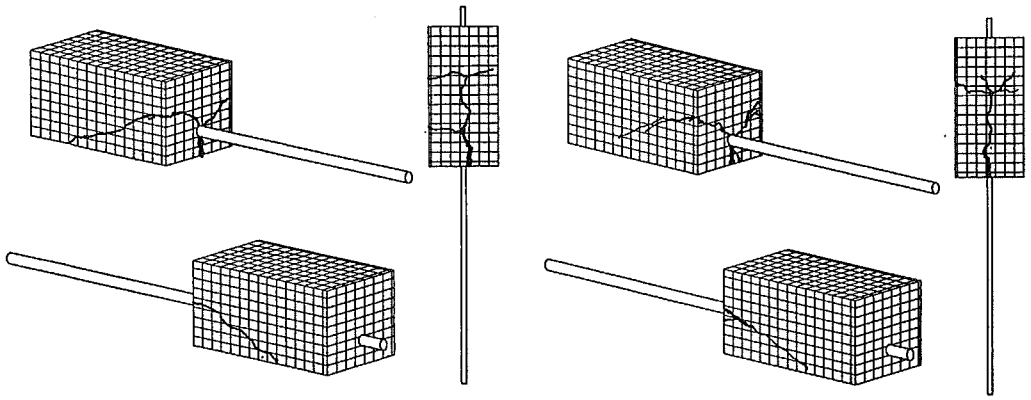

B6-08-619-04

S6-08-625-01

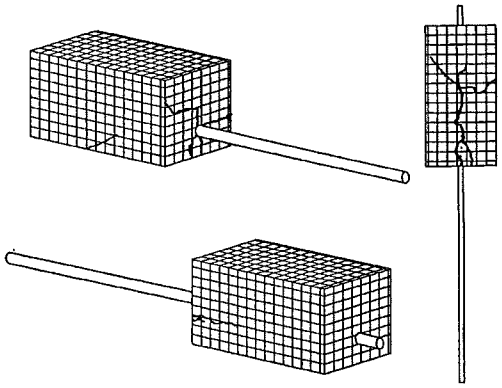

D6-08-925-02

Figure 4-20: Comparison of Crack Patterns for B6-08-619-04, S6-08-625-01, and D6-08-925-02

Mean experimental bond strength for all bonded lengths for the No. 6 black bars ranged from 18.7% above the predicted bond strength to 42.2% above the predicted bond strength based upon the OJB equation. The normalized mean experimental bond strength for the 316LN bar had a range of 14.5% to 35.7% above the predicted bond strength. Normalized experimental bond strength for the Duplex bars ranged from 3.8% above the predicted bond strength to 14.1% above the predicted bond strength.

Statistical t-tests were performed on the black bar experimental bond strength to determine if the experimental bond strength was different than the predicted bond strength (OJB, AASHTO, ACI, and Darwin), again with an emphasis on the AASHTO relationship. Test

parameters were similar to the No. 4 bar t-tests; the significance level, α, was 0.05. From these tests the black bar experimental bond strength was found to be different than the theoretical bond strength for all four relationships. Upon this conclusion another t-test was performed on the No. 6 black bar normalized experimental bond strength to determine if it was statistically greater than the predicted bond strength. From these statistical tests the black bar experimental bond strength was found to be greater than the predicted bond strength. The implications of this conclusion are that all bond tests involving the No. 6 bar are only valid if comparisons are made with respect to the black bar experimental bond strength; comparisons made with respect to the theoretical bond strength would not have any significant meaning. Hypotheses used for t-tests performed on black bar data as well as t-test results can be found in Table 4-9. In Table 4-9, μ_1 and μ_2 indicate the mean of the data being tested. In the black bar tests μ_1 is the mean of the black bar experimental bond strength and μ_2 is the theoretical bond strength. For the stainless t-tests μ_1 is always the stainless mean and μ_2 is either the mean of the black bar or the theoretical bond strength.

No. 6 Black Bar							
Hypotheses	Bonded Length	Black Bar	316LN Bar	OJB	AASHTO	ACI	Darwin
	4	--	--	$\mu_1 \neq \mu_2$	$\mu_1 \neq \mu_2$	$\mu_1 \neq \mu_2$	$\mu_1 \neq \mu_2$
	6	--	--	$\mu_1 \neq \mu_2$	$\mu_1 \neq \mu_2$	$\mu_1 \neq \mu_2$	$\mu_1 \neq \mu_2$
H_o: $\mu_1 = \mu_2$	6.5	--	--	$\mu_1 \neq \mu_2$	$\mu_1 \neq \mu_2$	$\mu_1 \neq \mu_2$	$\mu_1 \neq \mu_2$
H_A: $\mu_1 \neq \mu_2$	8	--	--	$\mu_1 \neq \mu_2$	$\mu_1 \neq \mu_2$	$\mu_1 \neq \mu_2$	$\mu_1 \neq \mu_2$
	10	--	--	$\mu_1 \neq \mu_2$	$\mu_1 \neq \mu_2$	$\mu_1 \neq \mu_2$	$\mu_1 \neq \mu_2$
	12	--	--	$\mu_1 \neq \mu_2$	$\mu_1 \neq \mu_2$	$\mu_1 \neq \mu_2$	$\mu_1 \neq \mu_2$
No. 6 316LN							
Hypotheses	Bonded Length	Black Bar	316LN Bar	OJB	AASHTO	ACI	Darwin
	6	$\mu_1 < \mu_2$	--	$\mu_1 \not< \mu_2$	$\mu_1 \not< \mu_2$	$\mu_1 \not< \mu_2$	$\mu_1 \not< \mu_2$
H_o: $\mu_1 = \mu_2$	8	$\mu_1 < \mu_2$	--	$\mu_1 \not< \mu_2$	$\mu_1 \not< \mu_2$	$\mu_1 \not< \mu_2$	$\mu_1 \not< \mu_2$
H_A: $\mu_1 < \mu_2$	10	$\mu_1 \not< \mu_2$	--	$\mu_1 \not< \mu_2$	$\mu_1 \not< \mu_2$	$\mu_1 \not< \mu_2$	$\mu_1 \not< \mu_2$
	12	$\mu_1 \not< \mu_2$	--	$\mu_1 \not< \mu_2$	$\mu_1 \not< \mu_2$	$\mu_1 \not< \mu_2$	$\mu_1 \not< \mu_2$
No. 6 Duplex							
Hypotheses	Bonded Length	Black Bar	316LN Bar	OJB	AASHTO	ACI	Darwin
	6	$\mu_1 < \mu_2$	$\mu_1 \not< \mu_2$	$\mu_1 \not< \mu_2$	$\mu_1 \not< \mu_2$	$\mu_1 \not< \mu_2$	$\mu_1 \not< \mu_2$
H_o: $\mu_1 = \mu_2$	8	$\mu_1 < \mu_2$	$\mu_1 < \mu_2$	$\mu_1 \not< \mu_2$	$\mu_1 \not< \mu_2$	$\mu_1 \not< \mu_2$	$\mu_1 \not< \mu_2$
H_A: $\mu_1 < \mu_2$	10	$\mu_1 < \mu_2$	$\mu_1 < \mu_2$	$\mu_1 \not< \mu_2$	$\mu_1 \not< \mu_2$	$\mu_1 \not< \mu_2$	$\mu_1 \not< \mu_2$
	12	$\mu_1 < \mu_2$	$\mu_1 < \mu_2$	$\mu_1 \not< \mu_2$	$\mu_1 \not< \mu_2$	$\mu_1 \not< \mu_2$	$\mu_1 \not< \mu_2$

Table 4-9: No. 6 Bar Statistical T-Test Results

T-tests were used to statistically compare stainless 316LN and Duplex 2205 normalized experimental bond strengths to black bar experimental bond strengths. Stainless normalized experimental bond strength was also compared to the theoretical bond. For the both statistical tests the null hypothesis, H_o, and the alternate hypothesis, H_a, was the same as the No. 4 bar statistical tests. The significance level, α, was again 0.05. It was also desired to compare the stainless 316LN experimental bond strength to the Duplex 2205 experimental bond strength, in order to determine if the Duplex bond strength was less than the 316LN bond strength.

From the t-tests involving the stainless bars the following conclusions can be made: There was no statistical reason to assume that the normalized experimental bond strength for both the stainless 316LN and the stainless Duplex 2205 bars was less than the predicted bond strength (for all bond relationships). There was reason to conclude that the stainless 316LN

experimental bond strength was less than the black bar bond strength for bonded lengths of 6-in and 8-in, but no reason to believe that that the experimental bond strength was less than the black bar experimental bond strength for bonded lengths of 10-in and 12-in. There was statistical reason to believe that the Duplex 2205 experimental bond strength was less than the black bar experimental bond strength for all bonded lengths. There was no statistical reason to assume that the Duplex 2205 bar normalized experimental bond strength was less than the predicted bond strength. There was also statistical reason to believe that the Duplex bond strength was less than the 316LN bond strength for all bonded lengths except the 6-in bonded length. T-test results for the No. 6 bars can be seen in Table 4-9.

From Figure 4-21, it can be seen that the conclusions based on the statistical analysis for the No. 6 bars are also valid. The normalized experimental bond strength for the No. 6 stainless 316LN bars do not seem to be less than the predicted bond strength based off the AASHTO relationship, rather the black bar experimental bond strength appears to be stronger than the predicted bond strength. However, it can also be seen that for the two shorter bonded lengths the stainless 316LN bars appear to have weaker bond strength than the black bar bond tests but still not less than the predicted bond strength. For the two longer bonded lengths, the 316LN bar is not less than the black bar experimental bond strength or theoretical bond strength. The statistical conclusions for the normalized bond strength for the stainless Duplex 2205 bars also make sense. Examining Figure 4-21 shows that a conclusion assuming the Duplex bond strength being not less than the predicted bond strength, but less than the experimental bond strength of black bar is affirmed.

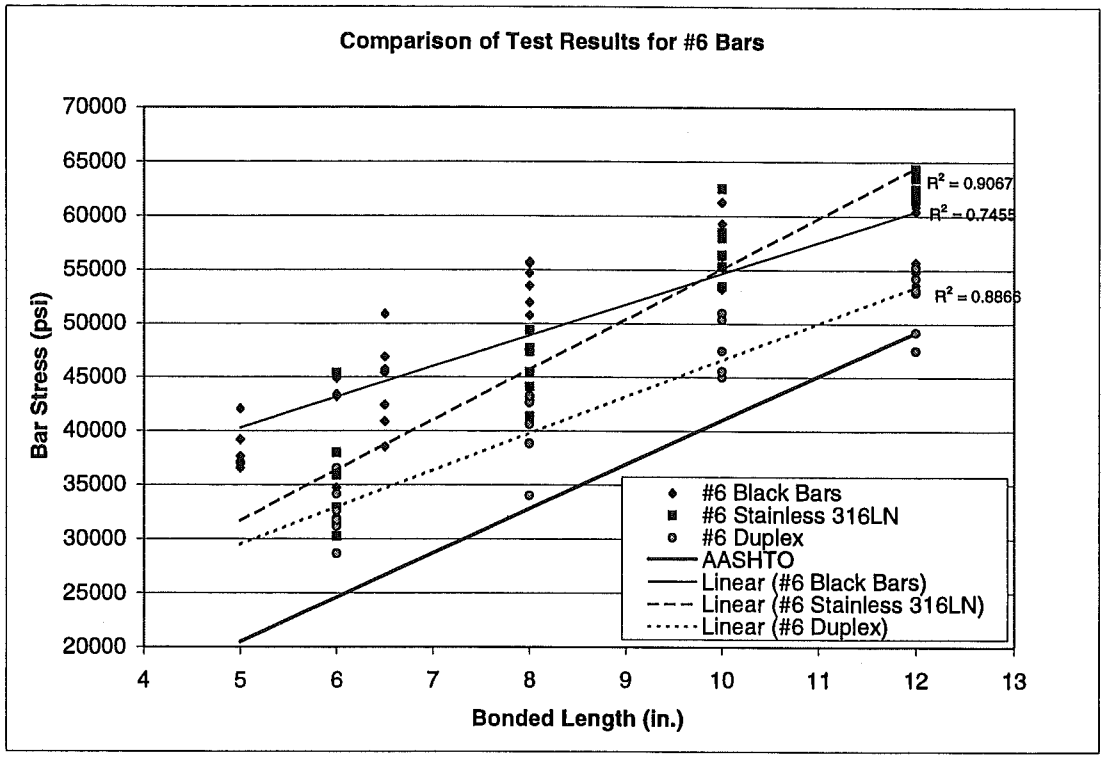

Figure 4-21: Linear Regression for No. 6 Bars

One probable cause for the No. 6 bond tests revealing atypical high bond strength could be the location of the upper reaction plate. The plate had to be moved closer to the bonded section of bar in order to eliminate flexural cracking failure. This action likely created confining stresses around the bonded section of bar resulting in higher bond strength results, due to an increase in the frictional component of bond.

The reduced bond strength capacity of the No. 6 Duplex bars could be caused by the weaker adhesion and friction components for this type of bar. The higher chromium content of the 2205 Duplex bars may be the source of this weaker adhesion and friction. Duplex bars had 22% chromium. The chromium content causes a passive film to form around the bar surface. This film may be different for the Duplex bars than the 316LN bars due to the rolling process and could be the cause for the reduction in adhesion and friction for the duplex bars by making the bar surface smoother than the A615 or the 316LN stainless bars. The No. 6 Duplex bars exhibited the bilinear curve for bonded lengths of 10-in. and 12-in. At these lengths neither of the other two types of bars displayed bilinear curves (as shown in

Figure 4-18). This indicates that something is different between the bond characteristics of the Duplex bars and the other two bar types for the No. 6 bars.

CHAPTER 5: CONCLUSIONS

The objective of this study was to compare bond strength over similar bonded lengths. The comparison was between A615 Gr. 60 reinforcing bar and two grades of stainless steel bar reinforcement, 316LN and Duplex 2205. A minimum of seven specimens was tested at each bonded length to provide a statistical sample of the bond strength for that particular bonded length. Bonded lengths were chosen to produce bar stresses between 55% and 100% yield of the A615 rebars. The test data were then compared statistically using t-tests to determine differences between the experimental bond strength and theoretical bond strength as well as differences between experimental bond strength for the black bars compared to the experimental bond strength of the two stainless types of reinforcement.

5.1 GENERAL CONCLUSIONS

A summary of the general bar and test properties can be made as follows:

- All three bar types had different yield strengths:
  - A615 Gr. 60 had yield strength of approximately 63 ksi.
  - Stainless 316LN had yield strength of approximately 91 ksi.
  - Stainless Duplex 2205 had yield strength of approximately 85 ksi.
- The range of bar stresses that the bond tests were conducted at included:
  - A615 Gr. 60 bars were tested in the bar stress range of 55% to 100% of yield for both bar sizes.
  - Stainless 316LN bars were tested in the bar stress range of 45% to 100% of yield for the No. 4 bars and 36% to 71% of yield for the No. 6 bars.
  - Stainless Duplex 2205 bars were tested in the bar stress range of 49% to 100% of yield for the No. 4 bars and 34% to 62% for the No. 6 bars.
- Similar crack patterns were observed for all bar types and sizes.

From the statistical analysis of the bond test data the following conclusions can be made for the range of bonded lengths tested:

- No. 4 black bar experimental bond strength is from a similar population as the theoretical bond strength population (AASHTO relationship).

- Stainless 316LN No. 4 bar experimental bond strength is not less than the predicted bond strength (AASHTO relationship).
- Stainless 316LN No. 4 bar experimental bond strength is not less than the No. 4 black bar experimental bond strength for all bonded lengths.
- Stainless Duplex 2205 No. 4 bar experimental bond strength is not less than the predicted bond strength. (AASHTO relationship).
- Stainless Duplex 2205 No. 4 bar experimental bond strength is not less than the No. 4 black bar experimental bond strength for all bonded lengths.

- No. 6 black bar experimental bond strength is from a different population than the theoretical bond strength population; further investigation revealed that the black bar experimental bond strength population was in fact greater than the theoretical bond strength population (AASHTO relationship).
- Stainless 316LN No. 6 bar experimental bond strength is not less than the predicted bond strength (AASHTO relationship).
- Stainless 316LN No. 6 bar experimental bond strength is less than the No. 6 black bar experimental bond strength for bonded lengths of 6-in and 8-in. Stainless 316LN No. 6 bar experimental bond strength is not less than the No. 6 black bar experimental bond strength for bonded lengths of 10-in and 12-in.
- Stainless Duplex 2205 No. 6 bar experimental bond strength is not less than the predicted bond strength (AASHTO relationship).
- Stainless Duplex 2205 No. 6 bar experimental bond strength is less than the No. 6 black bar experimental bond strength for all bonded lengths.
- Regression analysis plots of the data produces similar results as the t-tests.

When the stainless 316LN bars were compared to the AASHTO bond relationship, they were found to be statistically not less than the predicted bond strength. When the data were compared to the black bar experimental bond strength data, the No. 4 bars and the two longer bonded lengths of the No. 6 bars (10-in and 12-in) were found to be not less than the black bars, whereas the two shorter bonded lengths (6-in and 8-in) for the No. 6 bars were found to be less than the black bar experimental bond strength.

When the comparative study of the Duplex experimental bond strength was made the bond was found to be not less than the predicted bond strength. The No. 4 Duplex bond strength was also found to be not less than the black bar experimental bond strength. However, when the No. 6 Duplex experimental bond strength was compared to the black bar experimental bond strength, all bonded lengths were found to be less than the black bar experimental bond strength.

The most probable cause for the difference between the black bar and the Duplex bar was the bar surface condition. The Duplex bars appeared to have the smoothest surface which would cause weaker adhesion and friction components of bond. Because of the weaker adhesion, the formation of microcracks occurs earlier than the other two bar types. The smaller friction force causes specimen cracking to occur at a larger free-end displacement. For the longer bonded lengths the load-displacement relationship became drastically different between the different types of bars. The stainless 316LN bars continued to display results similar to the black bars, but the Duplex 2205 bars displayed the formation of microcracking and a reduced bond stiffness similar to the shorter bonded lengths. Because adhesion and friction may be the cause of the observed decreased bond capacity of the Duplex bars relative to the A615 Gr. 60 reinforcing bars, further research is suggested to investigate the difference. However, in all cases, the tested concrete-to-steel bond strength of the A615 Gr. 60, stainless 316LN and Duplex 2205 bars was greater than predicted by the AASHTO relationship.

5.2 SIGNIFICANCE OF RESULTS

With the integration of innovative materials being utilized in out nation's infrastructure, validity of using such materials must be considered. This study considered the use of stainless stress reinforcement as a replacement for A615 Gr. 60 reinforcement in concrete from a bond perspective. This study was not intended to define a new design method for stainless steel reinforcement utilizing its full material strength, nor was it intended to define an independent development length relationship for each stainless bar type tested. Rather, this investigation was performed to compare the bond strength of the concrete-to-stainless

steel reinforcement to concrete-to-A615 Gr. 60 reinforcing bars in service stress ranges up to yielding of the A615 bars.

Results indicated that a one-to-one replacement of stainless (316LN or Duplex 2205) bar for A615 Gr. 60 black bar would be suitable from a bond perspective of No. 4 and No. 6 reinforcing bars in normal strength concrete typical of that used in a Michigan bridge deck. All No. 4 stainless bars tested had a bond strength at least equal to the AASHTO predicted relationship and the No. 4 A615 Gr. 60 bars. While the No. 6 stainless bars has stronger bond than the A615 bars at longer bonded lengths, shorter lengths produced lower bond that the A615 bars. However, the conservatism of the AASHTO development length relationship (as well as other comparative relationships including OJB, ACI and Darwin) predicted lower bond strengths than observed at all bonded lengths for all bar types.

MDOT Bridge Design Guidelines (section 7.14.01 and 7.14.01A) do not need to be altered to reflect the results found in this study. Further research is required for determining changes to the lap-splice table.

5.3 FUTURE WORK

This research effort provides a solid foundation for understanding the bond of stainless steel reinforcement in concrete compared to standard A615 Gr. 60 (No. 4 and No. 6) reinforcing steel. For the bond strength of stainless steels to be fully incorporated into current design codes, a full-scale bond study is required. Such a study would include various bar sizes above No. 6 with bonded lengths that would produce bar stresses closer to the yield strength of the stainless steel reinforcement and would enable a full development length relationship to be derived. With that said, modifications to the test specimen used in the study herein would be needed to allow for longer bonded lengths. These studies involving larger bar sizes would also determine if any bond mechanic differences exist for the larger bars.

The AASHTO 16th ed. Standard Specifications and LRFD codes currently limit the use of reinforcing materials above Gr. 75, thereby limiting the potential use of high-strength materials to their fullest capacity. To fully utilize the material characteristics of the stainless steel reinforcement, a new design philosophy should be considered. This would account for

the non-linear (non-bimodal) relationship of the stainless stress-strain relationship, and possibly eliminate the concept of a yield plateau for reinforcing bars.

The microscopic study of bond would be useful to fully understand the adhesion difference between the two types of stainless bars and the black bar. Such an investigation may show initial bonding mechanisms that can potentially effect the bond behavior at higher stresses.

CHAPTER 6: REFERENCES

AASHTO (1996), "Standard Specifications for Highway Bridges," Sixteenth Edition, American Association of State Highway and Transportation Officials, Washington, DC.

Abrams, D. A. (1913), "Tests of Bond Between Concrete and Steel," *Bulletin No. 71*, University of Illinois Engineering Experiment Station, Illinois.

ACI Manual of Concrete Practice (1997), Part 3, Use of Concrete in Buildings - Design, Specifications, and Related Topics, Section 224.2R, American Concrete Institute, Farmington Hills, Michigan.

ACI Committee 318 (1999), "Building Code Requirements for Structural Concrete (318-99) and Commentary (318R-99)," American Concrete Institute, Farmington Hills, Michigan.

ACI Committee 408 (1966), "Bond Stress - The State of the Art," Report, American Concrete Institute, Detroit Michigan, November.

ACI Committee 408 (1990), "Bond Stress - The State of the Art," Report, American Concrete Institute, Detroit Michigan, November.

ACI Committee 408 (1992), "State-of-the-Art Report on Bond under Cyclic Loads," Report, American Concrete Institute, Detroit Michigan.

ASTM A370 (1997), Standard Test Methods and Definitions for Mechanical Testing of Steel Products.

ASTM A615/A 615M (1996), Standard Specification for Deformed and Plain Billet-Steel Bars for Concrete Reinforcement.

ASTM A617/A 617M (1996), Standard Specification for Axle-Steel Deformed and Plain Bars for Concrete Reinforcement.

ASTM A944 (1995), Standard Test Method for Comparing Bond Strength of Steel Reinforcing Bars to Concrete Using Beam-End Specimens.

ASTM A955 (1996), Standard Specification for Deformed and Plain Stainless Steel Bars for Concrete Reinforcement [Metric].

ASTM C231 (1997), Standard Test Method for Air Content of Freshly Mixed Concrete by the Pressure Method.

ASTM C31 (1996), Standard Practice for Making and Curing Concrete Test Specimens in the Field.

ASTM C39 (1996), Standard Test Method for Compressive Strength of Cylindrical Concrete Specimens.

ASTM C138 (1992), Standard Test Method for Unit Weight, Yield, and Air Content (Gravimetric) of Concrete.

ASTM C143 (1990), Standard Test Method for Slump of Hydraulic Cement Content.

Choi, Oan C., H. Hadje-Ghaffari, David Darwin, and Steven L. McCabe (1990a), "Bond of Epoxy-Coated Reinforcement to Concrete: Bar Parameters," *SL Report No. 90-1*, University of Kansas Center for Research, Lawrence, Kansas, January.

Choi, Oan C., D. Darwin and S.L. McCabe (1990b), "Bond Strength of Epoxy-Coated Reinforcement to Concrete," *SM Report No. 25*, University of Kansas Center for Research, Lawrence, Kansas, July.

Clark, A. P. (1946), "Comparative Bond Efficiency of Deformed Concrete Reinforcement Bars," *Journal of the American Concrete Institute*, Proc. V. 43, No. 4, December.

Cox, R. et al, "Stainless Steel in Concrete- State of the Art Report," *European Federation of Corrosion Publications, Number 18*, The Institute of Materials, London, England, 1996.

Darwin, David and Ebenezer K. Graham (1993), "Effect of Deformation Height and Spacing on Bond Strength of Reinforcing Bars," Structural Engineering and Engineering Materials, *SM Report No. 93-1*, University of Kansas Center for Research, Lawrence, Kansas, January.

Darwin, David and Michael L. Tholen (1996), "Effects of Deformation Properties on the Bond of Reinforcing Bars," Structural Engineering and Engineering Materials, *SM Report No. 42*, University of Kansas Center for Research, Inc., Lawrence, Kansas, October.

DenHartigh, Timothy C. (2001), "A Comparative Bond Study of Stainless Steel Reinforcement in Concrete," *MSCE Thesis*, Michigan Technological University, Houghton, Michigan.

Fédération Internationale du Béton (2000), "Bond of Reinforcement in Concrete - State of the Art Report," Task Group *Bond Models*, Lausanne, Switzerland.

Ferguson, P. M. and J. N. Thompson (1965), "Development Length of Large High Strength Reinforcing Bars," *Journal of the American Concrete Institute*, Proc. V. 62, No. 1, January.

French, Catherine, Roberto Leon, and Timothy Grundhoffer (1992) "Bond Behavior of Uncoated and Epoxy-Coated Reinforcement in Concrete", Center for Transportation Studies, *Structural Engineering Report No. 92-04*, University of Minnesota, May.

Foo, Ee-Lin (1998), "An Alternative Test for Bond Strength of Concrete Reinforcing Bars," *MSCE Thesis*, Michigan Technological University, Houghton, Michigan.

Hadje-Ghaffari, Hossain, David Darwin, and Steve McCabe (1991), "Effects of Epoxy-Coating on the Bond of Reinforcing Steel to Concrete," Structural Engineering and Engineering Materials, *SM Report No. 28*, University of Kansas Center for Research, Inc., Lawrence, Kansas, July.

Hester, Cynthia J., Shahin Salamizavaregh, David Darwin, and Steven L. McCabe (1990), "Bond of Epoxy-Coated Reinforcement to Concrete: Splices", *SL Report 90-1*, University of Kansas Center for Research, Lawrence, Kansas, May.

Jirsa, O., and Breen, J. E. (1981), "Influence of Casting Position and Shear on Development and Splice Lengths- Design Recommendations," *Research Report 242-3F*, Center for Transportation Research, Bureau of Engineering Research, The University of Texas at Austin, November.

Johnston, David W., and Zia, Paul (1980), "Bond Characteristics of Epoxy Coated Reinforcing Bars," Center for Transportation Engineering Studies, Department of Civil Engineering North Carolina State University at Raleigh, August.

Luke, J. J., B. S. Hamad, O. Jirsa, and J. E. Breen, (1981), "The Influence of Casting Position on Development and Splice Length of Reinforcing Bars," *Research Report 242-1*, Center for Transportation Research, Bureau of Engineering Research, The University of Texas at Austin, June.

Lutz, Leroy A., and Peter Gergley (1967), "The Mechanics of Bond and Slip of Deformed Bars in Concrete", *ACI Journal*, Proceedings Col. 64, No. 11, November, pp 711-721.

Mains, R.M. (1951), "Measurement of the Distribution of Tensile and Bond Stresses Along Reinforcing bars", *ACI Journal*, Proceedings V. 48, No. 9, November, pp. 225-252.

Michigan Department of Transportation, "Bridge Design Guidelines (1995)," April

Michigan Department of Transportation, "Special Provision for Reinforcement Stainless Steel (1999)," April.

Michigan Department of Transportation, "Standard Specifications for Construction (1996)," Second Edition, Lansing, Michigan.

Orangun, C.O., J.O. Jirsa, and J.E. Breen (1977), "A Reevaluation of Test Data on Development Length and Splices," *ACI Journal*, Proceedings, Col. 74, No. 3, March, pp. 114-122 Discussion, pp 470-473.

Sozen, Meta A., and Jack P. Moehle (1990), "Development and Lap-Splice Lengths for Deformed Reinforcing Bars in Concrete", *Report*, A Report to The Portland Cement Association, Skokie, IL and The Concrete Reinforcing Steel Institute, Schaumburg, IL., August.

Treece, R.A. and J.O. Jirsa (1989), "Bond Strength of Epoxy-Coated Reinforcing Bars," *ACI Material Journal*, V. 86, No. 2, March-April.

APPENDIX A - RELATIVE RIB AREA CALCULATIONS

Data used to calculate relative rib area for the reinforcing bars used in this study is found in this appendix.

- Relative rib area was computed using the mean of the measurements.

	#4 Black	#4 Stainless	#4 Duplex	#6 Black	#6 Stainless	#6 Duplex
Height of Rib	0.0328	0.0330	0.0283	0.0558	0.0553	0.0540
	0.0328	0.0371	0.0260	0.0590	0.0518	0.0588
	0.0303	0.0375	0.0313	0.0575	0.0520	0.0545
	0.0288	0.0288	0.0268	0.0583	0.0590	0.0538
Average	0.0311	0.0341	0.0281	0.0576	0.0545	0.0553
Coeff. of Var.	0.0634	0.1202	0.0827	0.0242	0.0623	0.0426
Length of Rib	0.1225	0.1235	0.1480	0.1280	0.2135	0.1900
	0.1220	0.1445	0.1530	0.1215	0.2130	0.1955
	0.1505	0.1360	0.1400	0.1330	0.2165	0.1950
	0.1465	0.1320	0.1430	0.1275	0.2010	0.1950
Average	0.1354	0.1340	0.1460	0.1275	0.2110	0.1939
Coeff. of Var.	0.1126	0.0651	0.0391	0.0369	0.0324	0.0134
Rib Spacing	0.3370	0.3305	0.3430	0.3630	0.5835	0.5185
	0.3285	0.3470	0.3480	0.3685	0.5795	0.5185
	0.3320	0.3240	0.3440	0.3510	0.5780	0.5100
	0.3415	0.3490	0.3385	0.3625	0.5880	0.5125
Average	0.3348	0.3376	0.3434	0.3613	0.5823	0.5149
Coeff. of Var.	0.0170	0.0364	0.0114	0.0204	0.0077	0.0084
Actual Bar Dia.	0.4615	0.4740	0.4840	0.6975	0.7060	0.717
	0.4630	0.4710	0.4850	0.6945	0.7080	0.7175
	0.4790	0.4715	0.4865	0.6920	0.7105	0.718
	0.4645	0.4705	0.4830	0.6940	0.7125	0.717
Average	0.4670	0.4718	0.4846	0.6945	0.7093	0.7174
Coeff. of Var.	0.0173	0.0033	0.0031	0.0033	0.0040	0.0007
Nominal Bar Dia.	0.5	0.5	0.5	0.75	0.75	0.75
Relative Rib Area	**0.0992**	**0.1083**	**0.0865**	**0.1728**	**0.1008**	**0.1156**

Table A-1: Relative Rib Area

APPENDIX B - REBAR YIELD TEST DATA

- Stress-strain curves from the yield tests are found in this appendix.
- Black bar data can be found in figures B-1 to B-2.
- Stainless 316LN data can be found in figures B-3 to B-4.
- Stainless Duplex 2205 data can be found in figures B-5 to B-6.

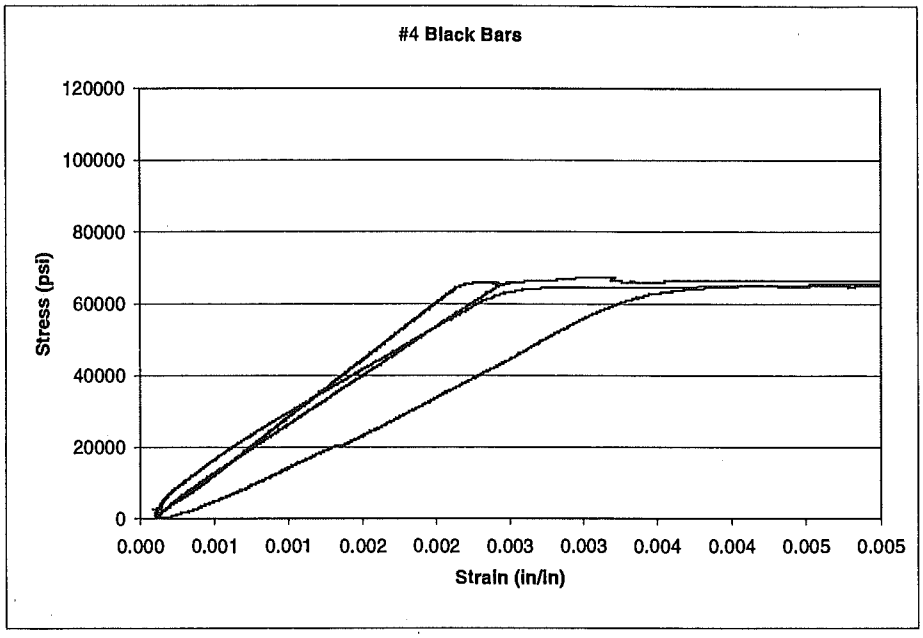

Figure B-1

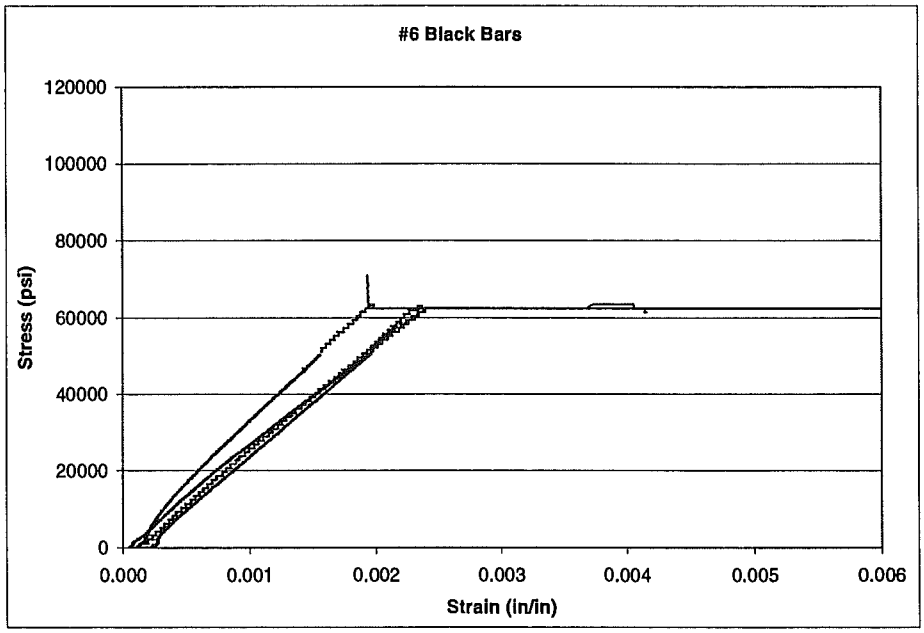

Figure B-2

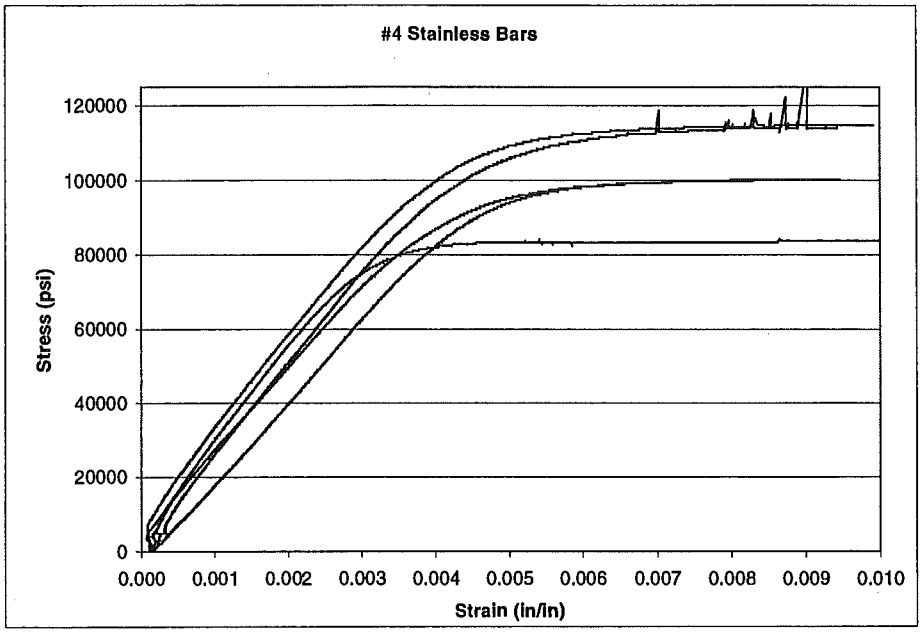

Figure B-3

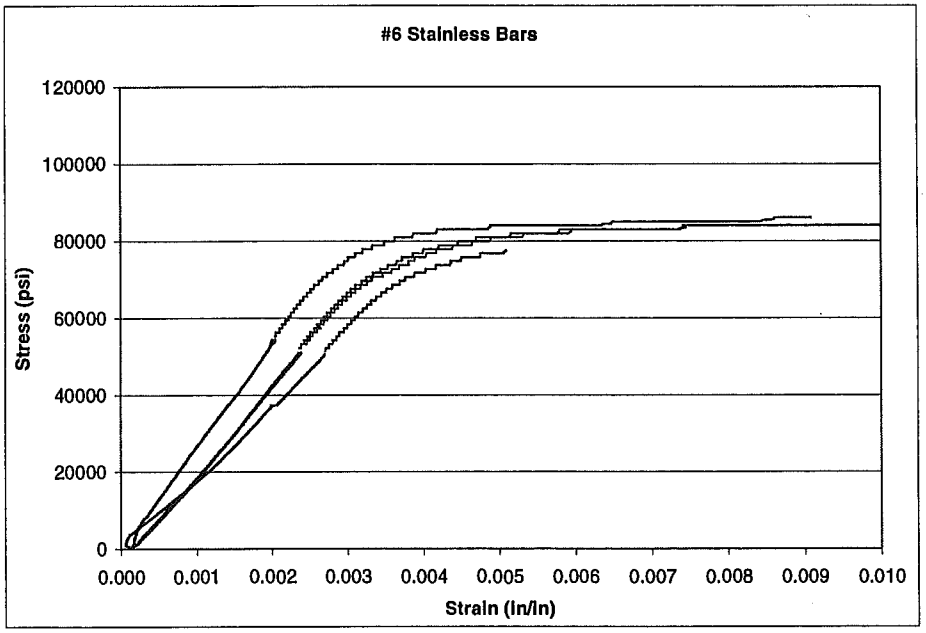

Figure B-4

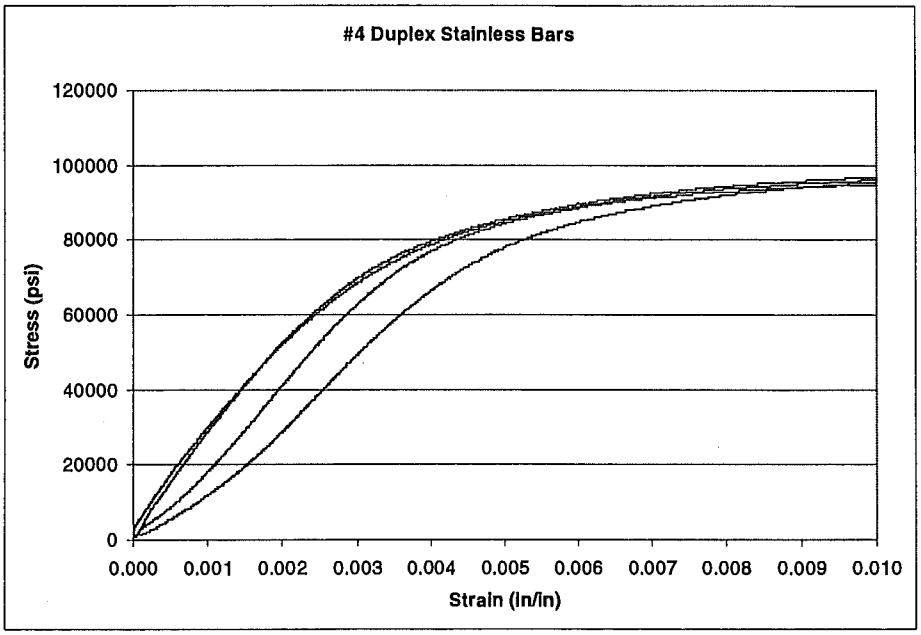

Figure B-5

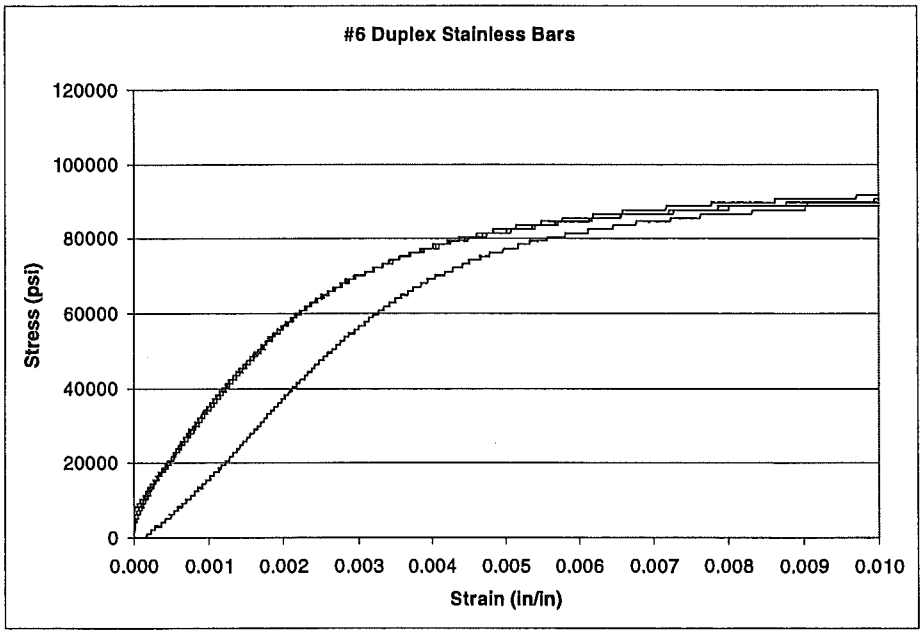

Figure B-6

APPENDIX C - CALCULATION OF THEORETICAL PULLOUT VALUES

- Theoretical pullout values used to compute bonded lengths can be found in this appendix.

- All calculated bond strength values are based on a concrete compressive strength of 5210 psi. This allows all bond strengths to be compared to the values in Chapter 4, i.e. the "Normalized Bond Strength" for the stainless bars and the "Load @ .002 in." for the black bars.

Theoretical Pullout Force Calculation for #4 Bar with 4-in. Bond:

Variables			
Length in Test		4	in
Bar Size		#4	
Area	A=	0.2	in^2
Diameter	d_b=	0.5	in
Concrete Strength	f'c=	5210	psi
Location Factor	a=	1	
Coating Factor	b=	1	
Size Factor	g=	0.8	
Lightweight Factor	l=	1	
Transverse Reinforcment Index	Ktr=	0	in
Cover or Spacing	c=	1.5	in
Darwin's Variables			
Number of Bars being developed	n=	1	bar
Side Cover	c_so=	3.375	in
Clear Space	CC=	100000	in
Clear space / 2	c_si=	50000	in
Bottom Cover	c_b=	1.5	in
min of c_si or .25 of c-so	c_s=	3.375	in
min of c_s or c_b	c_m	1.5	
Max of c_s or c_b	c_M	3.375	

Calculated Forces and Stresses (where P is load and fs is steel stress)		
"OJB" Equation	P= 7460.4433 lb	fs = 37995.73 psi
AASHTO Design Code	P= 7218.033 lb	fs = 36090.16 psi
1999 ACI Building Code	P= 5669.0298 lb	fs = 28872.13 psi
Darwin Equation	P= 7208.2296 lb	fs = 36711.21 psi

Table C-1: Calculation of #4 bar with 4-in. Bonded Length for Both Black and Stainless Bars

Theoretical Pullout Force Calculation for #4 Bar with 5.5-in. Bond:

Variables			
Length in Test		5.5	in
Bar Size		#4	
Area	A=	0.2	in^2
Diameter	d_b=	0.5	in
Concrete Strength	f'c=	5210	psi
Location Factor	a=	1	
Coating Factor	b=	1	
Size Factor	g=	0.8	
Lightweight Factor	l=	1	
Transverse Reinforcment Index	Ktr=	0	in
Cover or Spacing	c=	1.5	in
Darwin's Variables			
Number of Bars being developed	n=	1	bar
Side Cover	c_so=	3.375	in
Clear Space	CC=	100000	in
Clear space / 2	c_si=	50000	in
Bottom Cover	c_b=	1.5	in
min of c_si or .25 of c-so	c_s=	3.375	in
min of c_s or c_b	c_m	1.5	
Max of c_s or c_b	c_M	3.375	

Calculated Forces and Stresses (where P is load and fs is steel stress)		
"OJB" Equation	P= 9195.1664 lb	fs = 46830.60 psi
AASHTO Design Code	P= 9924.7953 lb	fs = 49623.98 psi
1999 ACI Building Code	P= 7794.916 lb	fs = 39699.18 psi
Darwin Equation	P= 8412.312 lb	fs = 42843.55 psi

Table C-2: Calculation of #4 bar with 5.5-in. Bonded Length for Both Black and Stainless Bars

Theoretical Pullout Force Calculation for #4 Bar with 7-in. Bond:

Variables			
Length in Test		7	in
Bar Size		#4	
Area	A=	0.2	in^2
Diameter	d_b=	0.5	in
Concrete Strength	f'c=	5210	psi
Location Factor	a=	1	
Coating Factor	b=	1	
Size Factor	g=	0.8	
Lightweight Factor	l=	1	
Transverse Reinforcment Index	Ktr=	0	in
Cover or Spacing	c=	1.5	in
Darwin's Variables			
Number of Bars being developed	n=	1	bar
Side Cover	c_so=	3.375	in
Clear Space	CC=	100000	in
Clear space / 2	c_si=	50000	in
Bottom Cover	c_b=	1.5	in
min of c_si or .25 of c-so	c_s=	3.375	in
min of c_s or c_b	c_m	1.5	
Max of c_s or c_b	c_M	3.375	

Calculated Forces and Stresses (where P is load and fs is steel stress)		
"OJB" Equation	P= 10929.89 lb	fs = 55665.47 psi
AASHTO Design Code	P= 12631.558 lb	fs = 63157.79 psi
1999 ACI Building Code	P= 9920.8022 lb	fs = 50526.23 psi
Darwin Equation	P= 9616.3944 lb	fs = 48975.89 psi

Table C-3: Calculation of #4 bar with 7-in. Bonded Length for Black Bars

Theoretical Pullout Force Calculation for #4 Bar with 8-in. Bond:

Variables			
Length in Test		8	in
Bar Size		#4	
Area	A=	0.2	in^2
Diameter	d_b=	0.5	in
Concrete Strength	f'c=	5210	psi
Location Factor	a=	1	
Coating Factor	b=	1	
Size Factor	g=	0.8	
Lightweight Factor	l=	1	
Transverse Reinforcment Index	Ktr=	0	in
Cover or Spacing	c=	1.5	in
Darwin's Variables			
Number of Bars being developed	n=	1	bar
Side Cover	c_so=	3.375	in
Clear Space	CC=	100000	in
Clear space / 2	c_si=	50000	in
Bottom Cover	c_b=	1.5	in
min of c_si or .25 of c-so	c_s=	3.375	in
min of c_s or c_b	c_m	1.5	
Max of c_s or c_b	c_M	3.375	

Calculated Forces and Stresses (where P is load and fs is steel stress)		
"OJB" Equation	P= 12086.372 lb	fs = 61555.39 psi
AASHTO Design Code	P= 14436.066 lb	fs = 72180.33 psi
1999 ACI Building Code	P= 11338.06 lb	fs = 57744.26 psi
Darwin Equation	P= 10419.116 lb	fs = 53064.12 psi

Table C-4: Calculation of #4 bar with 8-in. Bonded Length for Stainless Bars

Theoretical Pullout Force Calculation for #4 Bar with 8.5-in. Bond:

Variables			
Length in Test		8.5	in
Bar Size		#4	
Area	A=	0.2	in^2
Diameter	d_b=	0.5	in
Concrete Strength	f'c=	5210	psi
Location Factor	a=	1	
Coating Factor	b=	1	
Size Factor	g=	0.8	
Lightweight Factor	l=	1	
Transverse Reinforcment Index	Ktr=	0	in
Cover or Spacing	c=	1.5	in
Darwin's Variables			
Number of Bars being developed	n=	1	bar
Side Cover	c_so=	3.375	in
Clear Space	CC=	100000	in
Clear space / 2	c_si=	50000	in
Bottom Cover	c_b=	1.5	in
min of c_si or .25 of c-so	c_s=	3.375	in
min of c_s or c_b	c_m	1.5	
Max of c_s or c_b	c_M	3.375	

Calculated Forces and Stresses (where P is load and fs is steel stress)		
"OJB" Equation	P= 12664.613 lb	fs = 64500.34 psi
AASHTO Design Code	P= 15338.32 lb	fs = 76691.60 psi
1999 ACI Building Code	P= 12046.688 lb	fs = 61353.28 psi
Darwin Equation	P= 10820.477 lb	fs = 55108.24 psi

Table C-5: Calculation of #4 bar with 8.5-in. Bonded Length for Black Bars

Theoretical Pullout Force Calculation for #4 Bar with 10-in. Bond:

Variables			
Length in Test		10	in
Bar Size		#4	
Area	A=	0.2	in^2
Diameter	d_b=	0.5	in
Concrete Strength	f'c=	5210	psi
Location Factor	a=	1	
Coating Factor	b=	1	
Size Factor	g=	0.8	
Lightweight Factor	l=	1	
Transverse Reinforcment Index	Ktr=	0	in
Cover or Spacing	c=	1.5	in
Darwin's Variables			
Number of Bars being developed	n=	1	bar
Side Cover	c_so=	3.375	in
Clear Space	CC=	100000	in
Clear space / 2	c_si=	50000	in
Bottom Cover	c_b=	1.5	in
min of c_si or .25 of c-so	c_s=	3.375	in
min of c_s or c_b	c_m	1.5	
Max of c_s or c_b	c_M	3.375	

Calculated Forces and Stresses (where P is load and fs is steel stress)		
"OJB" Equation	P= 14399.336 lb	fs = 73335.22 psi
AASHTO Design Code	P= 18045.082 lb	fs = 90225.41 psi
1999 ACI Building Code	P= 14172.575 lb	fs = 72180.33 psi
Darwin Equation	P= 12024.559 lb	fs = 61240.58 psi

Table C-6: Calculation of #4 bar with 10-in. Bonded Length for Stainless Bars

Theoretical Pullout Force Calculation for #6 Bar with 5-in. Bond:

Variables			
Length in Test		5	in
Bar Size		#6	
Area	A=	0.44	in^2
Diameter	d_b=	0.75	in
Concrete Strength	f'c=	5210	psi
Location Factor	a=	1	
Coating Factor	b=	1	
Size Factor	g=	0.8	
Lightweight Factor	l=	1	
Transverse Reinforcment Index	Ktr=	0	in
Cover or Spacing	c=	1.5	in
Darwin's Variables			
Number of Bars being developed	n=	1	bar
Side Cover	c_so=	3.25	in
Clear Space	CC=	100000	in
Clear space / 2	c_si=	50000	in
Bottom Cover	c_b=	1.5	in
min of c_si or .25 of c-so	c_s=	3.25	in
min of c_s or c_b	c_m	1.5	
Max of c_s or c_b	c_M	3.25	

Calculated Forces and Stresses (where P is load and fs is steel stress)		
"OJB" Equation	P= 12500.211 lb	fs = 28294.69 psi
AASHTO Design Code	P= 9022.5412 lb	fs = 20505.78 psi
1999 ACI Building Code	P= 7086.2873 lb	fs = 16040.07 psi
Darwin Equation	P= 12941.008 lb	fs = 29292.45 psi

Table C-7: Calculation of #6 bar with 5-in. Bonded Length for Black Bars

Theoretical Pullout Force Calculation for #6 Bar with 6-in. Bond:

Variables			
Length in Test		6	in
Bar Size		#6	
Area	A =	0.44	in^2
Diameter	d_b =	0.75	in
Concrete Strength	f'c =	5210	psi
Location Factor	α =	1	
Coating Factor	β =	1	
Size Factor	γ =	0.8	
Lightweight Factor	λ =	1	
Transverse Reinforcment Index	Ktr =	0	in
Cover or Spacing	c =	1.5	in
Darwin's Variables			
Number of Bars being developed	n =	1	bar
Side Cover	c_so =	3.25	in
Clear Space	CC =	100000	in
Clear space / 2	c_si =	50000	in
Bottom Cover	c_b =	1.5	in
min of c_si or .25 of c-so	c_s =	3.25	in
min of c_s or c_b	c_m	1.5	
Max of c_s or c_b	c_M	3.25	

Calculated Forces and Stresses (where P is load and fs is steel stress)		
"OJB" Equation	P = 13724.72 lb	fs = 31066.41 psi
AASHTO Design Code	P = 10827.05 lb	fs = 24606.93 psi
1999 ACI Building Code	P = 8503.545 lb	fs = 19248.09 psi
Darwin Equation	P = 13743.73 lb	fs = 31109.44 psi

Table C-8: Calculation of #6 bar with 6-in. Bonded Length for Stainless Bars

Theoretical Pullout Force Calculation for #6 Bar with 6.5-in. Bond:

Variables			
Length in Test		6.5	in
Bar Size		#6	
Area	A=	0.44	in^2
Diameter	d_b=	0.75	in
Concrete Strength	f'c=	5210	psi
Location Factor	a=	1	
Coating Factor	b=	1	
Size Factor	g=	0.8	
Lightweight Factor	l=	1	
Transverse Reinforcment Index	Ktr=	0	in
Cover or Spacing	c=	1.5	in
Darwin's Variables			
Number of Bars being developed	n=	1	bar
Side Cover	c_so=	3.25	in
Clear Space	CC=	100000	in
Clear space / 2	c_si=	50000	in
Bottom Cover	c_b=	1.5	in
min of c_si or .25 of c-so	c_s=	3.25	in
min of c_s or c_b	c_m	1.5	
Max of c_s or c_b	c_M	3.25	

Calculated Forces and Stresses (where P is load and fs is steel stress)		
"OJB" Equation	P= 14336.976 lb	fs = 32452.28 psi
AASHTO Design Code	P= 11729.304 lb	fs = 26657.51 psi
1999 ACI Building Code	P= 9212.1735 lb	fs = 20852.10 psi
Darwin Equation	P= 14145.09 lb	fs = 32017.93 psi

Table C-9: Calculation of #6 bar with 6.5-in. Bonded Length for Black Bars

Theoretical Pullout Force Calculation for #6 Bar with 8-in. Bond:

Variables			
Length in Test		8	in
Bar Size		#6	
Area	A=	0.44	in^2
Diameter	d_b=	0.75	in
Concrete Strength	f'c=	5210	psi
Location Factor	a=	1	
Coating Factor	b=	1	
Size Factor	g=	0.8	
Lightweight Factor	l=	1	
Transverse Reinforcment Index	Ktr=	0	in
Cover or Spacing	c=	1.5	in
Darwin's Variables			
Number of Bars being developed	n=	1	bar
Side Cover	c_so=	3.25	in
Clear Space	CC=	100000	in
Clear space / 2	c_si=	50000	in
Bottom Cover	c_b=	1.5	in
min of c_si or .25 of c-so	c_s=	3.25	in
min of c_s or c_b	c_m	1.5	
Max of c_s or c_b	c_M	3.25	

Calculated Forces and Stresses (where P is load and fs is steel stress)		
"OJB" Equation	P= 16173.742 lb	fs = 36609.86 psi
AASHTO Design Code	P= 14436.066 lb	fs = 32809.24 psi
1999 ACI Building Code	P= 11338.06 lb	fs = 25664.12 psi
Darwin Equation	P= 15349.173 lb	fs = 34743.42 psi

Table C-10: Calculation of #6 bar with 8-in. Bonded Length for Both Black and Stainless Bars

Theoretical Pullout Force Calculation for #6 Bar with 10-in. Bond:

Variables			
Length in Test		10	in
Bar Size		#6	
Area	A=	0.44	in^2
Diameter	d_b=	0.75	in
Concrete Strength	f'c=	5210	psi
Location Factor	a=	1	
Coating Factor	b=	1	
Size Factor	g=	0.8	
Lightweight Factor	l=	1	
Transverse Reinforcment Index	Ktr=	0	in
Cover or Spacing	c=	1.5	in
Darwin's Variables			
Number of Bars being developed	n=	1	bar
Side Cover	c_so=	3.25	in
Clear Space	CC=	100000	in
Clear space / 2	c_si=	50000	in
Bottom Cover	c_b=	1.5	in
min of c_si or .25 of c-so	c_s=	3.25	in
min of c_s or c_b	c_m	1.5	
Max of c_s or c_b	c_M	3.25	

Calculated Forces and Stresses (where P is load and fs is steel stress)		
"OJB" Equation	P= 18622.763 lb	fs = 42153.31 psi
AASHTO Design Code	P= 18045.082 lb	fs = 41011.55 psi
1999 ACI Building Code	P= 14172.575 lb	fs = 32080.15 psi
Darwin Equation	P= 16954.616 lb	fs = 38377.40 psi

Table C-11: Calculation of #6 bar with 10-in. Bonded Length for Stainless Bars

Theoretical Pullout Force Calculation for #6 Bar with 12-in. Bond:

Variables			
Length in Test		12	in
Bar Size		#6	
Area	A=	0.44	in^2
Diameter	d_b=	0.75	in
Concrete Strength	f'c=	5210	psi
Location Factor	a=	1	
Coating Factor	b=	1	
Size Factor	g=	0.8	
Lightweight Factor	l=	1	
Transverse Reinforcment Index	Ktr=	0	in
Cover or Spacing	c=	1.5	in
Darwin's Variables			
Number of Bars being developed	n=	1	bar
Side Cover	c_so=	3.25	in
Clear Space	CC=	100000	in
Clear space / 2	c_si=	50000	in
Bottom Cover	c_b=	1.5	in
min of c_si or .25 of c-so	c_s=	3.25	in
min of c_s or c_b	c_m	1.5	
Max of c_s or c_b	c_M	3.25	

Calculated Forces and Stresses (where P is load and fs is steel stress)		
"OJB" Equation	P= 21071.784 lb	fs = 47696.76 psi
AASHTO Design Code	P= 21654.099 lb	fs = 49213.86 psi
1999 ACI Building Code	P= 17007.09 lb	fs = 38496.18 psi
Darwin Equation	P= 18560.059 lb	fs = 42011.38 psi

Table C-12: Calculation of #6 bar with 12-in. Bonded Length for Both Black and Stainless Bars

APPENDIX D - INSTRUMENT CALIBRATION DATA

- Data used to calibrate the LVDT and the Load Acquisition system can be found in this appendix.

- Two different load levels on the Tinius Olsen Testing Machine were used during the tests, the 24 kip setting and the 120 kip setting.
    - Data for the 24 kip load setting can be found on pages D-2 to D-3.
    - Data for the 120 kip load setting can be found on pages D-4 to D-5.

- LVDT calibration data can be found on pages D-6 to D-7

Sensor Definition: 24k Load

Identification	
Name:	Load
Number:	
Comments:	Tineus Load Signal; Potentiometer
Sensor Characteristics	
Output Type:	DC Voltage
Output Units:	mV
Excitation Type:	Unipolar DC Voltage
Excitation Source	Input Card
Excitation Units	V
Excitation Value	.5 V
Input Card Settings	
Input Card Selected	808FB1
Attenuation	No Restrictions
Card Gain	1
Post Gain	No Restrictions
Input Card Filtering	3 Pole Butterworth
Input Card Capabilities	
Can Balance	Yes
Can Sample And Hold	NO
Can ECheck	Yes
Can RCal	Yes
Programmable Gain	NO
Balance Type	No Restrictions
Calibration Curve Model	
Curve Model	None
Curve Type	Linear Best Fit
Eng. Units	
Eng. Units Desc	Pounds
Eng. Units Abbr	lbs
Cal Information	
Cal Type	RCal
Cal Target	0 lbs
Shunt Resistor	100 KOhms

Linear Best Fit

Sensor Value (mV)	Eng. Unit (lbs)
-16.5625	0
369.0625	2000
755.625	4000
1142.5	6000
1527.8125	8000
1914.0625	10000
2299.6875	12000
2686.25	14000
3072.1875	16000
3458.125	18000
3825.9375	20000
4210.3125	22000

Linear Slope and offset

Best Fit Slope	5.19828702041
Best Fit Offset	64.1036808097

Sensor Definition: 120k Load

Identification	
Name:	Load
Number:	
Comments:	Tineus Load Signal; Potentiometer
Sensor Characteristics	
Output Type:	DC Voltage
Output Units:	mV
Excitation Type:	Unipolar DC Voltage
Excitation Source	Input Card
Excitation Units	V
Excitation Value	5 V
Input Card Settings	
Input Card Selected	808FB1
Attenuation	No Restrictions
Card Gain	1
Post Gain	No Restrictions
Input Card Filtering	3 Pole Butterworth
Input Card Capabilities	
Can Balance	Yes
Can Sample And Hold	NO
Can ECheck	Yes
Can RCal	Yes
Programmable Gain	NO
Balance Type	No Restrictions
Calibration Curve Model	
Curve Model	None
Curve Type	Linear Best Fit

Eng. Units

Eng. Units Desc	Pounds
Eng. Units Abbr	lbs

Cal Information

Cal Type	RCal
Cal Target	0 lbs
Shunt Resistor	100 KOhms

Linear Best Fit

Sensor Value (mV)	Eng. Unit (lbs)
-0.3125	0
193.4375	5000
386.5625	10000
579.6875	15000
773.125	20000
966.875	25000
1159.0625	30000
1352.5	35000
1492.5	38500

Linear Slope and offset

Best Fit Slope	25.8352051310
Best Fit Offset	16.4751198491

Sensor Definition: Free End LVDT

Identification	
Name:	Free End LVDT
Number:	
Comments:	Sensotec +-0.1" LVDT 10VDC Serial #6605
Sensor Characteristics	
Output Type:	DC Voltage
Output Units:	V
Excitation Type:	Unipolar DC Voltage
Excitation Source	Input Card
Excitation Units	V
Excitation Value	10 V
Input Card Settings	
Input Card Selected	808FB1
Attenuation	No Restrictions
Card Gain	No Restrictions
Post Gain	No Restrictions
Input Card Filtering	3 Pole Butterworth
Input Card Capabilities	
Can Balance	Yes
Can Sample And Hold	NO
Can ECheck	Yes
Can RCal	Yes
Programmable Gain	NO
Balance Type	No Restrictions
Calibration Curve Model	
Curve Model	None
Curve Type	Linear Best Fit

Eng. Units

Eng. Units Desc	Inches
Eng. Units Abbr	in

Cal Information

Cal Type	RCal
Cal Target	0 in
Shunt Resistor	100 KOhms

Linear Best Fit

Sensor Value (V)	Eng. Unit (in)
-0.0975	-.01345
-0.082188	-.01125
-0.07625	-.0105
-0.062813	-.00865
-0.051563	-.00715
-0.03625	-.0051
-0.034375	-.0048
-0.023438	-.0033
-0.021563	-.00315
-0.014375	-.00225
-0.002813	-.0005
-0.000313	0
0.001875	.0001
0.003125	.0002
0.00375	.00035
0.005938	.0007
0.014063	.0018
0.01625	.00205
0.024688	.0032
0.032188	.00425
0.037813	.00505
0.047813	.0063
0.056563	.00755
0.080938	.01085
0.098125	.0132
0.111563	.015
0.125	.01675

Linear Slope and offset

Best Fit Slope	0.135770967264
Best Fit Offset	-1.46827755774E-4

APPENDIX E - WIRING DIAGRAMS

- Required information in order to successfully wire the LVDT and the Load Acquisition system is found in this appendix.

Data was electronically recorded through the Megadec 3016AC Data Acquisition System. The system operated on AC power and had 512 kilobytes of internal memory with a data sampling rate up to 25000 samples per second, depending on the number of channels to be sampled. Two channels were sampled throughout each bond test: one channel to record the testing machine load and one channel to record the free-end displacement measured by the LVDT. The TCS software was programmed to record at a rate of 10 samples per second.

The Tinius Olsen Testing Machine was used to apply vertical load to the specimen. The load data was taken directly from the testing machine via an internal variable resistor. The resistance between the terminals L and R was 100 ohms (see Figure E-1). Terminal C was connected to a wiper that could move between L and R while terminal T, not used in this study, was fixed in the middle of the resistor. The wiper was driven by gearing of the load dial servo-motor and changed proportionally from L to R as the load increased. Because of this variable resistor arrangement, the load signal was wired to the data acquisition system as a potentiometer. A standard terminal (STB 808FB-1) was used to connect the variable resistor to the AD FB 808-1 (120Ω) board within the data acquisition system. The wiring schematic is shown in Figure E-2.

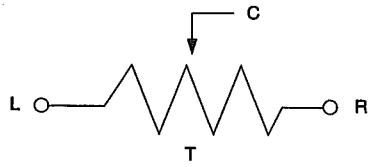

Figure E-1: Tinius Olsen Testing Machine Variable Resistor Schematic

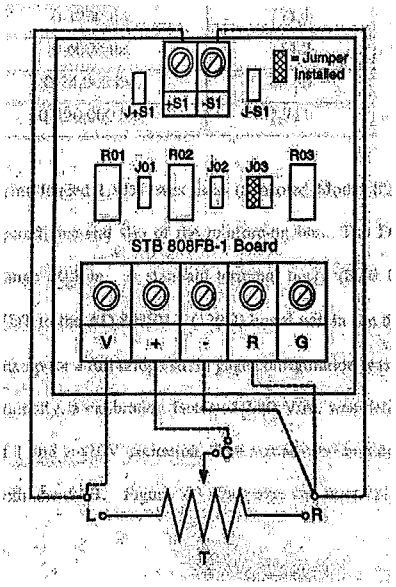

Figure E-2: Wiring Schematic for Tinius Load Signal to the Standard Terminal Board

The LVDT (Sensotec Model S2C-200) was used to measure the free-end displacement of the reinforcing bar. The LVDT had an accurate linear displacement range of ±0.1-in with a total displacement range of ±0.25-in. A standard terminal board (808FB-1) was used to connect the LVDT to the data acquisition system. A four-wire hook up for a full bridge strain gage configuration was used in the connection process. Calibration data can be found in Appendix D. Figure E-3 exemplifies the wire schematic for the LVDT connection to the 808FB-1 terminal board.

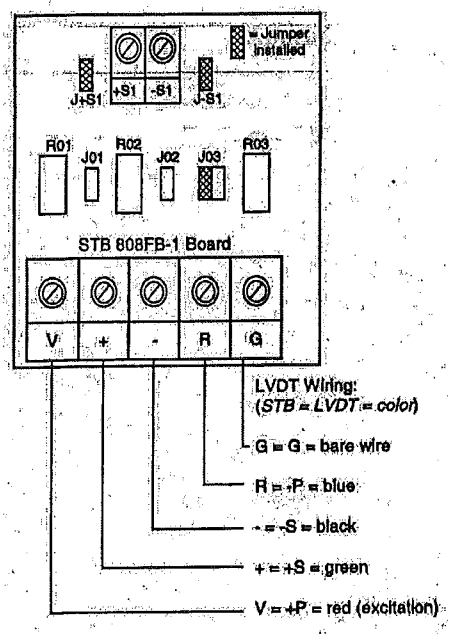

Figure E-3: Wiring Schematic for LVDT Connection to 808FB-1 Terminal Board

It should be noted that the current extension to the LVDT Wiring changes the colors depicted in Figure E-3 to the following: G = green, R = blue, (-) = orange, (+) = orange/white, V = blue/white.